THESIS APPROVAL

GRADUATE SCHOOL, KASETSART UNIVERSITY

Master of Engineering (Materials Engineering)

DEGREE

Materials Engineering | Materials Engineering

FIELD | **DEPARTMENT**

TITLE: A Study of Calcium Zeolite Type A from Eggshells Forming Using Binder, Compression and Polyurethane Foam as Template

NAME: Mrs. La-Orngdow Mulsow

THIS THESIS HAS BEEN ACCEPTED BY

THESIS ADVISOR

(Miss Nuchnapa Tangboriboon, Ph.D.)

DEPARTMENT HEAD

(Assistant Professor Wisit Locharoenrat, M.Eng.)

APPROVED BY THE GRADUATE SCHOOL ON _____

DEAN

(Associate Professor Gunjana Theeragool, D.Agr.)

THESIS

A STUDY OF CALCIUM ZEOLITE TYPE A FROM EGGSHELLS FORMING USING BINDER, COMPRESSION AND POLYURETHANE FOAM AS TEMPLATE

LA-ORNGDOW MULSOW

A Thesis Submitted in Partial Fulfillment of
the Requirements for the Degree of
Master of Engineering (Materials Engineering)
Graduate School, Kasetsart University
2012

La-Orngdow Mulsow 2012: A Study of Calcium Zeolite Type A from Eggshells Forming Using Binder, Compression and Polyurethane Foam as Template. Master of Engineering (Materials Engineering), Major Field: Materials Engineering, Department of Materials Engineering. Thesis Advisor: Miss Nuchnapa Tangboriboon, Ph.D. 112 pages.

The purpose of this research is to try to fabricate calcium zeolite type A from eggshells as a starting material via the sol-gel process. Forming using binder method, compression, and polyurethane foam as a template. The received samples were characterized phase formation by x-ray diffraction (XRD), microstructure by Scanning Electron Microscopy (SEM), pore size and specific surface area by Brunaues-Emmet-Teller (BET), mechanical properties of foam composite (gel_110+PU foam or gel_300+PU foam) by compression test, the functional groups by the Fourier Transformation Infrared Spectroscopy (FT-IR). Thermal properties of the endothermic-exothermic reaction by DTA and the percentage of weight loss were measured by TGA. In addition, micrographs of dispersion were characterized by Transmission Electron Microscope (TEM). The results demonstrated that $CaNaAlSi_2O_7$ can be fabricated to granules by using CMC as binder. The first method is granule preparation; granule product was prepared by coating on filter paper with granules dispersed on the filter paper by adhesive glue. The second method of samples prepared by compression was studied the specificion surface area that showed high surface area. The last method of sample preparat aims to produce polymer matrix composite (PMCs) between $CaNaAlSi_2O_7$ and PU foam as a matrix. The suitable composition of composite materials is 10% vol $CaNaAlSi_2O_7$ added into PU foam. The average particle size of $CaNaAlSi_2O_7$ is approximately 10μm, non-agglomeration, and good dispersion in the entire volume of PU foam. The composite foam cells are well ordered and uniform in size and shape. The true density, elastic modulus,and compressive strength of $CaNaAlSi_2O_7$ / PU composites are 1047g/cm^3, 0.0327 Kgf/mm^2, and 0.0188 Kgf/mm^2, respectively. The phase formation of $CaNaAlSi_2O_7$ / PU composites is shown both crystalline phase of tetragonal phase formations of $CaNaAlSi_2O_7$ and amorphous phase formation belonging to polyurethane (PU).

_____ _____ ___ / ___ / ____

Student's signature Thesis Advisor's signature

ACKNOWLEDGEMENTS

I would like to thank the Department of Materials Engineering at Kasetsart University for financial and analytical equipment support, the Petroleum and Petrochemical College, the Scientific and Technological Research Equipment Centre, at Chulalongkorn University for use of analytical equipment, and the Hutsman (Thailand) Ltd., for providing the chemical substances to prepare polyurethane as a PU foam. In addition, I would like to gratefully thank to Dr. Nuchnapa Tangboriboon for her advice, encouragement, and valuable suggestion for complete this research, Asst.Prof.Dr. Duangdrudee Chaysuwan for her thoughtfulness and good suggestions. Moreover, I also wish to thank my friends, technicians and lecturers at Department of Materials Engineering for their helpful and valuable knowledge.

Finally, I would like to thank my husband for his love, care and encouragement since first day until now and especially, my parents who are the most important in my life for encouragement, love and financial supports.

La-Orngdow Mulsow

March 2012

TABLE OF CONTENTS

LIST OF TABLES

LIST OF FIGURES

LIST OF FIGURES (Continued)

LIST OF FIGURES (Continued)

LIST OF FIGURES (Continued)

LIST OF FIGURES (Continued)

Appendix Figure

LIST OF FIGURES (Continued)

LIST OF FIGURES (Continued)

LIST OF ABBREVIATIONS

$CaNaAlSi_2O_7$	=	Calcium Zeolite Type A or Calcium Sodium Aluminosilicate
Gel_110	=	Calcium Zeolite Type A dried at 110°C.
Gel_300	=	Calcium Zeolite Type A calcined at 300 °C
10%gel_110 +PU foam	=	10%w/w of Calcium Zeolite Type A dried at 110°C composite with polyurethane foam
10%gel_300 +PU foam	=	10%w/w of Calcium Zeolite Type A calcined at 300°C composite with polyurethane foam
NaOH	=	Sodium hydroxide
M	=	Molar
L	=	Amount of alkali liquid
Si	=	Silicon element
Al	=	Aluminium element
SiO_2	=	Silica, silicon dioxide
Al_2O_3	=	Alumina, aluminium oxide
CaO	=	Calcium oxide
O_2	=	Oxygen gas
CO_2	=	Carbon dioxide gas
HCl	=	Hydrochloric acid
CMC	=	Carboxymethyl cellulose
TEM	=	Transmission Electron Microscope
BET	=	Brunauer-Emmet-Teller
PU	=	Polyurethane foam
STA	=	Simultaneous Thermal Analyzer
FT-IR	=	Fourier Transform Infrared Spectrometer
SEM	=	Scanning Electron Microscope
EDS	=	Electron dispersive spectroscopy

LIST OF ABBREVIATIONS (Continued)

XRD	=	X-ray diffraction
TGA	=	Themogravimetric analyzer
GP	=	Gas pycnometer
UTM	=	Universal testing machine
DTA	=	Differential thermal analysis
ASTM	=	American Society for Testing and Materials
KN	=	Kilogram newton
N/cm^2	=	Newton per square centimeter
m^2/g	=	Square meter per gram
MPa	=	Mega Pascal
cm^2	=	Square centimeter
cm^3	=	Cubic centimeter
nm	=	Nanometer
mm	=	Millimeter
mm^2	=	Square millimeter
cc	=	Cubic centimeter
g	=	Gram
N	=	Newton
Kgf	=	Kilogram force
rpm	=	Revolution per minute
μm	=	Micron
w/w	=	Weight per weight
ρ	=	Density
Å	=	Angstrom
°C	=	Degree of Celsius
f	=	Applied load
Std,Dev	=	Standard deviation
Ur	=	Uncertainty

A STUDY OF CALCIUM ZEOLITE TYPE A FROM EGGSHELLS FORMING USING BINDER, COMPRESSION AND POLYURETHANE FOAM AS TEMPLATE

INTRODUCTION

Over 200 years ago, a Swedish scientist discovered the first group of crystalline microporous aluminosilicate known as zeolite; zeolite derived from the Greek word *zeo* which means boil and *lithos* meaning stone (Van der Wall and Van Bekkum, 1998). Zeolite consists of open cells, three dimensional framework of tetrahedral AlO^{-}_{4} and SiO^{-}_{4} linked through shared oxygen molecules, crystalline microporous and aluminosilicate minerals. Due to their properties that have size and shape selectivity so its application can be used in ion-exchange, purification, desiccant or adsorbent and as a catalyst, these features are quite important in chemical, petrochemical and oil refining industries.

Calcium Zeolite Type A or Calcium Sodium Aluminosilicate ($CaNaAlSi_2O_7$) is one kind of all zeolite that is synthesized in different ways. The sol-gel process was used to synthesize zeolite type A in this research by using eggshells as the starting material (Nuchnapa *et al.*, 2010). After that design fabrication $CaNaAlSi_2O_7$ in three kind of samples was used as a foam catalyst by the binder, compression and polyurethane foam (PU) as a template for use in real life applications.

OBJECTIVES

1. To increase value by adding eggshells as the starting material for calcium zeolite type A or calcium sodium aluminosilicate synthesis.

2. To study the chemical composition of eggshells in order to synthesize calcium zeolite type A applied as an absorbent and catalyst foam.

3. To design various formation of calcium zeolite type A for proper use.

4. To investgate absorbtion of calcium zeolite type A by liquid and gas filtration.

5. To study the physical property of absorber-fabricated calcium zeolite type A for practical uses and future applications.

LITERATURE REVIEW

Nowadays, environmental problems are being solved by various institutions. The methods to solve the problems are known as reuse, reduce, and recycle depend on the type of materials. People are more interested in recycling, reusing, and reducing today than ever before, including waste from consumer, agricultural, and industrial products. In this research we would like to decrease pollution by using waste eggshells for use as a starting material for the synthesize of calcium zeolite type A ($CaNaAlSi_2O_7$) and for increasing value by designing and forming, by mixing with binder, compression and polyurethane foam as a template to work as a catalyst applicable for real world use.

The definition of calcium

Calcium is the chemical element with the symbol Ca, atomic number 20 and an alkaline earth metal in gray color. Ca is sometimes used as a reducing agent for extraction other elements. From reports, Ca element is the 5^{th} most abundant element in the earth's crust.

Calcium from eggshell

Since ancient times, eggs have been used as food and ingredients in many products. An eggshell contains two major layers with the primary function of protecting the chicken embryo (Nuchanapa *et al*., 2011). Eggshell's weight is approximately 10% of the total mass (Ca. 60g) of a hen's egg. The chemical composition (by weight) of eggshell has been reported as follows: calcium carbonate 94%, magnesium carbonate 1%, calcium phosphate 1% and organic matter 4% (Ziky *et al.,* 2009).

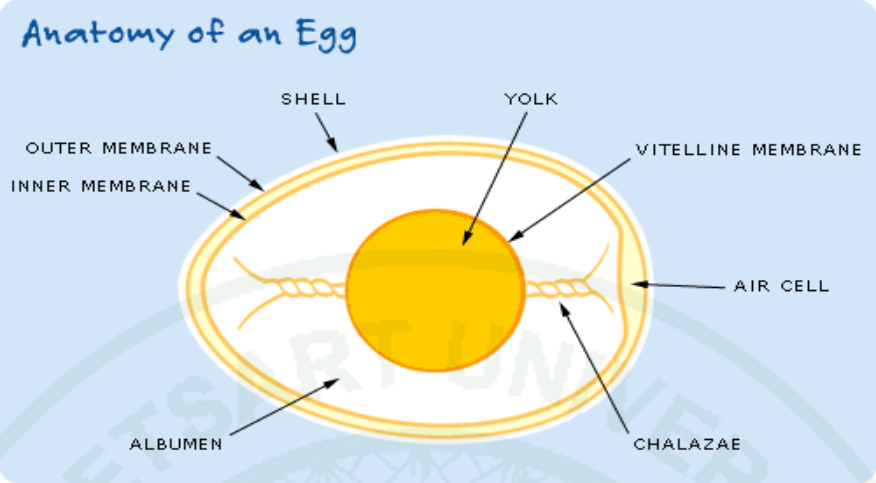

Figure 1 Anatomy of an Egg

Source: Anonymous (2012)

Calcium carbonate ($CaCO_3$) is the most abundant composition in eggshell with specific properties such as crystalline or powder, colorless, odorless, and insoluble in water, but it is soluble in weak acid. $CaCO_3$ can be converted into calcium oxide (CaO) or calcium hydroxide ($Ca(OH)_2$) by using calcinations as shown in figure 2.

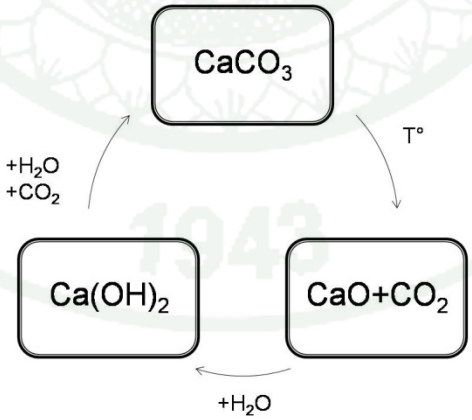

Figure 2 The reaction of $CaCO_3$, CaO, and $Ca(OH)_2$

Source: Khongnakhon and Kittikul (2009)

For eggshell applications, eggshell was studied many years ago as a starting material for several synthesis products. In 1998, Eric *et al* reported that eggshells were composed of a line up of three surface structures. The first and the second surface layers are composed of many types of proteins and fiber proteins but the external surface layer is composed of $CaCO_3$. In this research, eggshells are used as a starting material for the synthesis of hydroxyapatite compound that is a component in most organisms bones. First, eggshell was burned at 450°C for 2 h to remove any organic substances with a heating rate of 5 °C/min then calcined at 900°C for 2 h with the same heating rate in order to get calcium oxide (CaO). This is a hydroxyapatite's starting material.

In the same way, Csaba *et al.* (2006) used eggshells as the starting material to prepare a calcium phosphate compound. From their investigation of the first 30 minutes of calcined eggshell at 900°C found that the eggshell became black in color, and after 3 h became white in color because it changed to new phase formations and removed some organic material. The new phase formations were CaO, $Ca(OH)_2$, MgO, and others. Furthermore, waste eggshell was investigated in triglyceride transesterification with a view to determine its viability as a solid catalyst for use in biodiesel synthesis (Ziku *et al*., 2008). A temperature > 700°C for 1 h can change $CaCO_3$ to CaO. From this investigation, calcined eggshell exhibited high activity towards the transesterification of vegetable oil with methanol to produce biodiesel. The method of reusing eggshell waste to prepare catalyst could recycle the waste, minimizing contaminants, reducing the cost of catalyst, and making the catalyst environmentally friendly.

Nuchnapa *et al*. (2010) demonstrated that "Calcium Zeolite Type A ($CaNaAlSi_2O_7$) or Soda Melitite" can be synthesized from eggshells by the Sol-Gel process, with a ratio of $CaO:Al_2O_3:NaO:SiO_2$ is 1:1:2:8. The calcined temperature of the eggshells was 900°C for 1 h with a heating rate of 10°C/min to obtain the CaO starting material. Therefore, the proper calcined temperature of $CaNaAlSi_2O_7$ is 300°C for 1 h with 0.51 pore volume, 37.19 nm pore diameter, 55.15 m^2/g specific surface .

Witoon (2011) concluded that CaO derived from the eggshell waste is an attractive option for us as a CO_2 absorbent due to its potential low cost, environmentally benign nature and high CO_2 capture capacity. For all the above we can conclude that eggshell's application as a starting material derived from $CaCO_3$ can be used as a product to produce many kinds of materials.

Zeolite

What is zeolite?

Over 200 years ago, a Swedish scientist discovered a group of crystalline micro porous aluminosilicates known as zeolite. Zeolite is derived from the Greek word *zeo* which means boil and *lithos* meaning stone (Van der waal and van bek kum, 1998)

Zeolites are microporous crystalline solids with well-defined structures which generally consist of open cell, three dimensional, framework of tetrahedral AlO_4 and SiO_4 units linked through shared oxygen molecules, crystalline microporous and aluminosilicate minerals.

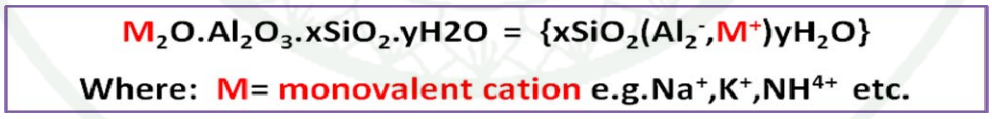

Figure 3 The normal composition of zeolite

Source: Bell (2001)

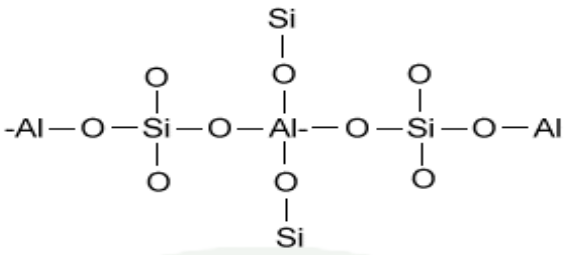

Figure 4 The framework of tetrahedral AlO^-_4 and SiO^-_4 units linked through shared oxygens

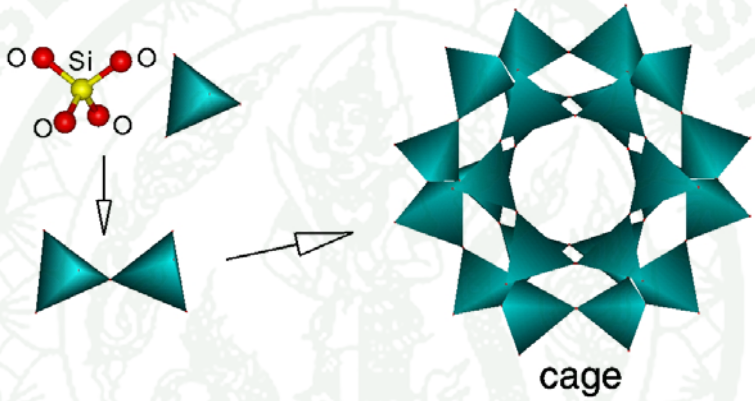

Figure 5 A defining feature of zeolite is that their frameworks are made up of 4-connected networks of atom.

Source: Bell (2001)

Due to their properties that have size and shape selectivity so that its application can be used in ion-exchange, purification, desiccant or adsorbent and as a catalyst. Catalysts are quite important in chemical, petrochemical and oil refining industries, other application are in agriculture, animal husbandry and construction (Bell, 2001). As table 1 shows estimated annual world production of zeolite in 1991.

Table 1 Estimated annual world production of zeolites in 1991

Application	Production (ton/year)
Ion exchange	825,000
Purification (Natural zeolite)	115,000
desiccant and adsorbent	40,000
Catalysis	100,000
Chemical	≈500
Petrochemical, special	≈5,000
Oil refinning, FCC cracking	≈95,000

Source: Van der waal and Van bek kum (1998)

Properties of zeolites

Properties of zeolite were above briefly expanded. For more understanding, discussion as follows: studies have shown that zeolite usually contains cations (e.g., Na^+, K^+, or NH_4^+) after synthesis. These positive ions are rather loosely held and can readily be exchanged for others in a contact solution. Figure 6 shows ion exchange between Na^+ and NH_4^+ of zeolite.

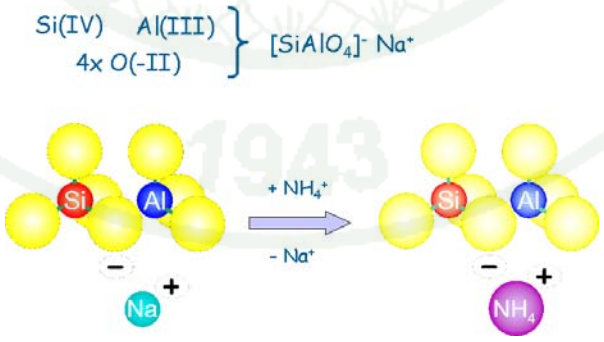

Figure 6 The presence of Al in the framework induces a negative charge that is balanced by an extraframework cation.

Source: Anonymous (2010)

Zeolite can be used as an ion-exchangers including for making softer water where Ca^{2+} and Mg^{2+} are removed from the water as shown in figure 7.

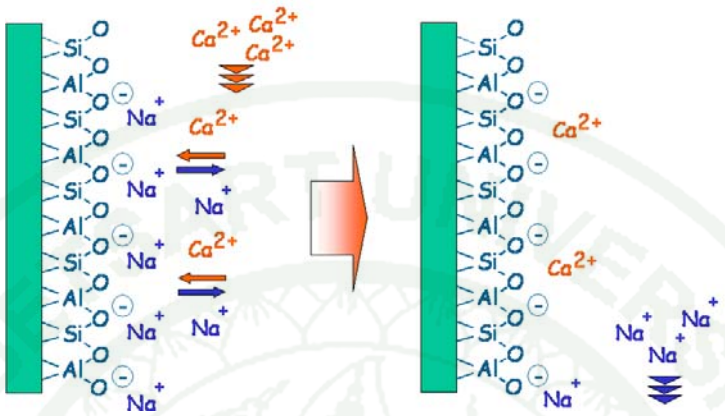

Figure 7 The diagram for making softer water by zeolite's ion-exchange.

Source: Anonymous (2010)

Zeolites have acidic properties. The protons which balance the negative charge of zeolite framework are not strongly bonded to the framework and are able to move within the pores and react with molecules which penetrate into the zeolite pore system. A protonated zeolite thus can act as a Bronsted acid. Furthermore, Lewis acidity can be caused by cations within the pores.

The pore sizes of zeolites are determined by their structures and may be varied slightly by ion-exchanging the zeolite, as shown in figure 9. The small cations can be positioned within the cage of zeolite structure. Specific cations may also be positioned on other sites than in the cages, whereas leading to even large open windows. The window sizes determine the accessibility of the zeolite pore system for other (e.g. organic) molecules

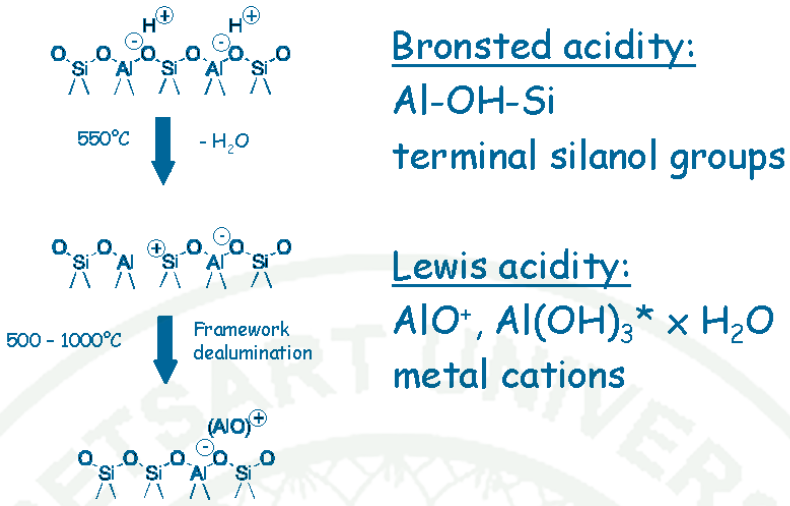

Figure 8 Bronsted acidity and Lewis acidity of zeolites

Source: Anonymous (2010)

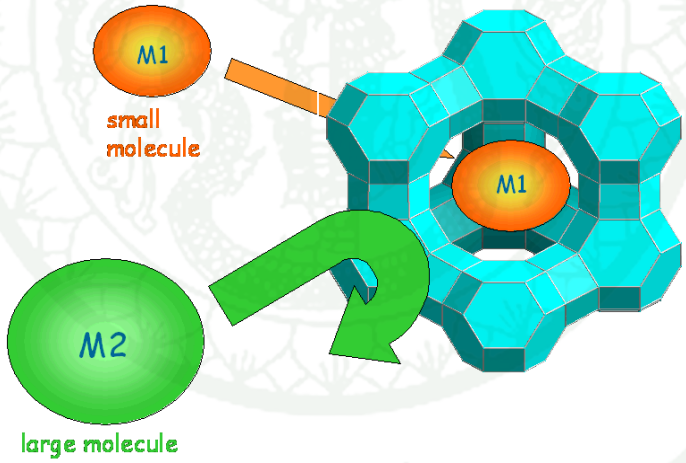

Figure 9 Molecular sieve effect of zeolites

Source: Anonymous (2010)

Van der waal and van bek kum (1998) reported that the high expectations of zeolite as selective catalysts for fine chemicals, arise from the uniform, molecular size and distribution of its micropores. This allows more selective reaction paths, due to

the restricted spatial confinement of the reaction site. In principle four different types of selectivity can be distinguished:

(i) Equilibrium Shift Selectivity.

The term equilibrium shift shape selectivity is used to describe the application of zeolite as adsorbent of one of the products molecules formed in an equilibrium reaction that is not used as a catalyst but rather as a non-reactive shape selective adsorbent.

(ii) Pore Size Shape Selectivity.

Also referred to as "reactant selectivity" that is mainly used in the catalytic upgrading of oil feedstocks as shown in figure 11.

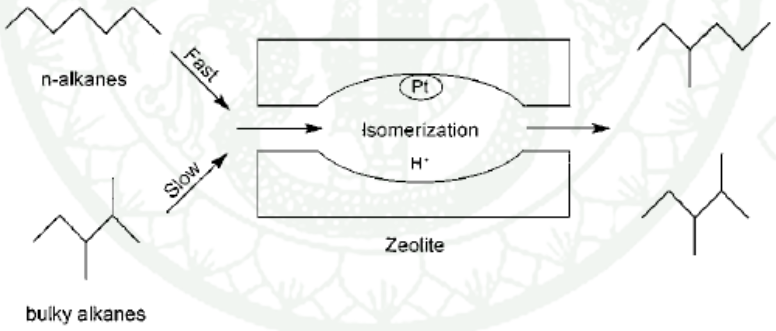

Figure 10 Pore size exclusion shape selectivity in the upgrading of oil feedstocks

(iii) Product Shape Selectivity.

The product shape selectivity shows in figure 1 as a good example for understanding.

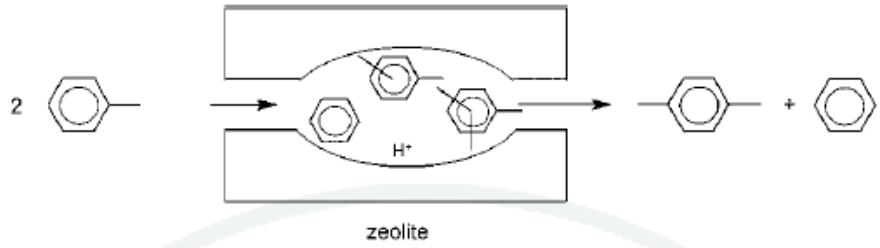

Figure 11 Product shape selectivity in the methylation of toluene over zeolite H-ZSM-5.

(iv) Transition-State Shape Selectivity.

This occurs when the spatial demands around the transition states to different products differ such that only certain, most preferably only one, reaction path is possible.

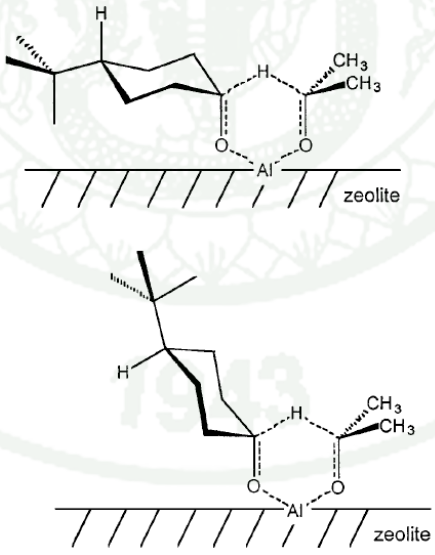

Figure 12 Transition states for the formation of *cis*-4-*tert*-butylcyclohexanol (top) and *trans*-4-*tert*-butylcyclohexanol (bottom) in the Meerwein-Ponndorf-Verley reduction of 4-*tert*-butylcyclohexanone using zeolite aluminum beta.

Classification of zeolites

In all, there are over 130 different framework structures are known. Zeolite is classified by the number of T-atoms in the pore openings of a cage window or channel wall. The small pore zeolites have 8-membered rings (about 0.45 nm); The medium pore zeolite have 10 membered rings (about 0.55 nm) and the large pore materials have at least 12T-atom in the ring (over 0.7 nm) (Van der waal and van bek kum, 1998)

Figure 13 Shows an overview of the pore sizes of commonly applied/used zeolite. Table 2 and table 3 show pore geometry of zeolites and trends in the properties of zeolite as a function of the Si/Al ratio.

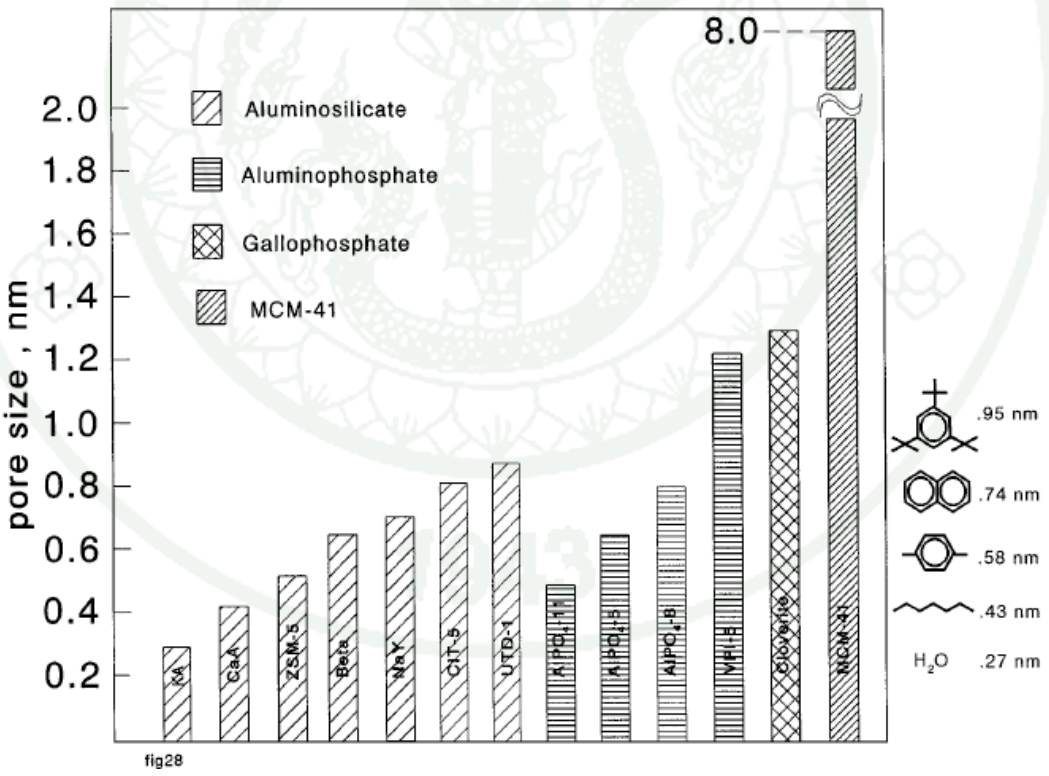

Figure 13 Pore sizes of zeolite

Source: Van der wall and van bec kum (1998)

Table 2 Pore geometry of zeolite

Pore geometry	Dimension	Molecular structure	Structure	Type
Channels	One dimensional	1 Straight	Parallel	LTL, UTD-1, TON, CIT-5
		2 Straight	Parallel	MOR
	Two dimensional	1 Straight, 1 sinusoidal	Perpened.	MFI
		2 Straight	Perpened.	MEL, P
	Three dimensional	1 Straight, 1 sinusoidal	Perpened.	BEA
			Tetrahedral	FAU (X, Y)
Cages + windows	Three dimensional		Cubic	LTA

Source: Van der wall and van bek kum (1998)

Table 3 Trends in the properties of zeolites as a function of the si/al ratio

Zeolite type	A	X	Y	MOR	MFI	Silicalite-1
Si/Al (minimum)	1	1	2.5	5	10	∞
	←		Number of cations		—	
	—		Stability vs. acidic solutions		→	
	—		Acid strength zeolite proton		→	
	—		Thermal stability		→	
	←		Hydrophilic character		—	
	—		Hydrophobic character		→	
	←		Affinity for polar molecules		—	
	—		Affinity for apolar molecules		→	

Source: Van der wall and van bek kum (1998)

To conclude, classification of zeolite depends on the pores and the framework structure which can be A, X, Y, L, and *etc.*,Type.

Zeolite A

Zeolite A is one kind of all zeolites which contains a small-pore in which the Si:Al ratio is 1 and the cages are linked octahedrically. The pore diameter varies from about 3 to 5 Å. Figure 14 shown structure and frame structure of zeolite A.

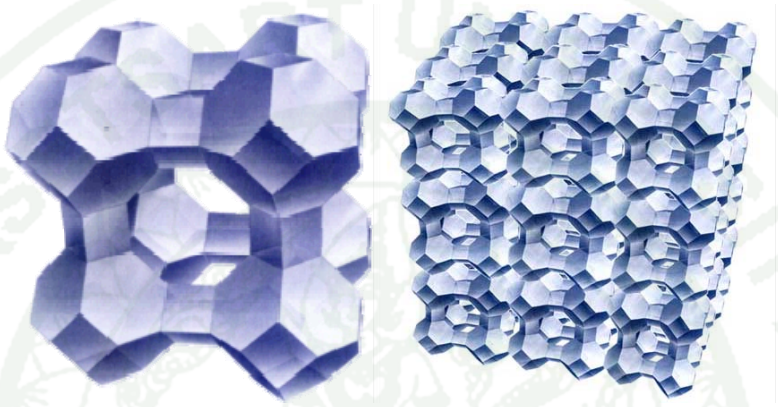

Figure 14 Structure and frame structure of zeolite A

Source: Anonymous (2012)

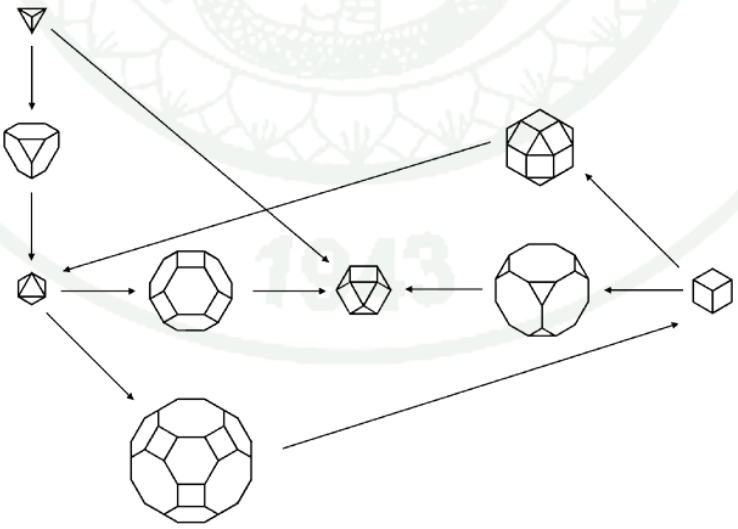

Figure 15 The octahedron structure

Source: Anonymous (2012)

Sol-Gel Processing

Sol-gel processing has attracted much interest both for the preparation of special powders and for forming thin coatings and cast or extruded shapes (James, 1989)

Methods in which a solution of metal compounds are converted into a solid body are sometimes referred to as liquid precursor methods. The sol-gel process is a liquid precursor solution that has attracted interest since the mid-1970s (Rahaman, 1995). The term sol-gel is used broadly to describe several processes in areas of chemistry and the chemical synthesis of inorganic materials such as ceramics and glasses. In the sol-gel process, a solution of metal compounds or a suspension of very fine particle in a liquid referred to sol. On the other hand, a sol is a suspension of colloidal particles in a liquid or a solution of polymer molecules. When sol is converted into a semi rigid mass referred to as gel. Gel is formed by linking colloidal particles with surface forces to form a network or when the polymer molecules are cross-linked or interlinked.

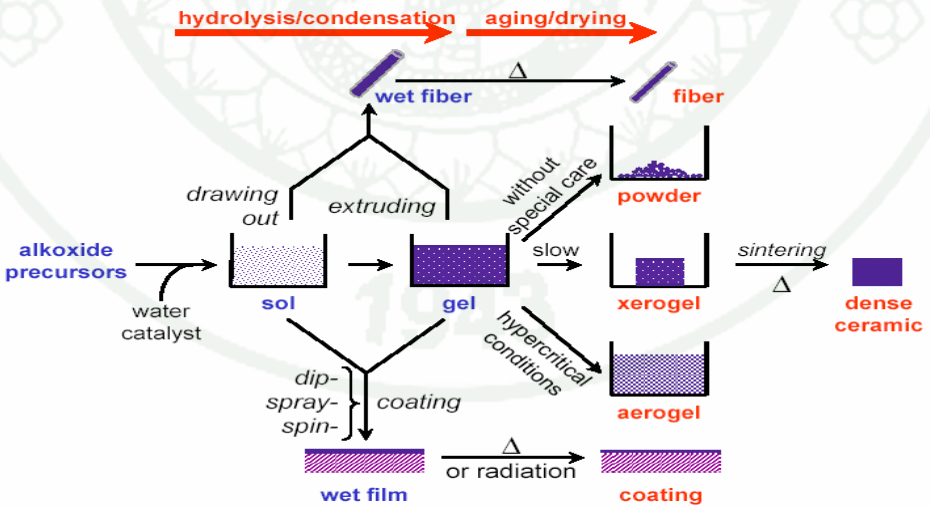

Figure 16 Basic flow charts for sol-gel processing using a solution and a suspension of fine particles.

Source: Khongnakhom and Kittikul (2009)

Sol-gel processes can be distinguished two different ways, depending on whether a sol or a solution is used. The simple flow chart of processing steps is shown in figure 16.

Type of Gels

To distinguish by sol-gel routes, type of gels are very important for the structure of ceramics fabrication, so considering the practical as well as the fundamental distinction between colloidal gels and polymeric gels are needed.

Colloidal gels consist of a skeletal network of essentially anhydrous particles held together by surface forces but polymeric gels are prepared by chemical reaction involving the hydrolysis, condensation, and polymerization of metal alkoxides in solution. The gels are formed by the entanglement and cross-linking of the growing polymer chains. The polymeric gel route has seen considerable use during the last 15-20 years for fabrication of ceramics and glasses. The use of liquid starting materials such as a solution of metal alkoxides provides distinct advantages for the preparation of pure, chemical homogeneous materials. Table 4 compares advantages and disadvantages of the polymer gel route.

Metal alkoxide (Metal-Organic compounds)

Metal alkoxide are especially used in sol-gel processing. Sometimes, it is also referred to as metal-organic compounds. An organometallic has a metal-carbon(M-C) bond where as a metal-organic need not have M and C directly bonded. Metal alkoxides have the general formula $M(OR)_z$, where M is a metal of valence z and R is an alkyl group. It also can be considered as either a derivative of an alcohol, ROH or in which R is replaced by a metal to $M(OH)_x$ (Rahaman, 1995).

Table 4 Advantages and Disadvantages of the Polymeric Gel Route Compared with Conventional Fabrication Methods of Ceramics and Glasses

Advantages	Disadvantages
1. High purity	1. Expensive raw materials
2. High chemical homogeneity with multicomponent systems	2. Large shrinkage during fabrication
3. Low temperature of preparation	3. Drying step leads to long fabrication times
4. Preparation of ceramics and glasses with novel compositions	4. Limited to the fabrication of small articles
5. Ease of fabrication for special products such as films and fibers	5. Special handling of law materials usually required

Source: Rahaman (1995)

The sol-gel process for metal alkoxides

The sol-gel process can be divided into three stages:

(i) Gel formation by hydrolysis and condensation reaction

Taking the example of a tetravalent metal, the reaction may be expressed as follows.

Hydrolysis:

$$M(OR)_4 + H_2O \rightarrow M(OR)_3OH + ROH \qquad (1)$$

Condensation:

$$M(OR)_3OH + M(OR)_4 \rightarrow (RO)_3\text{-M-O-M-}(OR)_2 + ROH \qquad (2)$$

(polymer)

Gel formation by hydrolysis and condensation reactions were polymerized with interlinking and cross-linking of the polymer chains which eventually leads to an increased viscosity of the reaction mixture and thus became the gel product with aging of polymeric gels (Rahaman, 1995).

(ii) The gel must be dried to remove the liquid prior to conversion to the final article. The simplest method is conventional drying which removes the liquid by evaporation in air or in an oven. However, drying must be carried out slowly and under carefully controlled conditions. Another way, the gel may be dried is by removal of the liquid under supercritical condition in order to gel highly porous. In this stages may be referred to as alcogel, hydrogel, xerogel or aquagel and aerogel. For more understanding, the meanings were referred as follows.

- Alcogel is an excess volume of alcohol that is used as a common solvent in the preparation of the gel.

- Hydrogel is colloidal gels that consist of a particulate network in which the pores are filled with an aquesous liquid.

- Xerogel is the gel produced by conventional drying.

- Aerogel is the gel produced by supercritical drying.

Moreover, Drying involves the interaction of three independent processes: (i) evaporation, (ii) shrinkage, and (iii) fluid flow in pores. These processes are ever complex process.

For ceramic drying, a function of the moisture content is defined in two ways, called the dry basis and the wet basis. However, the dry basis is commonly used (Rahaman, 1995).

Moisture Content (Dry Basis) = (Wet Mass – Dry Mass)/Dry Mass

Moisture Content (Wet Basis) = (Wet Mass – Dry Mass)/Wet Mass

(iii) Conversion of the dried gel into the final product by firing. The gel formed by hydrolysis, condensation, and gelation of the initial solution is dried and ground to produce a powder. However, dried gels with lower strength and easier to grind, and the extent of contamination introduced during grinding is lower. For powders produced from dried gels, the benefits in sintering are due to the amorphous structure and high surface area. After gel is already dried and calcined then ground to produce a powder.

Binder

A binder is a general term of the resinous ingredient that holds together a material composite. This may be the continuous phase and also could be the continuous resin phase in a molding compound or adhesive formulation (Charles and edward, 2003). Besides, the binder meaning can be referred to the word base which is the resin base in polymeric formulation.

Although the above meaning is used in polymer term. Similarly, binder is also used in ceramic processing. For binder meaning in ceramics, binder is polymer molecules and coagulation colloidal particles that are adsorbed and bridged between ceramic particles. However, these binder may be used as additives to provide several different practical functions in ceramic processing such as a wetting agent, or increasing viscosity. In more condensed systems such as granules for pressing, extrusion bodies, cast bodies, and unfired ceramic coatings (James,1989)

Binder compositions

Today, binders are used in processing a wide variety of tradition ceramics and more advanced ceramic systems. Two types of binder materials are colloidal particle

type and molecular type which each type can be separated into organic and inorganic as shown in table 5.

Table 5 Binder materials

Colloidal Particle Type			
Organic Microcrystalline Cellulose		Inorganic KaolinBall, clay, Bentonite	
Molecular Type			
Organic	Examples	Inorganic	Example
Natural gums	Xanthan gum, Gum arabic	Soluble silicates	Sodium silicate
Polysaccharides	Refined starch, dextrine	Organic silicates	Ethyl silicate
Lignin extracts	Paper waste liquor	Soluble phosphates	Alkali phosphates
Refined alginate	Na, NH_4 alginate	Soluble aluminates	Sodium aluminate
Cellulose ethers	Methyl cellulose, hydroxyethyl cellulose, sodium carboxymethyl cellulose		
Polymerized alcohols	Polyvinyl alcohol		
Polymerized butyral	Polyvinyl butyral		
Acrylic resins	Polymethyl methacrylate		
Glycols	Polyethyleneglycol		
Waxed	Paraffin, wax emulsions, microcrystalline wax		

Source: James (1989)

For more expanding, the refined natural materials are more expensive than clay binders but less expensive than the refined and synthetic organic polymers. Organic molecular binders may be introduced as aqueous or non-aqueous solution, liquid emulsions, or liquid melts. Common binders such as polyvinyl alcohol and the cellulose types are purchased as a powder and must be dissolved in water before admixing (James, 1989).

Molecular binders

In this research interested in molecular binders, especially cellulose ethers. Molecular binders are low-to high-molecular polymer molecules that adsorb on the surfaces of particles and bridge them together. The functionality of the polymer Molecule may be nonionic, anionic, or cationic. Most of the polymer binder used in ceramic processing are nonionic or mildly anionic (James, 1989)

Carboxymethyl cellulose

Carboxymethyl cellulose (CMC) or cellulose gum (Anonymous, 2012) is a cellulose derivative with carboxymethyl groups (-CH_2-COOH) bonded to some of the hydroxyl groups of the glucopyranose monomers that make up the cellulose backbone. The other names are carmellose, E466 that is often used as its sodium salts, sodium carboxymethyl cellulose. The figture 17 shows CMC structure unit which is a derivative of cellulose formed by its reaction with alkali and chloroacetic acid. Most CMCs dissolve rapidly in cold water and are mainly used for controlling viscosity without gelling. Some CMCs do not dissolve well in cold water but do dissolve well in hot water, this depends on functionality (Martin, 2011).

For CMC's application, CMC is used in food science, food additives as a viscosity modifier or thickener, and to stabilize emulsions in various products. As a food additive, it has E number E466 and non-food products have a k-y number which is used in toothpaste, detergent, textile sizing, various paper products, and pharmaceuticals as a thickening agent. The important advantages of CMCs are high viscosity and being non-toxic so many products have CMC's constituents including in this research, CMCs were used as a binder for making granules.

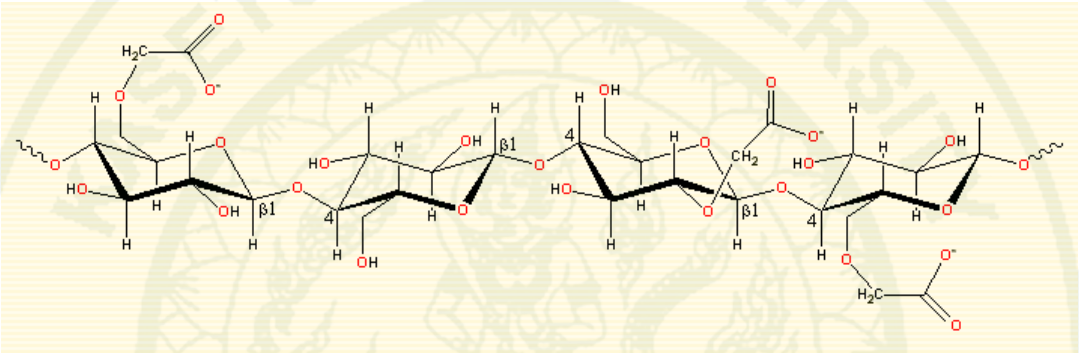

Figture 17 Carboxymethylcellulose (CMC) structure unit.

Source: Martin (2011)

Granules

The term granules refer to large agglomerates (≈100-1000 μm in size) that are deliberately formed by the addition of a granulating agent (e.g., a polymer-based binder) to the powder, followed by tumbling or spray drying. These large, nearly spherical agglomerates improve the flow ability of the powder during filling and compaction in complex molds. The approximate size ranges of the various types of particles are summarized in table 6.

Granules can be produced by direct granulation and spray-drying for direct granulation. Powdered granules may be produced directly by compaction, extrusion, and spray granulation process. The catalyst supports can be produced in this way by fine powder premixed with a percentage a wetting liquid or a binder solution then compacted in a tableting die or between briquetting rolls or belts. The granules were compacted at about 10 MPa making dense, hard and strong. Spray-drying is the process of spraying a slurry into a warm drying medium to produce nearly spherical powder granules that are relatively homogeneous, a lot of materials are widely used for preparing granules such as powders of ferrites, titanates, other electrical ceramic compositions, alumina, carbides nitrides, and porcelain bodies. This process need the use of a spray-dryer for production which is quite expensive. Thus, we have designed an easier way to produce zeolite granules without the use of a machine yet still get granules as shown in the method in this report (James, 1989).

Table 6 Size range for particles in ceramic processing

Type of particle	Size range
Powder	
Colloidal particle	1 nm to 1μm
Coarse particle	1-100 μm
Granule	100μm to 1 mm
Aggregate	>1 mm

Source: Rahaman (1995)

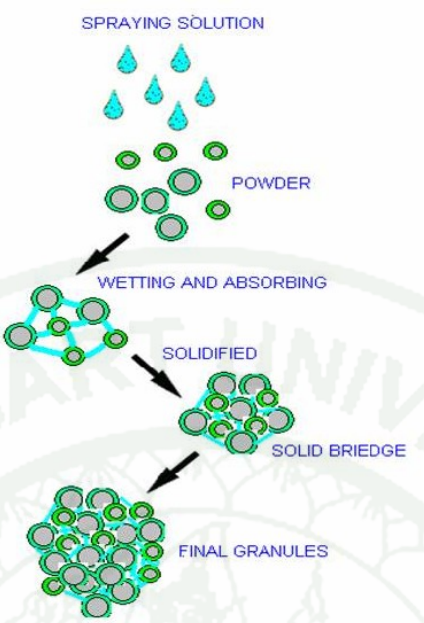

Figure 18 Granulation process

Source: Anonymous (2012)

Plastic Foams

Foams or plastic foams are materials which are popular because they are light weight, easy moving and have a wide range of uses for example, foam for packaging in food, other packaging, cold and hot insulators, yoga mat, using in arts.,*etc*.

Foam or plastic foams are cellular materials that occur from blowing agent that work to decrease the density of a plastic foam such as Pentane, Methylene Chloride. Foams can separate to be rigid foam, semi rigid foam and flexible foam. Normally, rigid foam is closed cell so their applications are in making furniture and \ industrial use, but flexible foam is open cell, so when compressed the air can escape and when force is released the foam will return to its original form. This applies to things such as cushions. Generally, foams have a cell size of about 0.05-1.00 mm but sometimes have more than a 1 mm cell size such as thermoset modified PVC foams (Hanwatanakul, 2007)

To consider what the type of foam is, we can classify by using compressive strength at 10% deformation with DIN 53421 or ISO 844 standard testing. If it is rigid foam, the compressive strength should be more than 0.08 MPa. For semi rigid foam it should be 0.015 to 0.08 MPa and flexible foam should be less than 0.015 MPa (Hanwatanakul, 2007)

Type of Foams

The foam can be classified according to the 2 types as follows:

- Thermoset foam is the plastic foam that cannot be recycled such as polyurethane foam (PU foam), *etc.*

- Thermoplastic foam is recyclable plastic foam such as polystyrene foams (PS foam), polyethylene foams (PE foams), *ect.*

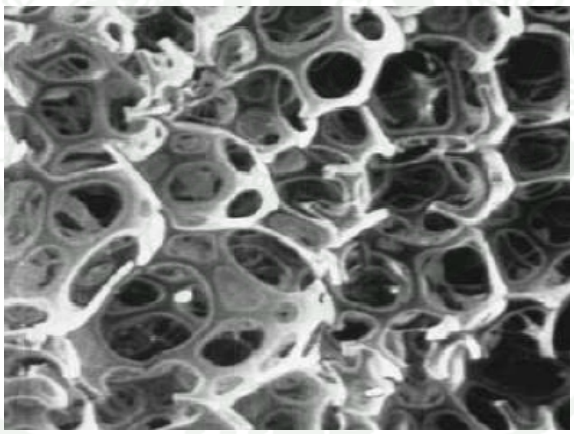

Figure 19 Open cell of flexible polyurethane foam.

Source: Hanwatanakul (2007)

Polyurethane (PU)

Polyurethane (PU) are linear polymers that have a molecular backbone containing a carbamate group (-$NHCO_2$). These groups, called urethane, consist of polymers derived from the reaction between isocyanates and polyols.

History of Polyurethane (PU)

For history of polyurethane, PU chemistry was first studies by the German chemist, Friedrich Bayer in 1937 (Perry, 2011). He produced early prototypes by reacting toluene diisocyanate with dihydric alcohols. From this work one of the first crystalline PU fibers, Perlon U, was developed. The devilment of elastic polyurethanes began as a program to find a replacement for rubber during the days of World War II. In 1940, the first PU elastomers were produced. These compounds gave malleable gums that could be used as an adequate alternative to rubber. When scientists found that PU could be made into fine threads, they were combined to make more lightweight, stretchable garments. In 1953, the first commercial production of a flexible PU foam was began in the United States. This material was useful for foam insulation. In 1956, more flexible, less expensive foams were introduced. During the late 1950s, moldable PU was produced. Over the years, improved polyurethane polymers have been developed including spandex fiber, PU coatings, and thermoplastic elastomers.

Advantages to Polyurethane (PU)

PU is a unique material that offers the elasticity of rubber combined with the toughness and durability of metal (Perry, 2011). It can be produced in four different forms including elastomer, coating, flexible foam, and cross-linked foam. Elastomers are materials that can be stretched but will eventually return to their original shape. Their application for use requires strength, flexibility, abrasion resistance, and shock absorbing qualities. For thermoplastic polyurethane elastomers can be molded and shaped into different parts like materials for automobile parts, ski boots, roller skate

wheels, cable jackets, and other mechanical goods. In this research, a researcher interested in flexible polyurethane foam with opened cell structure with the ultimate in abrasion resistance and physical properties. There properties can be used as the templates to produced catalyst foam.

Polyurethane has many advantages, these include (Anonymous, 2012);

- Abrasion resistant

Parts made of PU will often outwear other materials by a margin of 5 to 50/one when severe abrasion is a factor. It has been proven to be vastly superior to rubber plastic and metal in many applications. Oil and solvent resistant, PU has excellent resistance to oils, solvents, fats, greases and gasoline.

- Load bearing capacity

PU has higher load-bearing capacity than any conventional rubber. Due to this characteristic, it is an ideal materials for load wheels, heavy duty couplings, metal-forming pads, shock pads, expansion joints and machine mounts.

- Tear resistant

Tear-strength ranges between 500-100 Ibs./linear inch, which is far superior to rubbers. As a result, urethane is often used as drive belts, diaphragms, roll covers, cutting pads, gaskets and chute liners.

- Weather resistant

PU has outstanding resistance to oxygen, ozone, sunlight and general weather conditions.

- Excellent noise abatement properties

The hard urethanes are now being used as gears in products where engineers desire sound reduction. The soft urethanes are used to replace rubbers for improved sound/vibration dampening.

- Flex-Life

Most formulations offer extremely high flex-life and can be expected to outlast other elastomer materials where this feature is an important requirement. Dust boots, bellows, diaphragms, belts, couplings and similar products are made from urethane for this reason.

- Electrical properties

PU has excellent electrical insulating properties and is used successfully in many molded wire and cable harness assemblies.

- Heat and cold resistant

Continuous use above 225°F is not recommended nor is urethane recommended in hot water over 175°F. At low temperature, PU will remain flexible down to -90°F. A gradual stiffening will occur at 0°F, but will not become pronounced until much lower temperatures are obtained.

Raw Materials to Produce Polyurethane (PU)

A variety of raw materials are used to produce polyurethanes. These include monomers, polymers, and stabilizers which protects the integrity of the polymer and colorants.

One of the key reactive materials required to produce polyurethanes are diisocyanate and the other reacting materials are compounds that contain multiple alcohol groups (OH), called polyols. There are many kinds of polymers that have isocyanate (NCO) groups which can be used for production of polyurethane, examples include toluene diisocyanate (TDI), polymeric isocyanate (PMDI), *etc.*

For polyols materials often used for this purpose are polyester polyols which are polymers formed from cyclic ethers. Various polyether polyols that are used include polyethylene glycol, polypropylene glycol, and polytetramethylene glycol. These materials are generally utilized when the desired polyurethane is going to be used to make flexible foams or thermoset elastomers.

Some polyurethanes are needed to avoid damage from heat, light, atmospheric contaminants, and chlorine. Many additives are added to protect the polymer such as one type of stabilizer that protects against light degradation, a UV screener called hydroxybenzotriazole. Antioxidant compounds which inhibit discoloration and for certain applications may also be added.

Synthesis of polyurethane

Synthesis polymers, like polyurethane, are produced by reacting monomers in a reaction vessel. In order to produce polyurethanes, a step known as condensation-reaction is performed. In this type of chemical reaction, the monomers contain reacting end groups namely a diisocyanate (OCN-R-NCO) react to a diol (HO-R-OH).

The first step of this reaction results in the chemical linking of the two molecules leaving a reactive alcohol (OH) on one side and a reactive isocyanate (NCO) on the other. These groups react further with other monomers to form a larger, longer molecule. This is a rapid process which yields high molecular weight materials even at room temperature. Polyurethane are important commercial uses typically containning other functional groups in the molecule including esters, ethers, amides, or urea groups (Perry, 2011).

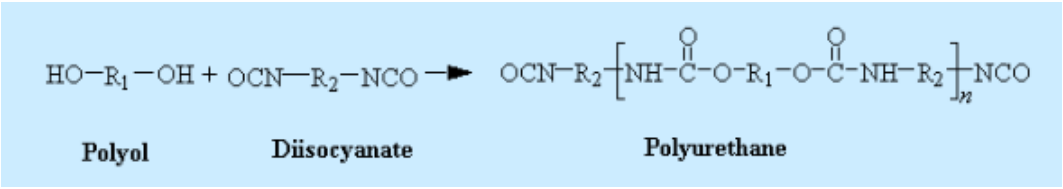

Figure 20 Reaction between diisocyanate with polyol

Source: Anonymous (2012)

The Figure 21 and Figure 22 shows reactions of polyurethane between composition of hydroxyl groups with diisocyanate. Normally using R group of longer HO-R-OH to produce flexible polyurethane.

When TDI reacted with polyol which is a exothermal reaction to produce polyurethane as shown in Figure 23

Figure 21 Reaction between Toluene diisocyanate with polyol

Source: Hanwatanakul (2007)

Figure 22 Nucleophilic addition of R-OH across C=N

Source: Hanwatanakul (2007)

To decrease exothermal, high molecule polyols or prepolymer isocyanate that occur from the reaction between polyol and diisocyanate were used by reaction with some parts of polyols to work at medium to high viscosity of polymers so the isocyanate groups will be at the end of the polymer chain. Polyols are the constituent part of several hydroxyl that can be used to produce foam by crosslinking polymer chains.

Foam was produced from carbondioxide (CO_2) which occurred by a reaction between isocyanate and water (H_2O). Carbondioxide causes gel to bubble and become foam. The complete reaction needed to use surfactants to create small open cells and used methylchloride like a blowing agent.

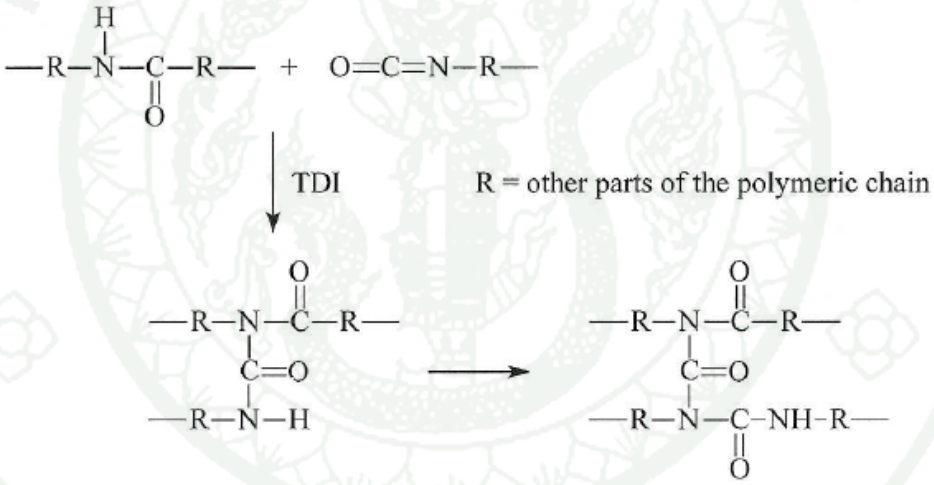

Figure 23 Nucleophilic addition of R-OH across C=N

Source: Hanwatanakul (2007)

Chemicals needed to produce polyurethane

- Catalyst agent

The most proper and popular catalyst agent is tertiary amines and organic tin compounds.

- Surfactants

The most popular surfactant is liquid silicone help to produce foam by adding approximately 0.2-2.0% to obtain gel homogeneous open cells.

- Flame Retardants

Flame retardants are necessary agents to add to polyurethane foam because foam s are easily combustible because the foam structure has a large surface area, this result makes foam rapidly burn out. Retardants which have phosphorous (P), boron (B), antimony (Sb) are added to polyurethane foam.

- Blowing agent

Fluorocarbon 11 and 12 were used as a blowing agent to produce rigid polyurethane foam for use as an insulator with very low thermal conductivity.

Other literature reviews

Peng *et al*. (2000) expanded on the preparation of ceramic foam distribution in polyurethane. From their research, 20% v/v of ceramic was added into the polymer phase which consists of resin and an isocyanate component stirred at 2,000 rpm for 300 s in order to get an even distribution of the ceramics. After that the resin and the isocyanate component were mixed together by a stirrer at 2400 rpm for 20 s then poured into the cardboard so as to rise freely. This reaction takes about 24 h. As a result, the ceramic foam's open cells had a 150 μm pore size with homogeneous ceramic's dispersion and high degree of reliculation in polyurethane.

Watanabe *et al.* (2005) reported that Linde Type A Zeolite or LTA ($(x_{12/m})(Si_{12}Al_{12}O_{48})\bullet nH_2O$), x = cation, m = charge number, LTA) is the highest cation exchange capacity; CEC. LTAs have widely been used as ion exchangers for ammonium and cadmium. Furthermore, It can be used as an absorbent of radioactive

elements such as cesium, iodine, *etc*. For LTA preparation, 0.5g of Na-LTA was left in 1500 ml of 0.5 M $CaCl_2$ for 24 h to cause ion-exchange between Ca^{2+} and Na^{2+}. Next, the sample was filled by using 0.45 μm size of membrane filter then washed with liquor to eliminate excess ions. The obtained Ca-LTA was dried at 100°C for 24 h. From their conclusion, this research successful synthesized a nanocomposition between hydroxyapatite layers formed and zeolite by using ion-exchange reaction.

Chuapradit *et al.* (2005) investigated polyaniline/zeolite LTA composites and electrical conductivity response towards CO. They studied about types dopant, concentrations dopant, the amount of LTA zeolite, and pore size volume of zeolite which found that zeolite 4A had decreased electrical conductivity response with 40% w/w concentration whereas zeolite 4A and 5A was the best because of the larger pore size with 5Å (zeolite 3A= 4Å, zeolite 4A= 3Å). Normally, LTA zeolite were synthesized in the form of Na^+, $Na_{12}Al_{12}Si_{12}O_{48}27H_2O$ with three-dimension pore structure and 8 oxygen of pore diameter including to pore size 2.3-4.2 Å that depend on cation.

Narine *et al.* (2006) studied rigid polyurethane (PU) forms which were synthesized from canola oil, castor oil, and soybean. These plants have structural properties similar to polyurethane foams that can produce polyol. For the method, polyol was added of crosslink agent, catalyst, surfactant then stirred 2 min, after that was poured aromatic diphenyl metharo diisocynate (MDI) was stirred at 1500 rpm for 40 s in the case of canola oil and castor oil while soybean was stirred for 90 s. The foam samples were post cured at room temperature for 4 days to finish the reaction. The analysis reported that the soybean had several -OH, $-OCH_3$ groups which made low activity efficiency and not a complete reaction. Besides, the high amount of isocyanate has an effect as a catalyst killer that can be proven with a mechanical property experiment. The mechanical properties were tested by compressive properties according to ASTM D1620-00. All samples were prepared by cylindrical teflon molds with a diameter of 60 mm, and length of 36 mm. The condition testing is 3.54 mm/min of cross-head speed, 500 kgf of load cell until the foam thickness at 15% of the previous thickness, and 10% deformation. In addition, the thermal

property was studied by TGA and found that the decomposition temperature of polyurethane foam started at 200°C and when studied about pores diameter demonstrated 0.25 mm of canola-PU foams was invisible to the eye.

From our previous study eggshells were studied as a starting material to produce a hydroxyapatite compound. The eggshells were calcined at 300°C to 1000°C for 1, 3, 5, h optimum conditions were at 900°C for 1 h because of low electrical conductivity, spherical particle with good dispersion, high microporous, high surface area, distribution as well, and no remaining organic compounds.

Linde Type A Zeolite (LTA)-Goethite nanocomposite was synthesized by adding sodium orthosilicate to goethite followed by adding sodium aluminate and NaOH solution. At 100°C of the Goethite (œ-FeOOH) temperature is iron minerals and this is most of the components of the soil. The objective of this research is to synthesize nanocomposites from natural materials and use this way to synthesize according to international zeolite association's synthesis commission for each experiment. The obtained nanocomposite had a ratio of zeolite is (Kugbe *et al.,* 2008) $3.17Na_2O:Al_2O_3:1.93SiO_2128H_2O$.

Nuchnapa *et al.* (2010) successfully synthesized calcium zeolite type A ($CaNaAlSi_2O_7$) or soda melitite with a ratio of $CaO:Al_2O_3:Na_2O:SiO_2$ is 1:1:2:8. The conditions were calcined at 300°C for 1 h by using Sol-Gel process. The obtained samples had 0.51 pore volume, 37.19 nm pore diameter, 55.15 m^2/g specific surface .

MATERAIALS AND METHODS

Materials

1. Eggshells from a local cafeteria of faculty of engineering at kasetsart university

2. Hydrophilic fumed silica (SiO_2), 99.8% silica, The specific surface area is 206 m^2/g, The pH is 3.9, and particle size is 40 μm: WACKER Chemic, AG, Germany.

3. Precipitated sodium aluminosilicate, 82% silica, 10% alumina, 6% sodium oxide, 0.04% iron oxide: United Silica (Siam) Ltd., Thailand.

4. Sodium hydroxide pellets: Molecule Co., Ltd., Thailand, purity > 98.0% hydrochloric acid (analytical reagent, AR), Lab-Scan Co., Ltd., Thailand.

5. DALTOPED®FF45804 (Ethane-1-2-diol+Diethylene glycol, Density 1.1 g/cm^3 at 25°C) and SUPRASEC®2749 (pre-polymer, diisocyanate, density 1.2 g/cm^3 at 25°C) are starting-material to produce polyurethane foam, Huntsman (Thailand) Ltd.

6. CMC 1,000 (caboxy methyl cellulose), Amarin CERAMICS CORP., Ltd. UHU Gmbt & Co, KG, Germany.

Instruments

1. Mortar and Pestle
2. Porcelain Crucible
3. Volumetric Pipette 10 ml
4. Graduated Pipette 5 ml

5. Beaker 50 ml
6. Graduate Cylinder 10 ml
7. Volumetric Flask 500 ml, 1,000 ml
8. Font Dropper
9. Glass Rod
10. Spatular
11. Parafilm
12. Rubber Bulb
13. Rubber Gloves
14. Digital Weight Scale
15. High Temperature Furnace Linn High Therm 1,200°C (Linn High Therm, Germany)
16. Oven WTB binder, Germany 300°C
17. X-Ray Diffraction: XRD (Philip, PW 3040/00, Natherlands)
18. Scanning Electron Microscope: SEM (Philip, XL 30&EDX, Natherlands)
19. Fourier Transform Infrared Spectrometer: FT-IR (Perkin Elmer, Spectum one)
20. Simultaneous Thermal Analyzer: STA (Netzsch, 409)
21. Sieve 200 Mesh (75 Micron), 140 Mesh (106 Micron), 100 Mesh (150 Micron), 70 Mesh (212 Micron), 50 Mesh (300 Micron), Endecotts Ltd.,England.
22. Machaical stirrer (RW 16 basic IKALABORTECHNIN, Thailand)
23. Stopwatch
24. Transmission Electron Microscope: TEM (JEM-2100)
25. Brunauer-Emmet-Teller: BET (AUTOSORB-1 (QUANTA CHROME)/BET)
26. Filter papers, Qualitative Cricles 70Ø Cat No 1001 070, Whatman Internation

Ltd Maidstone England.

27. Universal Testing Machine: UTM (50 KN), Houns field, H50ks, England.
28. Oven, Espec, PH-110,USA.
29. Differential Thermal Analysis (DTA), Perkin Elener.

30. Themogravimetric Analyzer (TGA), Q50V6.7 Build 203.
31. Gas Pycnometer: GP (Quantachrome, Ultrapycnometer 1,000)

Methods

1. Preparation of calcium zeolite type A by sol-gel process

1.1 Calcium chloride solution preparation

Calcium oxide (CaO) was prepared from eggshells by the following steps; washed and dried at room temperature, crushed and calcined under atmospheric pressure at 900°C for 1 h (the percentage of ceramic yield of calcium oxide content in the product by STA was equal to 74.42) with a heating rate of 10°C/min, the 0.5 g of air cooled CaO was dissolved in 20 ml of 1 M HCl to obtain the $CaCl_2$solution.

1.2 Sodium aluminosilicate solution preparation

Sodium aluminosilicate solution was obtained by mixing 0.8 g of fumed silica powder (SiO_2), 5.0 g of precipitated sodium aluminosilicate and 1.0 g of sodium hydroxide (NaOH) with 20 ml distillated water.

1.3 Synthesis of cacium zeolite type A

The calcium zeolite type A ($CaNaAlSi_2O_7$) was obtained by pouring the mixture solution of 1.1 into the mixture solution of 2.2 stirred then left at room temperature for 24h, known as the sol-gel process (Nuchnapa *et al*., 2011). The gel sample was dried at 110°C for 24 h (gel_110) and calcined at 300°C for 1 h (gel_300) to obtain $CaNaAlSi_2O_7$ powder. The molar ratios of this synthesis of $CaO:Al_2O_3:Na_2O:SiO_2$ is 1:1:2:8.

2. Forming-designed of calcium sodium aluminosilicate or calcium zeolite type A ($CaNaAlSi_2O_7$)

2.1 Granulation

Granules were produced from calcium sodium alumino silicate which was dried and calcined at 110°C, 300°C (gel_110 and gel_300), respectively. Carboxy methyl cellulose (CMC) was used as binder to mix with calcium zeolite type A.

Figure 24 Granules packed into the column.

At first, adding 1 g CMC in water heat at 60-70°C, and let CMC melted. A melted solution of CMC was obtained then the 10 g powder of gel_110/gel_300 was added into the solution and stirred until solution and powder are homogeneous. Finally step, rounder-glide by using sieve passing size 200, 140, 100, 70 and 50 mesh for size separate granulation.

2.2 Granules coat on filter papers

The filter paper was coated granules by UHU latex as adhesive.

2.3 Compression by Uniaxial pressing

The gel_110 and gel_300 were pressed by uniaxial pressing to study theirs properties and structures.

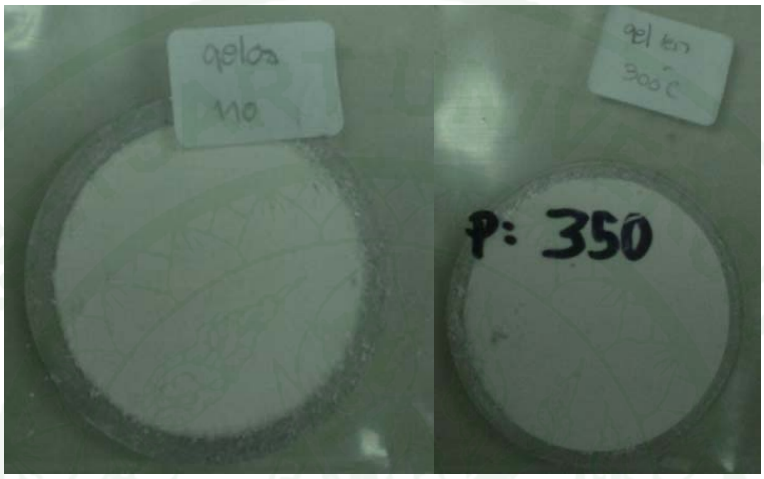

Figure 25 Uniaxial pressing of samples.

2.4 Polyurethane foam as template (Catalyst foam preparation)

Catalyst foam was prepared by using polyurethane foam (PU) as a template (DALTOPED®FF 45804 and SUPRASEC®2749 from Huntsman (Thailand). The FF45804 is polyols and the 2749 was used as pre-polymer with a ratio of 100:98w/w.

Figure 26 Pre-polymer and polyols for preparing polyurethane foam(PU)

The catalyst foam was prepared by stirring the FF45804 for 3 min at 1200 rpm then 10% w/w of gel_110/gel_300 was added to the FF 45804 mixture, after 1 min, the 2749 mixture was rapidly added and uniformly stirred until complete exothermic reaction, observed by heating to skin hand.

Figure 27 A foam composite sample

3. Characterization

There are many instruments and methods used in this research to characterize mechanical, physical and chemical properties such as SEM, FT-IR, DTA, TGA, TEM, STA, XRD, GP, BET, QUANTASORB-1,*etc.*

For mechanical properties characterization, pure PU foam and foam composite samples were tested under flexural loading condition to assess the flexural properties. The compressive strength and modulus parallel to the rising direction of foam samples were measured by a universal testing machine (QMat 5.44 M-series-10KN) according to ASTM D-695 compressive of rigid plastic[X Head] and ASTM D1621. The specimens had dimensions of 25.4×25.4×12.7 mm^2 and the crosshead speed of compression was set at 1.2 mm/min (Xia *et al*., 2005).

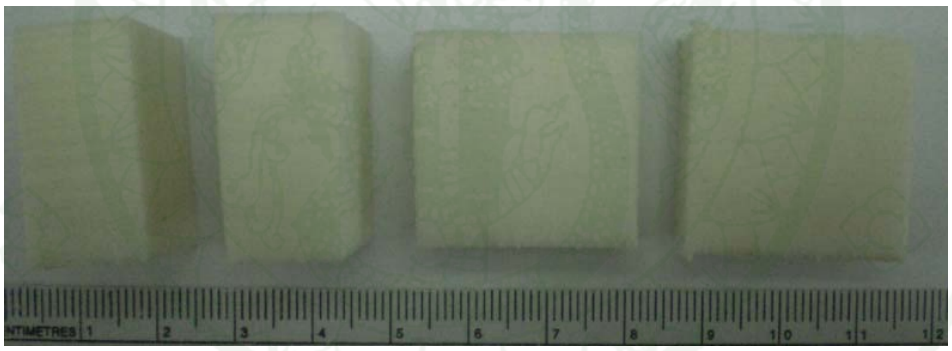

Figure 28 The specimen samples were measured by a universal testing machine size 25.4×25.4×12.7 mm^3

The thermal properties were measured by using a Simultaneous Thermal Analyzer (STA), Differential Thermal Analyzer (DTA) and Thermo Gravimetric Analyzer (TGA). The samples were tested with a heating rate 10°C/min under atmospheric pressure.

X-Ray Diffraction (XRD) was operated to determine the crystalline phase of samples. Samples were analyzed using double-crystal wide-angle goniometry. Scans were measured from 5 to 80°2θ, 25-35°2θ, with a step size of 0.03°2θ and preset time of 1s. The international center for Diffraction Data Standard (JCPDS) patterns was used to identify position of crystalline phases.

Microstructures were observed by using a Scanning Electron Microscope (SEM). In addition, Micrographs were obtained using a Transmission Electron Microscope (TEM, JEM-2100) equipped with EDS for x-ray microanalysis and NBD for nano beam diffraction. The TEM sample preparation was done on a grid to investigate the morphology and microstructure with an acceleration voltage of 80-200 KV, magnifications from 50 to 1.5 million times were used.

Functional groups were characterized by Fourier Transform Infrared Spectra (FT-IR) which recorded on a Perkin Elmer, model spectrum one spectrometer with a spectral resolution of 4 cm^{-1}, in the rang of 4,000-400 cm^{-1} and a number of scan of 64.The samples were measured by the single-crystal potassium bromide, KBr.

The specific surface area, adsorption and/or desorption isotherms, pore size and surface distributions were measured using an AUTOSORB-1 (QUANTACHROME) to measure the quantity of gas adsorbed onto or desorbed from the solid surface at some equilibrium vapor pressure by the static volumetric method.

Gas pycnometer (Quanta chrome, Ultrapycnometer 1000) was used measuring samples true density and surface area analyzer (Quantachrome, Autosorb-1) was used for characterization of Multipoint BET (m^2/g), Total pore volume(cc/g) and average pore diameter(Å) which measured samples were dispersed in a water medium and vibrated in an ultrasonic cleaner for 20 min.

RESULTS AND DISCUSSION

1. Characterized results

1.1 Simultaneous Thermal Analysis (STA)

Thermal property of eggshell was characterized by simultaneous thermal Analyzer (STA) with a heating rate 10°C/min under air atmosphere, as shown in figure 29. The differential thermal analysis (DTA) and the thermogravimetric curves TG/DTG of the raw eggshells show an endothermic reaction at highest peak of 924.7°C which approximately started from 800°C to 950°C and broad band peak at about 650°C, the first stage can be attributed to absorbed water molecules and loss of organic compounds, whereas carbon dioxide was lost between 700-800°C. The second stage exhibited a major weight loss at 924.7°C, corresponding to 46.40 wt% was due to the change of $CaCO_3$ phase to CaO phase which could be confirmed by the XRD and the FTIR results, as shown in figure 34 and 35.

Wei *et al.,* 2009 reported that natural eggshell had macropores and a generally irregular crystal structure. From their studied which indicated that the structure of eggshell changed with calcinations temperature. Below 700°C, the size and shape of particles were similar to that of natural eggshell. Above 800°C, the size of particles decreased and the particle shape became more regular and displayed diffraction reflections characteristic of CaO.

For this study, calcined temperature at 900°C for 1 h was used in order to make CaO as a starting material as previously reported (Nuchnapa, 2010) that the temperature 900°C for 1 h was then suitable for the use as the calcinations temperature to ensure complete conversion to CaO.

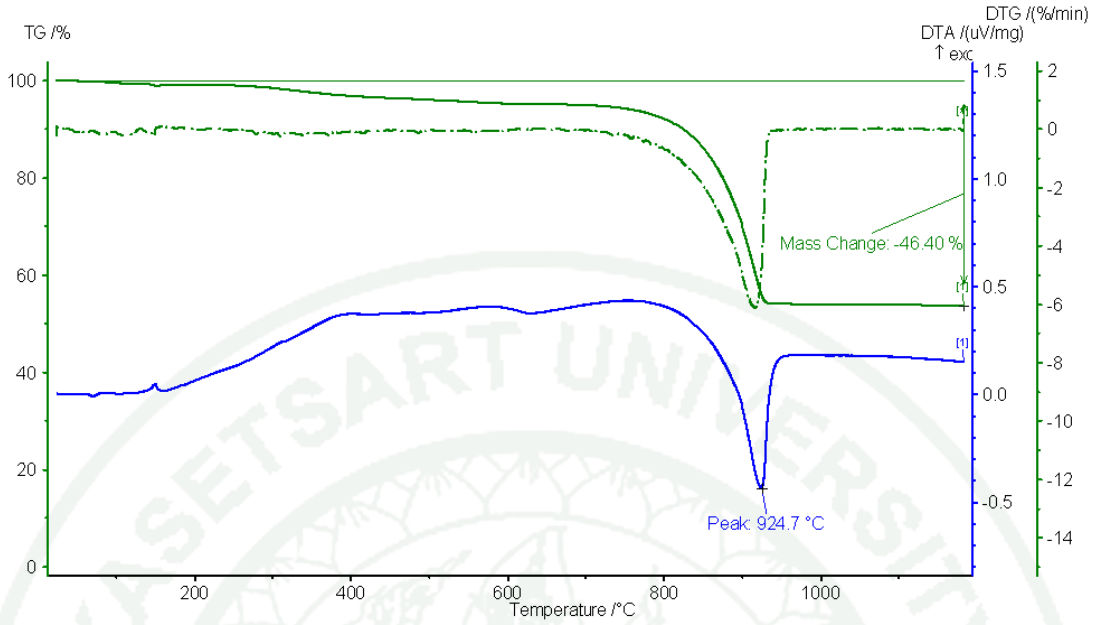

Figure 29 Simultaneous Thermal Analysis (STA) of eggshell

1.2 The percentage of volatile water testing

Table 7 The percentage of volatile water from wet $CaNaAlSi_2O_7$ gel dried at 110°C

No.	Wet weight(g)	Dry weight(g) Or gel_110	Volatile water(g)	%Volatile Water
1	87.461	20.429	67.032	76.680
2	87.176	15.687	71.489	82.010
3	88.555	20.299	68.256	77.010
4	39.687	9.360	30.327	76.415
5	73.232	15.231	58.001	79.220
6	70.414	19.963	50.451	71.650
7	35.756	8.013	27.743	77.590
		Avg.		77.235
		SD		3.138
		Ur, 95%		2.805

The percentage of volatile water from wet $CaNaAlSi_2O_7$ gel dried at 110°C for 24 h in the oven, as shown in table 7. Drying is an important process in producing raw material for ceramics and shaped products ready for firing or calcinations. During drying, heat is transported to the liquid in the body, and evaporated liquid is transported into the surrounding atmosphere. After initial heating, the product dries at a constant rate during which shrinkage commonly occurs (James, 1989) thus there is an average of 77.24% volatile water.

1.3 Particle size analyzer

Calcium sodium aluminosilicate or calcium zeolite type A ($CaNaAlSi_2O_7$) was synthesized by sol-gel process then dried at 110°C for 24 h (gel_110) then the dried gel calcined at 300°C for 1 h (gel_300) and characterized the particle size distribution as shown in figures 30 and 31. Both data show the same range of particle diameter from about 0.5-90 μm. In addition, gel_110 has approximately 65% of 10 μm particle diameter and gel_300 has about 60% of 10 μm particle diameter. This result presented that the calcined temperature at 300°C can change the $CaNaAlSi_2O_7$ particle because of more a little bit of agglomeration of particles leads to particle packing and increased density as supported by table 8 that is gel_300 has higher true density then gel_110.

1.4 Transmission Electron Microscope (TEM)

Figures 32 (a-c) and 33 (a-c) show the TEM micrographs of crushed-eggshell with different magnifications of (a) 50 k; (b) 30 k and (c) 12 k and The TEM's figure of calcined-eggshell at 900°C for 1 h with different magnification of (a) 50 k, (b) 30 k and (c) 12 k, respectively. From comparison, calcinations of eggshells had moderately good dispersion more than raw eggshells because of agglomeration of small particles.

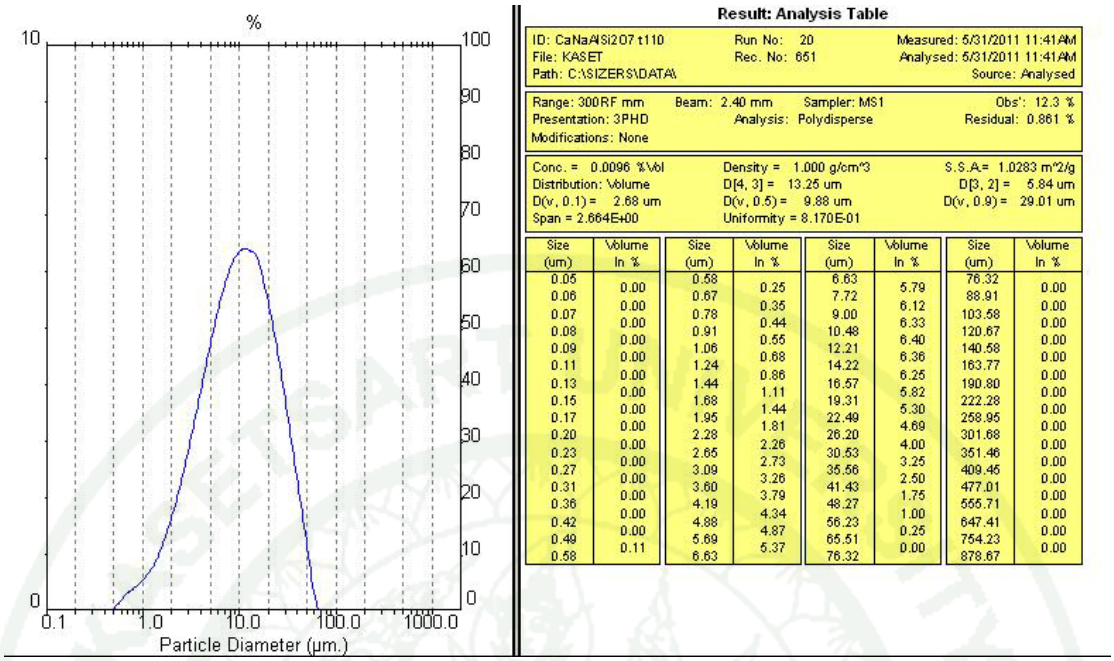

Result: Analysis Table

ID: CaNaAlSi2O7 t110 | Run No: 20 | Measured: 5/31/2011 11:41AM
File: KASET | Rec. No: 651 | Analysed: 5/31/2011 11:41AM
Path: C:\SIZERS\DATA\ | Source: Analysed

Range: 300RF mm | Beam: 2.40 mm | Sampler: MS1 | Obs': 12.3 %
Presentation: 3PHD | Analysis: Polydisperse | Residual: 0.861 %
Modifications: None

Conc. = 0.0096 %Vol | Density = 1.000 g/cm^3 | S.S.A.= 1.0283 m^2/g
Distribution: Volume | D[4, 3] = 13.25 um | D[3, 2] = 5.84 um
D(v, 0.1) = 2.68 um | D(v, 0.5) = 9.88 um | D(v, 0.9) = 29.01 um
Span = 2.664E+00 | Uniformity = 8.170E-01

Size (um)	Volume In %	Size (um)	Volume In %	Size (um)	Volume In %	Size (um)	Volume In %
0.05	0.00	0.58	0.25	6.63	5.79	76.32	0.00
0.06	0.00	0.67	0.35	7.72	6.12	88.91	0.00
0.07	0.00	0.78	0.44	9.00	6.33	103.58	0.00
0.08	0.00	0.91	0.55	10.48	6.40	120.67	0.00
0.09	0.00	1.06	0.68	12.21	6.36	140.58	0.00
0.11	0.00	1.24	0.86	14.22	6.25	163.77	0.00
0.13	0.00	1.44	1.11	16.57	5.82	190.80	0.00
0.15	0.00	1.68	1.44	19.31	5.30	222.28	0.00
0.17	0.00	1.95	1.81	22.49	4.69	258.95	0.00
0.20	0.00	2.28	2.26	26.20	4.00	301.68	0.00
0.23	0.00	2.65	2.73	30.53	3.25	351.46	0.00
0.27	0.00	3.09	3.26	35.56	2.50	409.45	0.00
0.31	0.00	3.60	3.79	41.43	1.75	477.01	0.00
0.36	0.00	4.19	4.34	48.27	1.00	555.71	0.00
0.42	0.00	4.88	4.87	56.23	0.25	647.41	0.00
0.49	0.00	5.69	5.37	65.51	0.00	754.23	0.00
0.58	0.11	6.63		76.32		878.67	0.00

Figure 30 Average particle diameter of gel_110

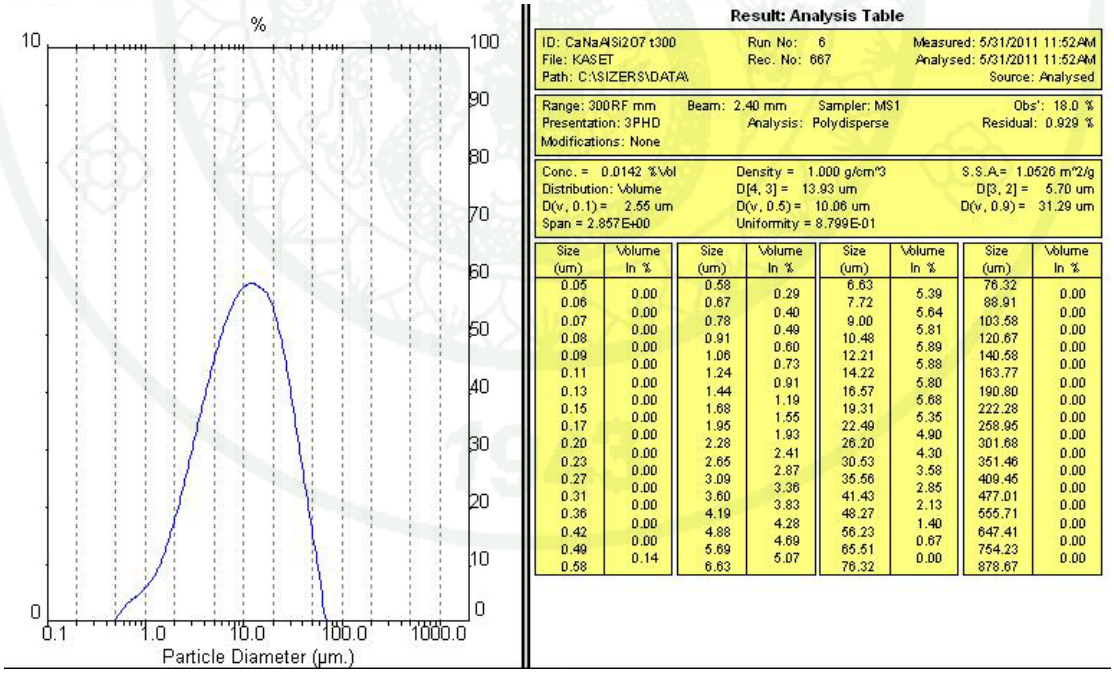

Result: Analysis Table

ID: CaNaAlSi2O7 t300 | Run No: 6 | Measured: 5/31/2011 11:52AM
File: KASET | Rec. No: 667 | Analysed: 5/31/2011 11:52AM
Path: C:\SIZERS\DATA\ | Source: Analysed

Range: 300RF mm | Beam: 2.40 mm | Sampler: MS1 | Obs': 18.0 %
Presentation: 3PHD | Analysis: Polydisperse | Residual: 0.929 %
Modifications: None

Conc. = 0.0142 %Vol | Density = 1.000 g/cm^3 | S.S.A.= 1.0526 m^2/g
Distribution: Volume | D[4, 3] = 13.93 um | D[3, 2] = 5.70 um
D(v, 0.1) = 2.55 um | D(v, 0.5) = 10.06 um | D(v, 0.9) = 31.29 um
Span = 2.857E+00 | Uniformity = 8.799E-01

Size (um)	Volume In %	Size (um)	Volume In %	Size (um)	Volume In %	Size (um)	Volume In %
0.05	0.00	0.58	0.29	6.63	5.39	76.32	0.00
0.06	0.00	0.67	0.40	7.72	5.64	88.91	0.00
0.07	0.00	0.78	0.49	9.00	5.81	103.58	0.00
0.08	0.00	0.91	0.60	10.48	5.89	120.67	0.00
0.09	0.00	1.06	0.73	12.21	5.88	140.58	0.00
0.11	0.00	1.24	0.91	14.22	5.80	163.77	0.00
0.13	0.00	1.44	1.19	16.57	5.68	190.80	0.00
0.15	0.00	1.68	1.55	19.31	5.35	222.28	0.00
0.17	0.00	1.95	1.93	22.49	4.90	258.95	0.00
0.20	0.00	2.28	2.41	26.20	4.30	301.68	0.00
0.23	0.00	2.65	2.87	30.53	3.58	351.46	0.00
0.27	0.00	3.09	3.36	35.56	2.85	409.45	0.00
0.31	0.00	3.60	3.83	41.43	2.13	477.01	0.00
0.36	0.00	4.19	4.28	48.27	1.40	555.71	0.00
0.42	0.00	4.88	4.69	56.23	0.67	647.41	0.00
0.49	0.00	5.69	5.07	65.51	0.00	754.23	0.00
0.58	0.14	6.63		76.32		878.67	0.00

Figure 31 Average particle diameter of gel_300

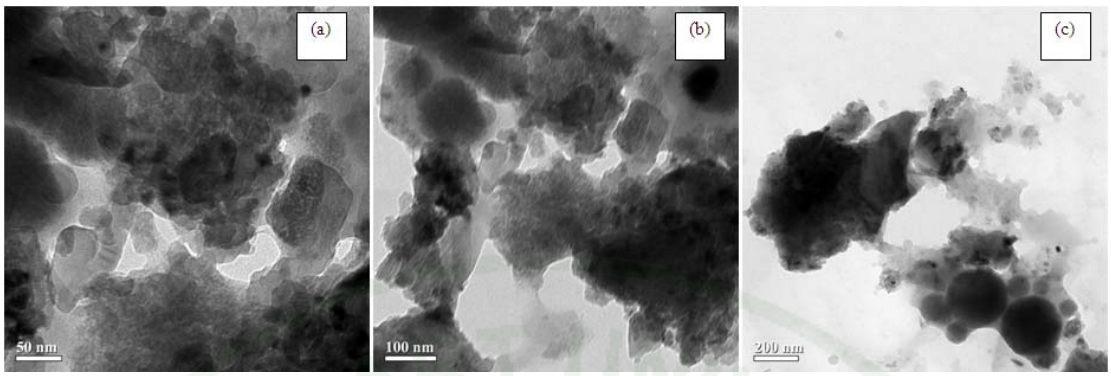

Figure 32 The TEM micrographs of crushed-eggshell with different magnifications of (a) 50 k, (b) 30 k and (c) 12 k

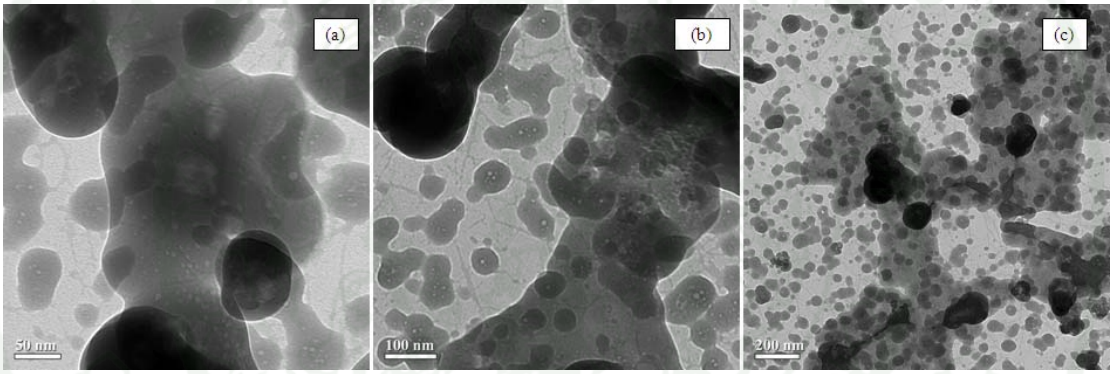

Figure 33 The TEM's figure of calcined-eggshell at 900°C for 1 h with different magnifications of (a) 50 k, (b) 30 k and (c) 12 k

1.5 X-Ray Diffraction (XRD)

The XRD peak pattern of eggshell is shown in Figure 34 (a) with the number of 01-085-1108 according to the International Center for Diffraction Data (JCPDS) of 2θ and (hkl) values equal to 29.466 (104), 36.039 (110), 39.489 (113), 43.244 (2302), 47.685 (018), 48.615 (116) and 48.615 (122) indicating the rhombohedral formation of calcium carbonate ($CaCO_3$). The Figure 34 (b) shows a peak pattern of CaO, number 00-037-1497 with 2θ and (hkl) are equal to 32.604 (111), 37.347 (200), 53.856 (220), 64.154 (311), 67.375 (222) and 79.665 (400) indicating the cubic phase formation. Furthermore, the Figures 34 (c) and 34 (f)

demonstrated peak patterns of catalyst gel at 110°C (gel_110) and catalyst gel at 300°C (gel_300) with the JCPDS numbers 01-076-0479 and 01-071-2066 of 2θ and (hkl) are equal to 31.805 (211), 45.432 (220), 56.452 (222), 29.310 (201), 68.714 (521) and 75.263 (420) indicating the tetragonal formation of calcium sodium aluminosilicate.

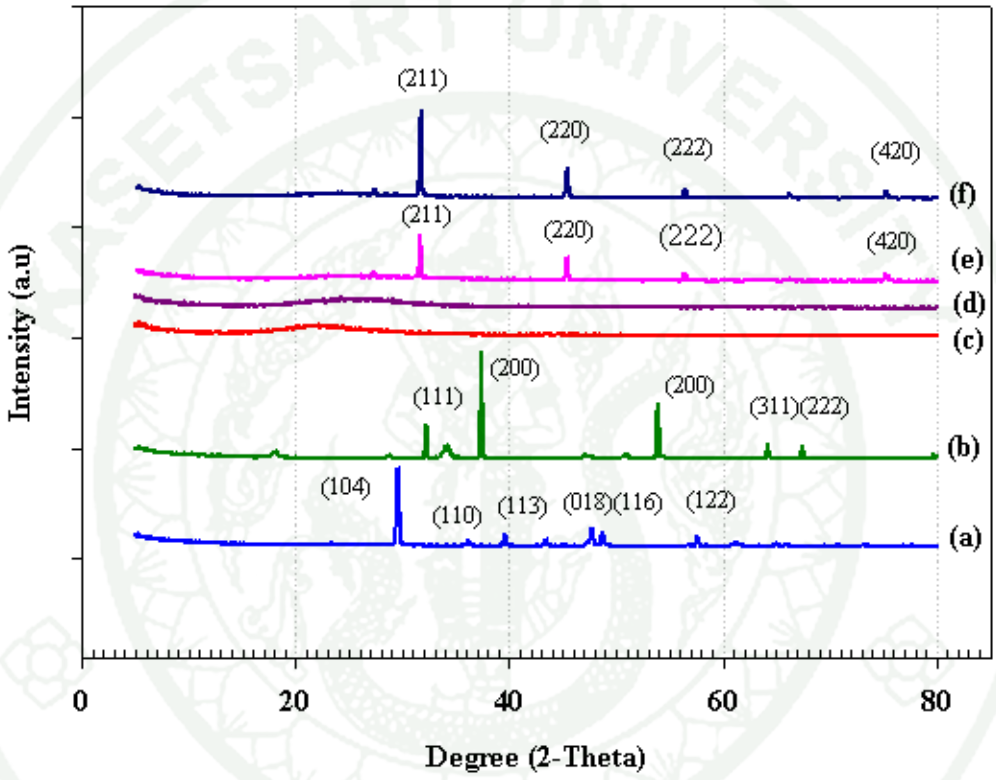

Figure 34 X-ray diffraction (XRD) patterns comparison of (a) eggshell, (b) CaO, (c) fumed SiO_2, (d) aluminosilicate, (e) dried gel_110 and (f) dried gel_300

1.6 Fourier Transform Infrared Spectrometer (FT-IR)

The Figure 35(a) shows the FT-IR (Perkin Elmer, Spectum one) spectrum of the calcined eggshell to be CaO. The wave number of peak at 3642.13 cm^{-1} belongs to OH of $Ca(OH)_2$ due to moisture absorption of CaO. The broad band peak occurs around 1440.33 cm^{-1} corresponding to the Ca-O. Figures 35(b) and 35(c) are FTIR spectra of catalyst gel at 110°C (gel_110) and catalyst gel 300°C (gel_300) at 500-550

cm^{-1} indicating Al-O-C, Si-O-Al, Si-O and Si-O-Si bonding consistent with the data reported (Nuchnapa *et al*., 2010). In addition, the FTIR spectra at 463.43, 794.40 and 1446.04 cm^{-1} show the characteristic of the β-Ca-O-Si, Ca-O-Si, and strong C=O vibration, respectively, which indicated the $CaNaAlSi_2O_7$.

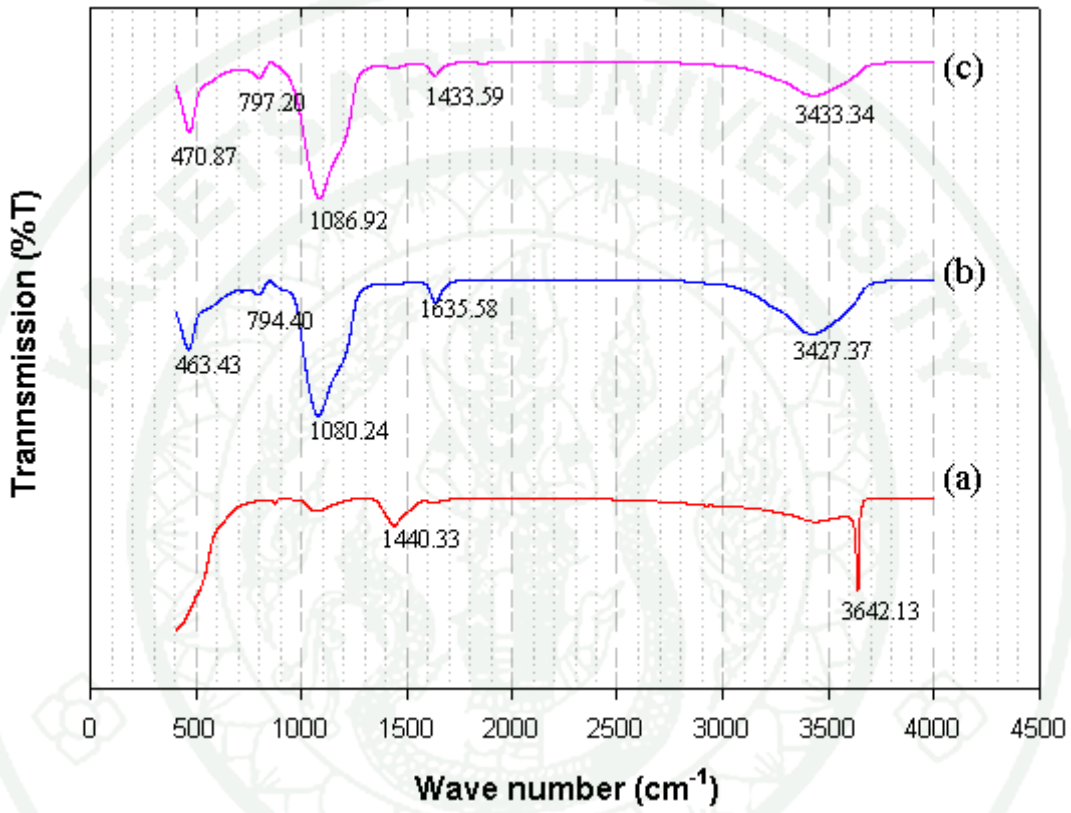

Figure 35 The Fourier Transformation Infrared Spectroscopy (FT-IR) spectra of (a) CaO, (b) gel_110 and (c) gel_300

1.7 Gas Pycnometer

The true density of gel_110 and gel_300 were characterized by gas pycnometer, as shown in table 8. The calcined gel at 300°C has a true density of 1.91 g/cc and dried gel at 110 °C has a true density of 1.90 g/cc. From comparison, gel_300 has a slightly higher true density than gel_110 because the calcined temperature at 300°C.

Density is usually increased due to calcination which causes the removal of water, carbon dioxide, sulphur dioxide, and certain volatile compounds. However increasing the density of the substance is the primary focus.

Table 8 True density of gel_110 and gel_300

Sample names	True density (g/cc)
1. gel_110	1.90
2. gel_300	1.91

Note The gel_110 is dried gel at 110°C and gel_300 is dried gel at 300°C both is $CaNaAlSi_2O_7$

1.8 Brunauer-Emmet-Teller (BET)

The specific surface area, total pore volume, and average pore diameter of catalyst gel were analyzed by Brunauer-Emmet-Teller (BET), as shown in table 9. The catalyst gel at 300°C (gel_300) exhibited higher surface area, pore volume and pore diameter values than the data values of catalyst gel at 110°C (gel_110) due to densification, internal voids in the material reduce the mass and diffusion of some residue gas such as carbon dioxide (CO_2) gas out of material.

Table 9 Multipoint BET, total pore volume, and average pore diameter of gel_110 and gel_300

Sample names	Multipoint BET(m^2/g)	Total pore volume(cc/g)	Average pore diameter(Å)
1. gel_110	37.91	0.2917	307.8
2. gel_300	38.89	0.3728	383.4

2. Granulation

2.1 Bulk density

Table 10 Bulk density of different size granules of gel_110 and gel_300

Sieve size (μm)	Bulk density(g/cm^3)	
	gel_110	gel_300
212	0.552±0.013	0.415±0.015
150	0.506±0.018	0.381±0.017
106	0.466±0.048	0.369±0.015
75	0.410±0.018	0.329±0.007
Bottom 75	0.381±0.019	0.302±0.006

Note gel_110 is dried gel at 110°C and gel_300 is dried gel at 300°C

Bulk density is a property of powders, granules and other "divided" solids. It is defined as the mass of many particles of the material divided by they occupy. The total volume includes particle volume, inter-particle void volume and internal pore volume.

Bulk density is defined as the weight per unit volume of material. Bulk density is primarily used for powders or pellets. The test can provide a gross measure of particle size and dispersion which can affect material flow consistency and reflect packaging quantity.

Bulk density (ρ) = mass (M) / volume (Vt)

Remarks: 1. Bulk density depend on water content and particle size avoid adsorption or desorption of water before determination.

2. To obtain reliable results, make sure the powder is at room temperature when analysis (Anonymous, 2012).

Table 10 shows bulk density of different size granules by using CMC binder at 212, 150, 106, 75 and bottom 75 µm sieve size of gel_110 and gel_300. All of granule's gel_300 sieve size had bulk density (g/cm^3 or g/cc) less than granule's of gel_110 consistent with table 9 which illustrated multipoint BET (m^2/g), total pore volume (cc/g), and average pore diameter of gel_300 (Å) higher than gel_110 which mean less mass at the same total volume.

2.2 Transmission Electron Microscope (TEM)

Figures 36 (a-c) and 37 (a-c) show the TEM micrographs of dried gel_110 granulation is on 212 µm and 75 µm sieve size, respectively with different magnifications of (a) 50k (b) 30k (c) 12k. The micrographs of the gel_110 of 212 and 75 µm sieve size granules point out small size particles with a moderately good dispersion (Nuchanpa *et al.*, 2010), also both of 212 and 75 µm of gel_110 have the same dispersion attributes. Likewise, figures 38 (a-c) and 39 (a-c) show the TEM micrographs of dried gel_300 granulation on 212 µm sieve size (70 Mesh) and 75 µm (200 Mesh) sieve size, respectively with different magnifications of (a) 50k, (b) 30k and (c) 12k and can be explained similarly in figures 36 and 37.

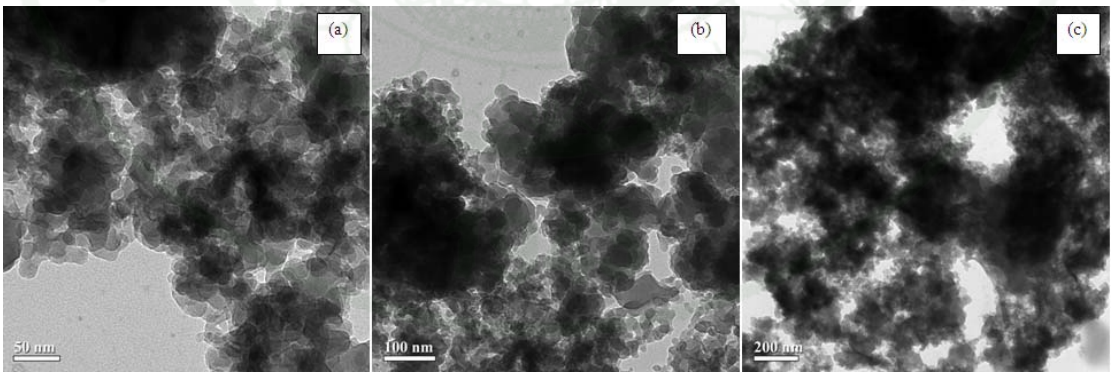

Figure 36 The TEM micrographs of dried gel_110 granulation is on 212 µm sieve size (70 Mesh) with different magnifications of (a) 50k, (b) 30k and (c) 12k

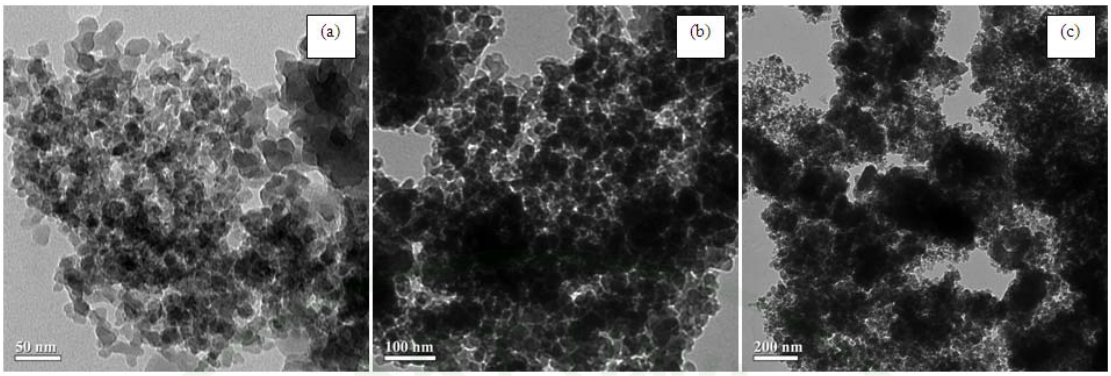

Figure 37 The TEM micrographs of dried gel_110 granulation on 75 µm sieve size (200 Mesh) with different magnifications of (a) 50k, (b) 30k and (c) 12k

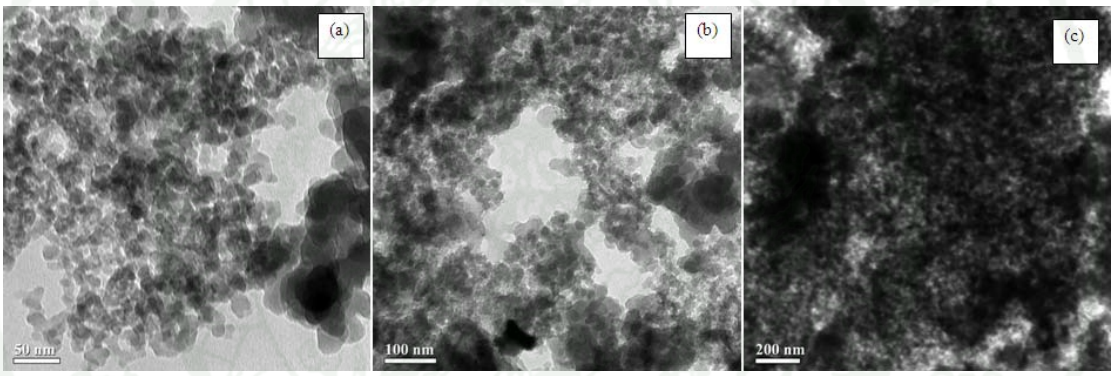

Figure 38 The TEM micrographs of dried gel_300 granulation on 212 µm sieve size (70 Mesh) with different magnifications of (a) 50k, (b) 30k and (c) 12k

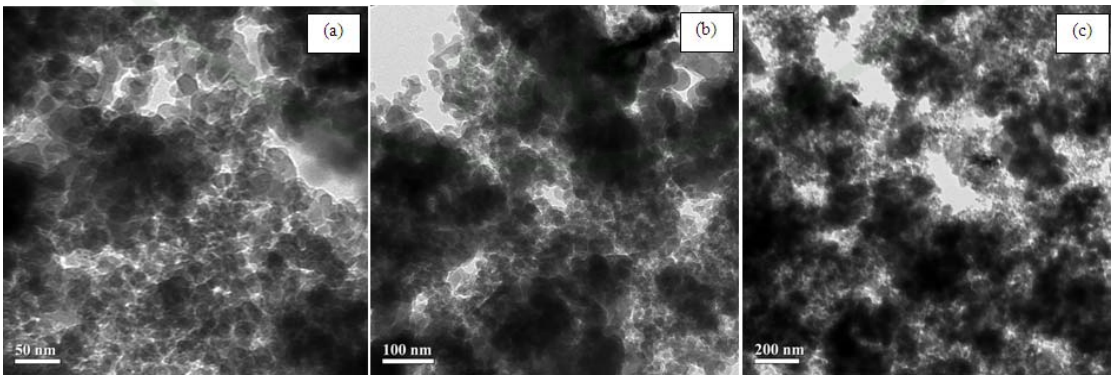

Figure 39 The TEM micrographs of dried gel_300 granulation on 75 µm sieve size (200 Mesh) with different magnifications of (a) 50k, (b) 30k and (c) 12k

2.3 Scanning Electron Microscope (SEM)

Sieving is the classification of particles in terms of their ability or inability to pass through an aperture of controlled size. Particle are introduced onto a stack of sieves with successively finer apertures below, and the particles are agitated to induce translation until blocked by an aperture smaller than the particle size.

In this study, sieving techniques made using CMC binder to produce granules. The SEM's figures of gel_110 and gel_300 at different sieve size (212, 150, 106 and 75 µm sieve size) and magnification (100x, 500x, and 3000x) shown in figure 40 to 47. Granules of gel_110 and gel_300 at different sieve sizes in all figure show small particles close the size on sieve passing and spherical in shape.

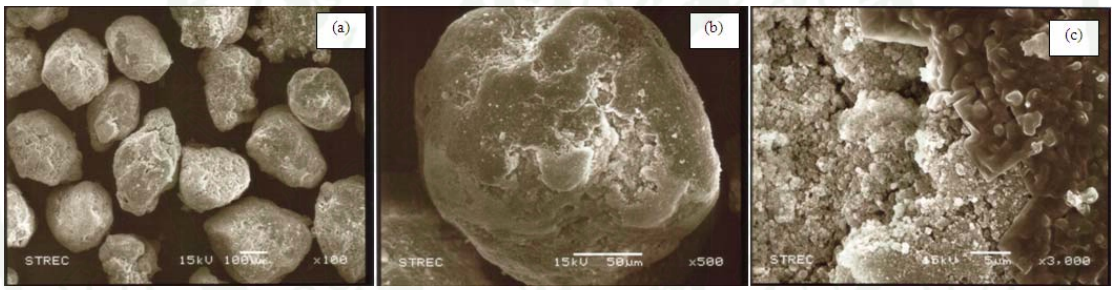

Figure 40 The SEM micrographs of dried gel_110 granules on 212 µm sieve size (70 Mesh) with different magnifications of (a) 100x, (b) 500x and (c) 3000x

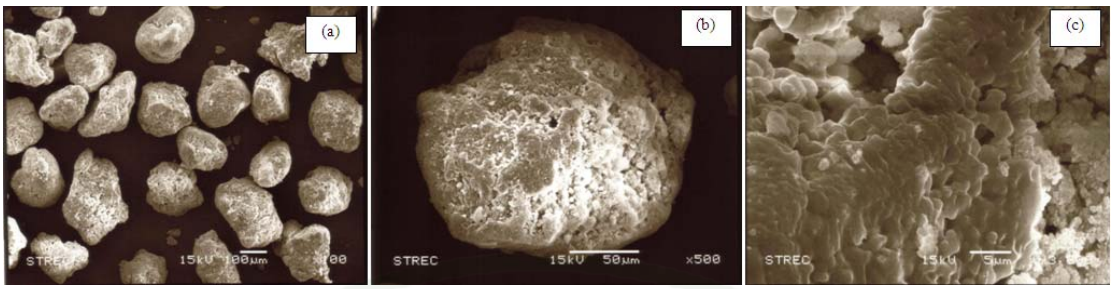

Figure 41 The SEM micrographs of dried gel_110 granules on 150 µm sieve size (100 Mesh) with different magnifications of (a) 100x, (b) 500x and (c) 3000x

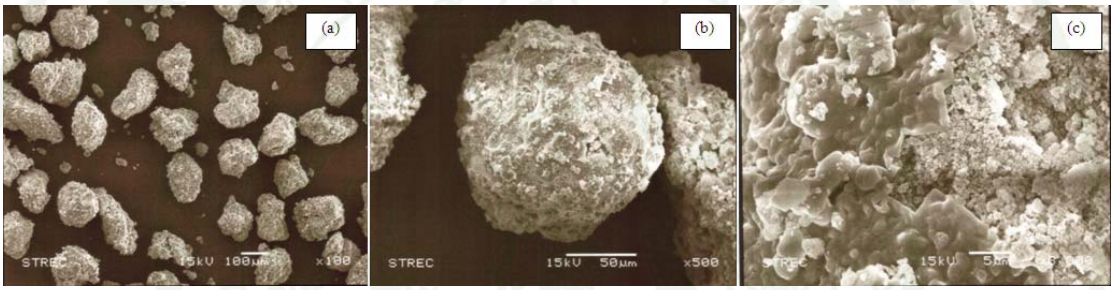

Figure 42 The SEM micrographs of dried gel_110 granules on 106 µm sieve size (140 Mesh) with different magnifications of (a) 100x, (b) 500x and (c) 3000x

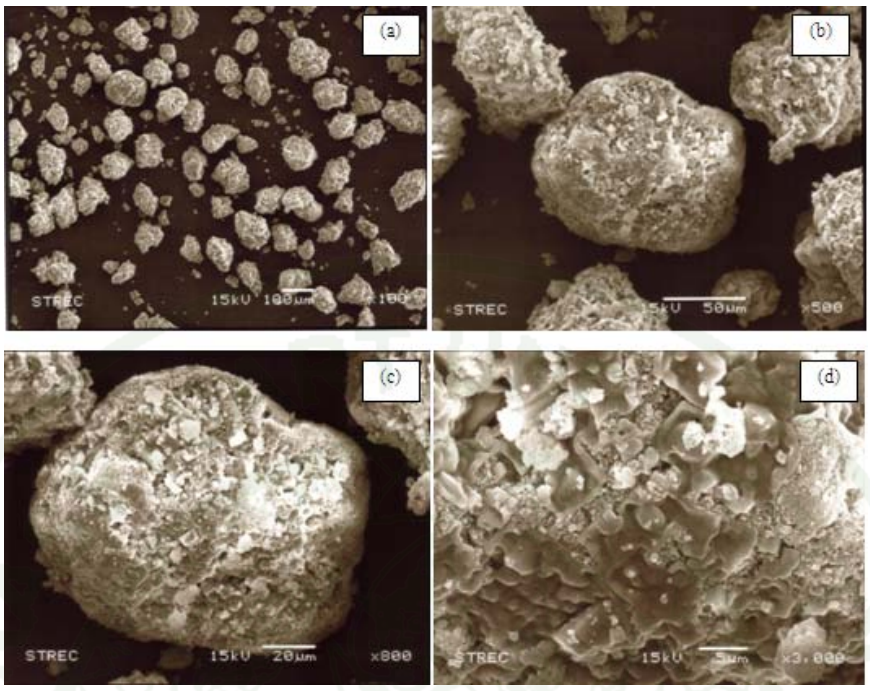

Figure 43 The SEM micrographs of dried gel_110 granules on 75 µm sieve size (200 Mesh) with different magnification s of (a) 100x, (b) 500x, (c) 800x and (d) 3000x

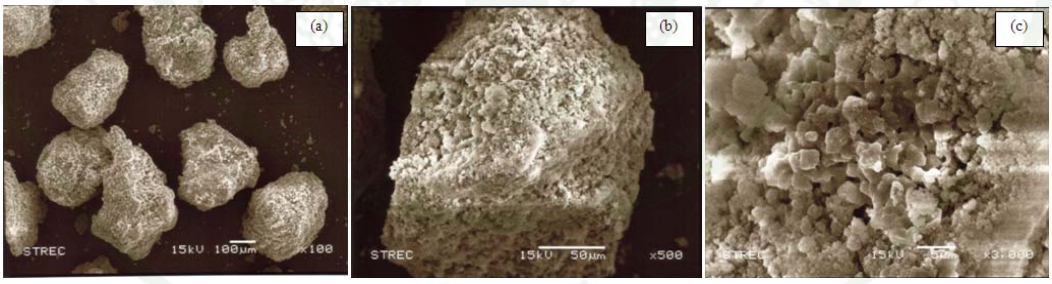

Figure 44 The SEM micrographs of dried gel_300 granules on 212 µm sieve size (70 Mesh) with different magnifications of (a) 100x, (b) 500x and (c) 3000x

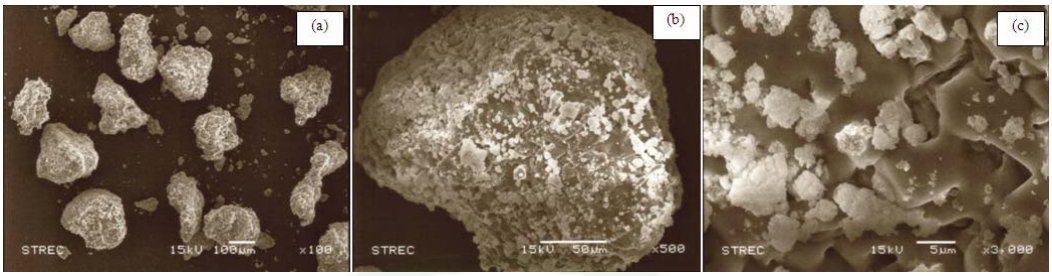

Figure 45 The SEM micrographs of dried gel_300 granules on 150 µm sieve size (100 Mesh) with different magnifications of (a) 100x, (b) 500x and (c) 3000x

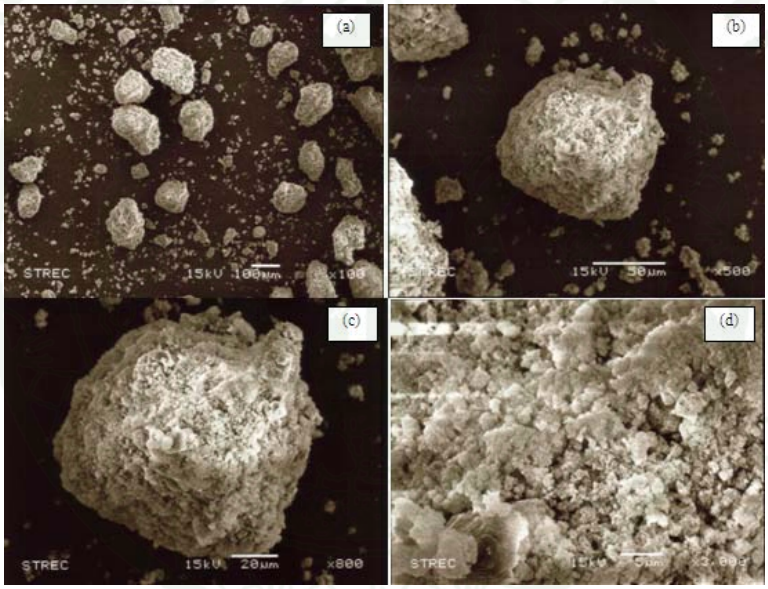

Figure 46 The SEM micrographs of gel_300 granules on 106 µm sieve size with different magnifications of (a) 100x, (b) 500x, (c) 800x and (d) 3000x

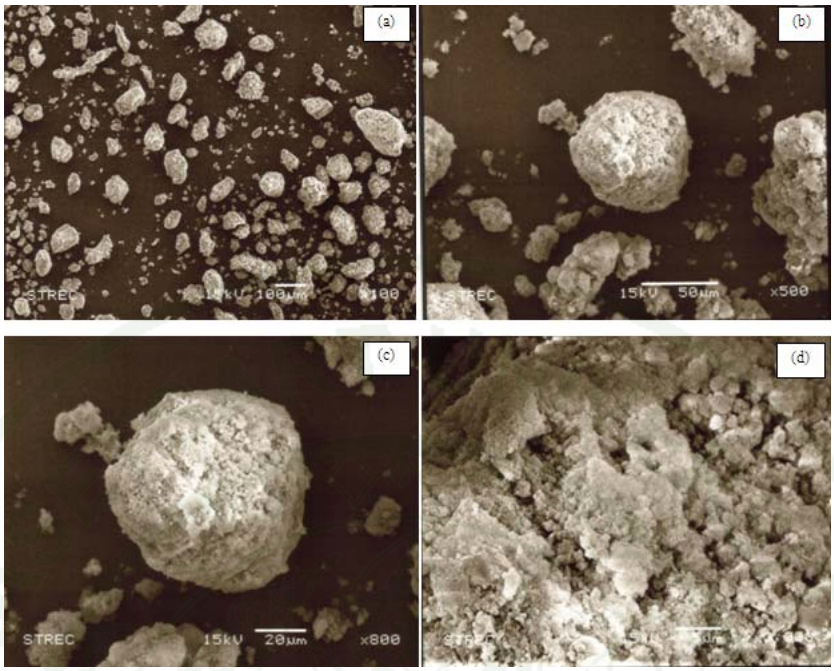

Figure 47 The SEM micrographs of gel_300 granules on 75 µm sieve size with different magnifications of (a) 100x, (b) 500x, (c) 800x and (d) 3000x

2.4 The Fourier Transformation Infrared Spectroscopy (FT-IR)

The figure 48 shows FT-IR spectra of (a) CaO, (b) gel_110, (c) gel_300, (d) CMC and (e) granules of gel_300+CMC. The CaO, gel_110 and gel_300 were previously explanted but their wave lengths were put here because of comparison between CMC's wave number and gel_300+CMC granules.

Figure 48 (d) shows the FT-IR spectrum of carboxymethyl cellulose (CMC) which found the carboxyl, methyl, and hydroxyl functional groups at wave number of 1610.64, 1424.43 and 1328.09 cm^{-1}, respectively. These wave numbers are similarly demonstrated in the report at wave number of 1618, 1426, and 1300 cm^{-1}. According to reported data, broad absorption band at 3436.01 cm^{-1} is due to the stretching frequency of the hydroxyl group (-OH) (the wave number reported at 3432 cm^{-1}). The band at 2920.60 cm^{-1} is due to carbon hydrogen bond (C-H) stretching vibration which is reported at 2909 cm^{-1}. The presence of a strong absorption band at 1610.64 cm^{-1} confirmed the presence of carboxyl group (-COO). This is reported at

1603 cm^{-1}. Furthermore, the bands around 1424.43 and 1328.09 cm^{-1} are assigned to- CH_2 scissoring and hydroxyl group (-OH) bending vibration which is close to the data reported at 1423 and 1325 cm^{-1}, respectively. Finally, the band at 1054 cm^{-1} is due to >CH-O-CH_2 stretching which is reported at 1061 cm^{-1} (Heydarzadeh *et al.*, 2009).

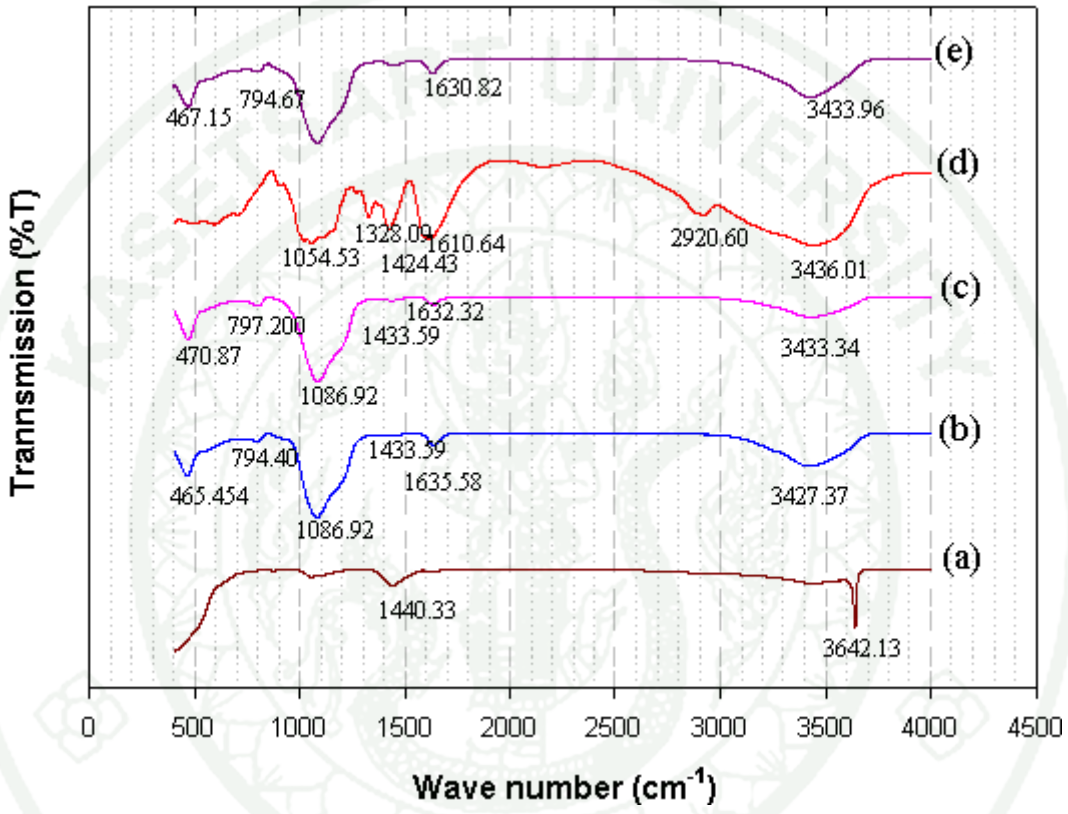

Figure 48 The Fourier Transformation Infrared Spectroscopy (FT-IR) spectra of (a) CaO, (b) gel_110, (c) gel_300, (d) CMC and (e) granules of gel_300+CMC on 150 µm sieve size

Figure 48 (e) shows the spectra of gel_300 was mixed with CMC to produce granules (granules of gel_300+CMC) of 150 µm sieve size. The granules of gel_300+CMC show wave lengths at 467.15, 794.67, 1630.82 and 3433.96 cm^{-1} which are spectrum of gel_300 when compared to figure 48 (c). The spectra of CMC did not show gel_300+CMC may because the sample preparation contained a few amounts of CMC in the sample was tested thus it could not be detected spectra of

CMC. Another reason, the granules of gel_300+CMC show broaden spectrum at 3433 cm^{-1} same as of gel_300 that show belonging to -OH group.

3. Granules coat on filter papers

3.1 Scanning Electron Microscope (SEM)

Filter paper is a semi-permeable paper barrier placed perpendicular to a liquid or air flow. It is used to separate fine solids from liquids or air. In this research, we used the filter paper with calcium zeolite type A for forming to use in molecular sieving. To produce granules coated on filter paper, UHU latex was used as a adhesive to coat granules on the filter paper then study their images at different expansion.

Figure 49 shows SEM's figures paper with different magnifications of (a) 100x, (b) 500x, (c) 1000x and (d) 2000x. The cellulose filter paper has porosity as exhibited in figure 49 (a) to 49 (d). Figures 50 (a-d) shows SEM's figure of UHU latex coated on filter paper with different magnification. After coated UHU latex, the filter paper still had porosity then granules of gel_110 and gel_300 was added into the filter paper surface which was coated by UHU latex in addition to smooth and flat as shown in figure 51 (a-d) to 52 (a-d). The granules coated on the filter paper was badly distribution and disordered yet good coating on the filter paper. This means it need more control for real operation, but this result show calcium zeolite type A covered on the pores of litter paper. Therefore, this fabrication method on filter paper is not good enough for using the $CaNaAlSi_2O_7$ should be prepared in nanosize smaller than the porosity of filter paper. In addition, we only investigated forming so there were no test results for this product, also can not measure the thickness of this products because we did not have suitable instrumentation for measurement.

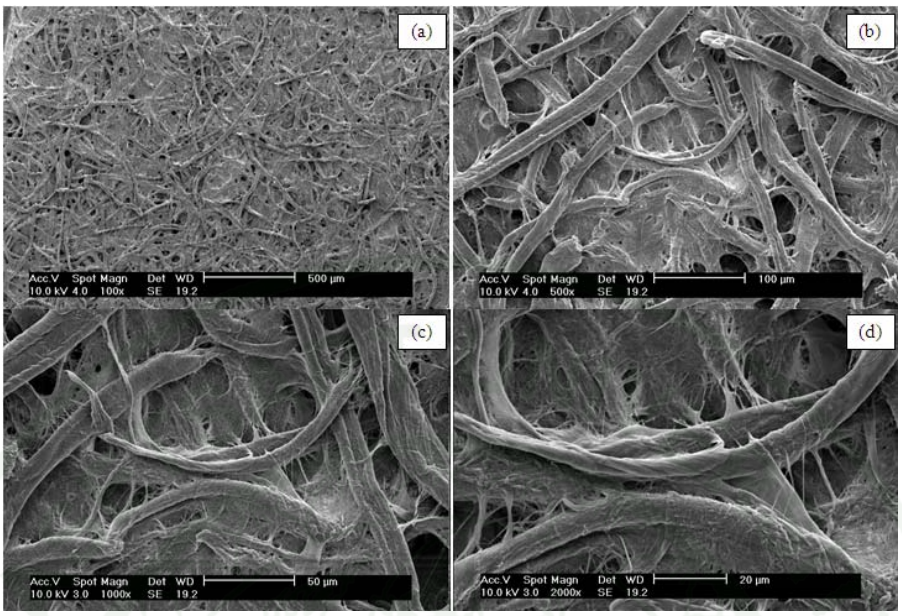

Figure 49 The SEM micrographs of filter paper with different magnifications of (a) 100x, (b) 500x, (c) 1000x and (d) 2000x

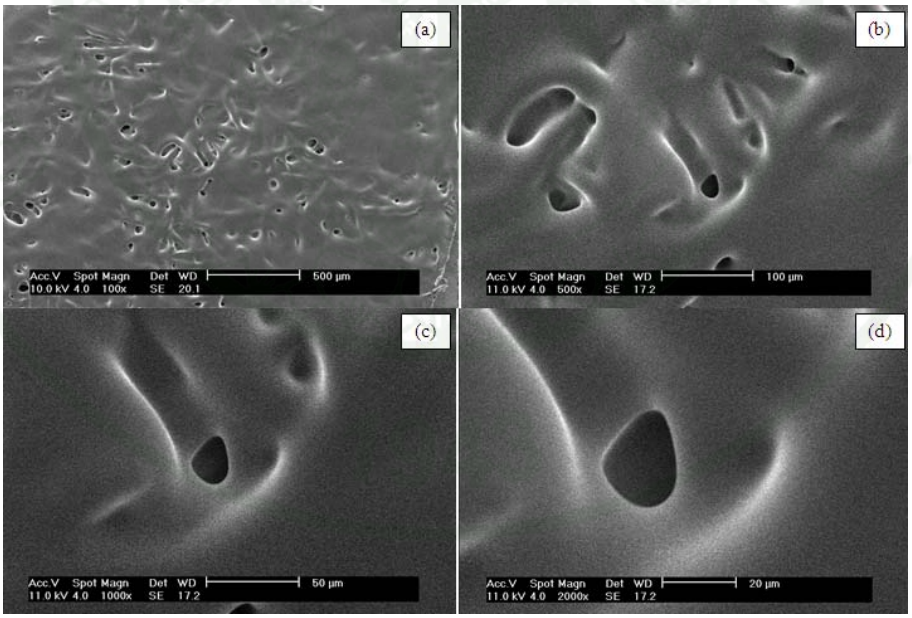

Figure 50 The SEM micrographs of UHU latex coated on filter paper with different magnifications of (a) 100x, (b) 500x, (c) 1000x and (d) 2000x

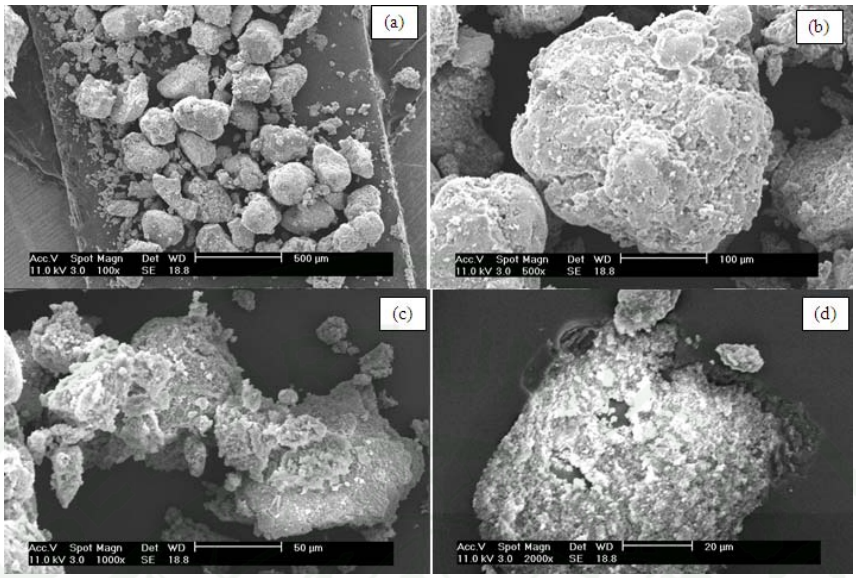

Figure 51 The SEM micrographs of 212 µm gel_110 granules coat on filter paper by using UHU latex coater with different magnifications of (a) 100x, (b) 500x, (c) 1000x and (d) 2000x

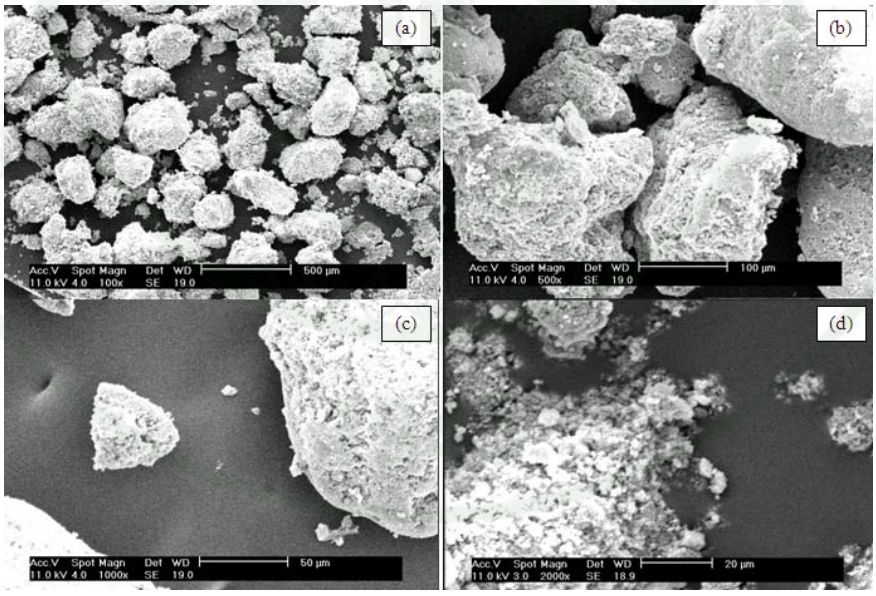

Figure 52 The SEM micrographs of 212 µm gel_300 granules coated on filter paper by using UHU latex coater with different magnifications of (a) 100x, (b) 500x, (c) 1000x and (d) 2000x

4. Compression by uniaxial pressing

4.1 Scanning Electron Microscope (SEM)

In this part, we studied the forming of calcium zeolite type A by using compressive force with uniaxial pressing as shown in figures 53 to 54. Figures 53 (a-d) and 54 (a-d) show SEM's figures of gel_110 and gel_300 compressive force by uniaxial pressing at 350 N with different magnifications of: (a) 100x (b) 500x (c) 1000x (d) 2000x. The micrograph exhibited smooth surface because of preparing by compression.

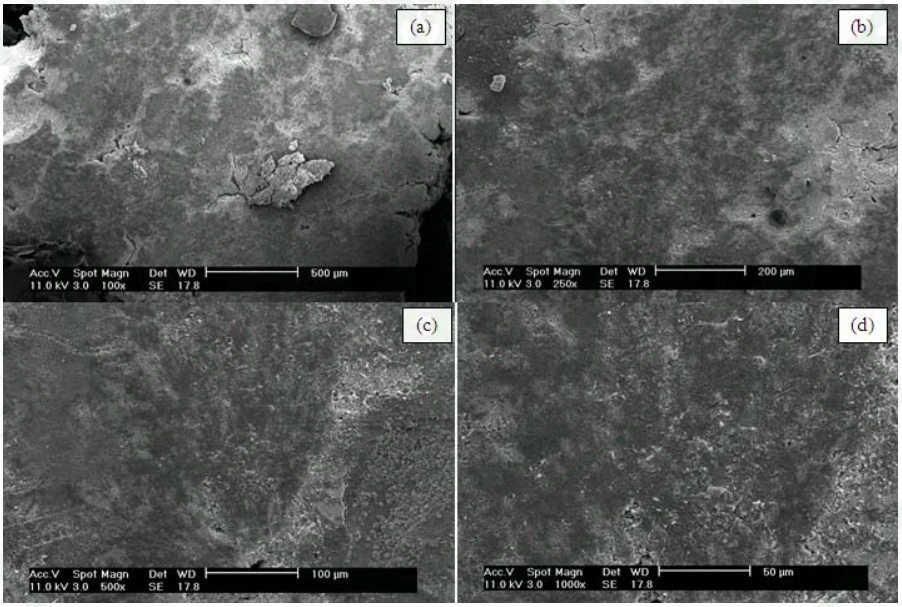

Figure 53 The SEM micrographs of gel_110 compression by uniaxial pressing at 350 N with different magnifications of: (a) 100x, (b) 500x, (c) 1000x and (d) 2000x

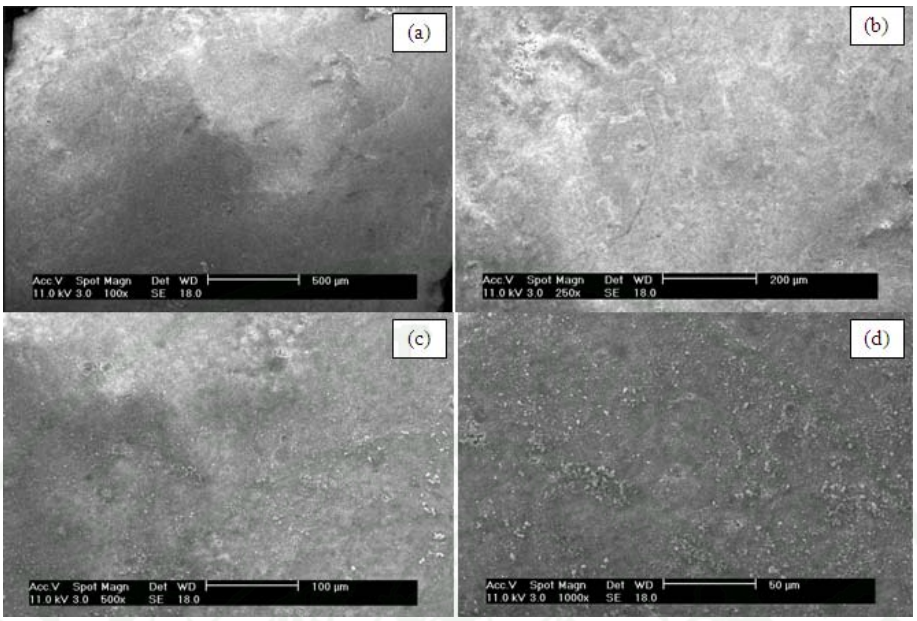

Figure 54 The SEM micrographs of gel_300 compression by uniaxial pressing at 350 N with different magnifications of:(a) 100x, (b) 500x, (c) 1000x and (d) 2000x

5. Polyurethane foam as template (Catalyst foam preparation)

5.1 Differential Thermal Analysis (DTA)

The thermal stability of catalyst and PU composite foam was determined by differential thermal analysis (DTA, Perkins-Elmer TAC7/DX, DTA7, USA) under a nitrogen atmosphere (Figure 55). The samples were heated from 30° to 950°C with a heating rate 10°C/min. The result shows an exothermic reaction of PU foam started to degrade from 530°C to 650°C (Figure 59a). Furthermore, the catalyst-composite foams (10%gel_300°C+PU foam) have an endothermic peak at 790°C shown onset at 786°C (Figure 59b) due to re-crystalline of catalyst gel in PU foam matrix.

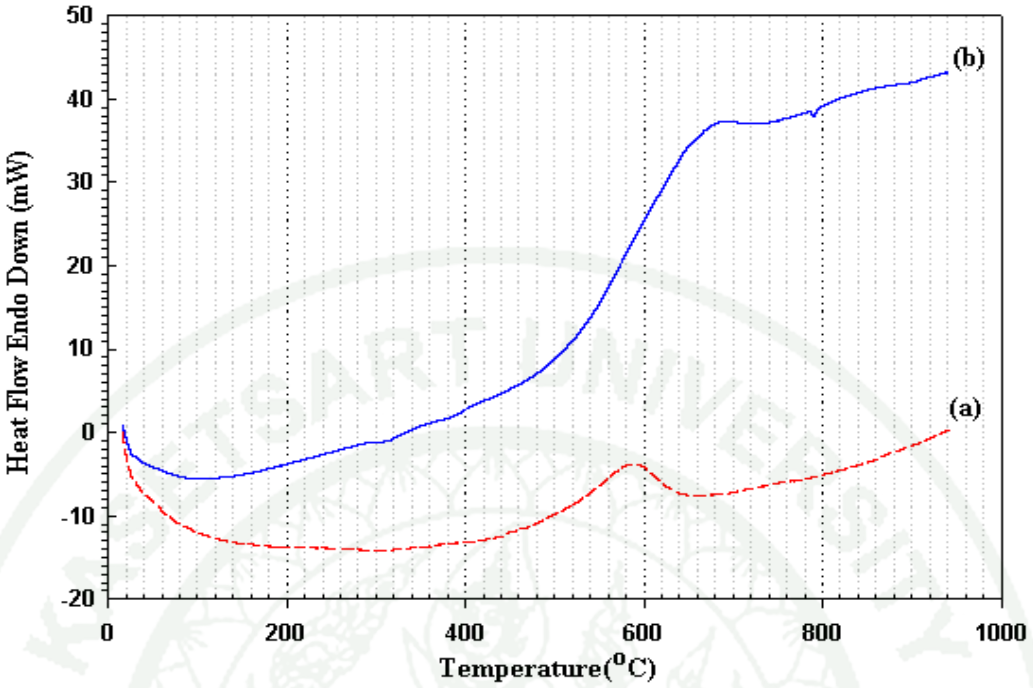

Figure 55 Differential thermal analysis (DTA) of (a) PU foam and (b) 10%gel_300+PU foam

5.2 Themogravimetric Analysis (TGA)

Figure 56 shows thermogravimetry thermal analysis (TGA) testing (TGAQ50 V6.7 Build 203) of PU foam (Figure 56a) and 10%gel_300+PU foam (Figure 56b). TGA uses heat to force reactions and physical changes in materials. Also provides quantitation measurement of mass change in materials associated with transition and thermal degradation. TGA records change in mass from dehydration, decomposition, and oxidation of a sample with time and temperature. In this characterization, samples (10-15 mg) were degraded in flowing nitrogen at a heating rate of 10°C/min from room temperature to 950°C. TGA curve in figure 56a shows that the decomposition of the PU foam started at approximately 200°C and ended at around 400°C. In the first stage, the fastest rate of loss was at 329.39°C (from the report at 335°C) the second stage involved an estimated weight loss of 88.69% with the fastest rate of loss situated at 500°C for sample. The degrading process is complex and depends on several factors such as urethane bonds, polyol type, dangling chains

and unreacted isocyanate (Suresh *et al*., 2007). In the first stage, the sample degradation processes lost the -NCO groups to urethane bonds, others literature have be explained that the first stage degraded of hard segment and the second stage degraded of soft segment that is decomposition process of the polyols' backbone.

Figure 56a shows TGA curve of 10%gel_300+PU foam which exhibited three stages of decomposition in the first stage, the fastest rate of loss was at 235.38°C with on estimated weight loss of 88.69%. In the second stage, the fastest rate of loss was at 302.05°C with an estimated weight loss of 10.74% and the third stage, the fastest rate at loss was at 377.50°C with an estimated weight loss of 61.00%. All this data pointed out that the 10%gel_300+PU foam has inferior thermal property compared to pure PU foam due to the fact that zeolite can hinder bonds between threshold segments of polyurethane chains but still have high a temperature for polymers including work as a template for calcium zeolite type A. For the third stage, it still may degrade the polyurethane chain because calcium sodium aluminosilicate or calcium zeolite type A ($CaNaAlSi_2O_7$) had endothermic peaks at 787° and 1102°C (Nuchnapa *et al*., 2010) that corresponds with figure 54 (b). TGA curve of figure 56 (b) still has %weight loss from temperature 400°C to 950°C.

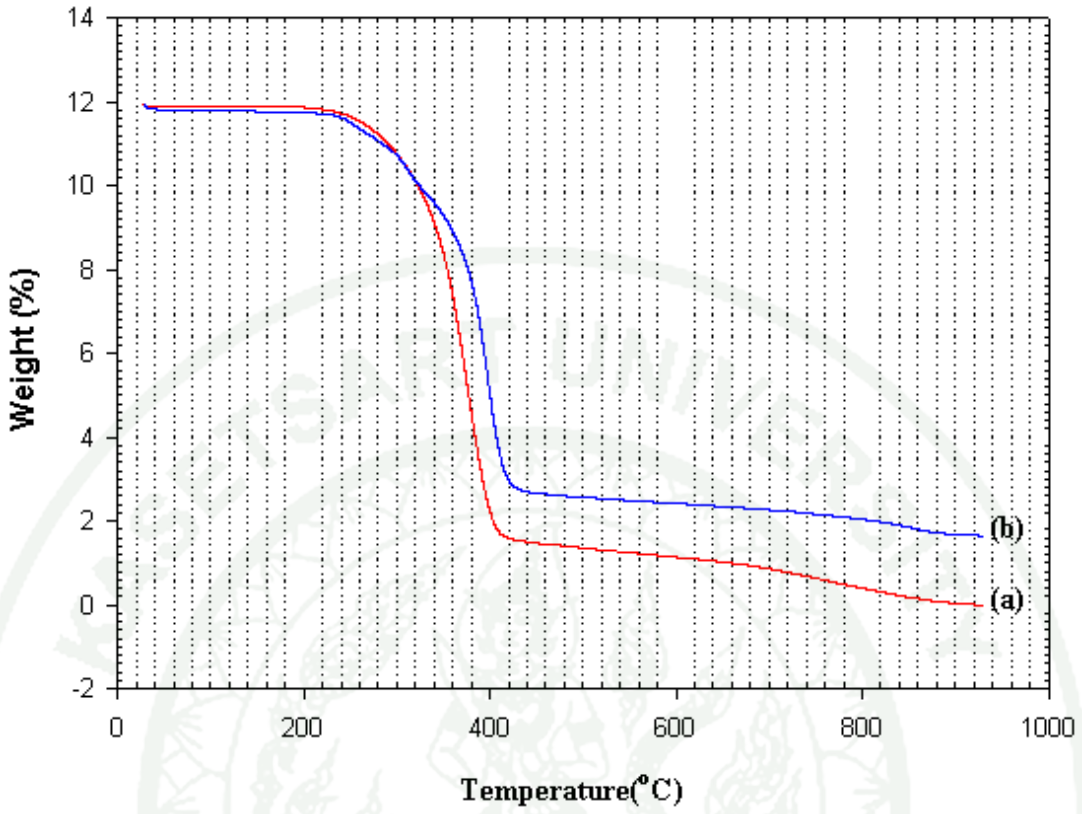

Figure 56 Themogravimetric Analsis (TGA) of (a) PU foam and (b) 10%gel_300+PU foam

Figure 57 shows the SEM photographs analyzed by Scanning Electron Microscope (SEM) (Philips, XC, Netherland) of pure PU foam and pure PU foam added with 10 vol% catalyst gel at 300°C (10%gel_300+PU foam). The cell edges and cell walls of pure PU foam are distinctly visible with almost uniform cell structures throughout. Cell size as seen in the (SEM) is approximately 200-250 µm. The samples added 10%gel_300+PU foam are shown in Figures 57 (d), 57 (e) and 57 (f). The 1%, 2%, 5%, 15 vol%, 20 vol%, 30 vol% and 50 vol% of catalyst gel were added into PU foam as shown in appendix A1-A10. The higher percentage of catalyst added into PU foam is not good for making catalyst composite foam formation due to the agglomeration of catalyst within the interconnecting cells of PU foam. Therefore, the best composition of composite materials is adding 10 vol% $CaNaAlSi_2O_7$ into PU matrix with uniform structure and non-agglomeration of catalyst powder. The composite foam cells still are well ordered and uniform in size and shape. However,

open cells of the composite foam seem smaller than that of pure PU foam. According to the SEM image results of catalyst composite foam added 10 vol% catalyst gel at 110°C (10%gel_110+PU foam) into PU foam matrix are similar SEM micrographs of catalyst composite foams added with 10 vol% catalyst gel at 300°C (10%gel_110+PU foam) into PU foam matrix.

5.3 Scanning Electron Microscope (SEM)

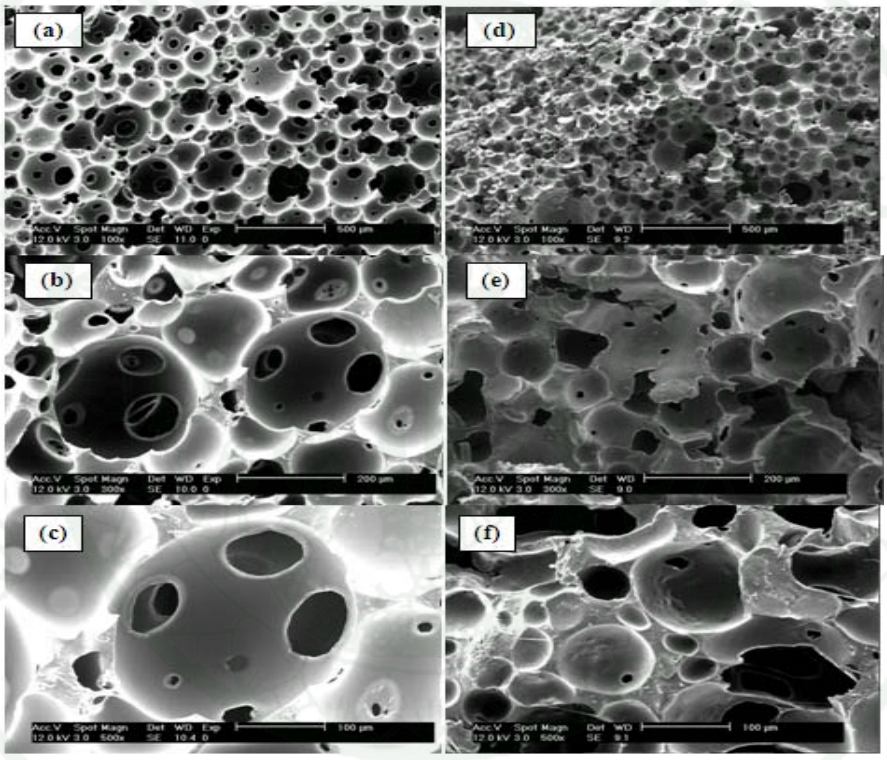

Figure 57 SEM pictures of: (a) pure PU foam at 100x, (b) PU foam at 200x, (c) PU foam at 500x, (d)10%gel_300+PU foam at 100x, (e) 10%gel_300+PU foam at200x and (f)10%_gel 300+PU foam at 500x

5.4 X-Ray Diffraction (XRD)

The Figure 58 shows XRD peak pattern comparison between pure PU foam and catalyst composite foams. The step scan used present time at 1s with 2θ = 5°-80°. The XRD peak patterns of pure PU foams and catalyst composite foams exhibited amorphous regions, so the step scan measured in the range of 2θ = 5°-80°. However, the XRD peak patterns of $CaNaAlSi_2O_7$ powder show crystalline phase in the range of 2θ equal to 25°-35° as shown in Figure 59. The peak patterns of figures 63b, 63c, 63d and 63e were demonstrated at 2θ about 32° which indicated the tetragonal formation of calcium sodium aluminosilicate.

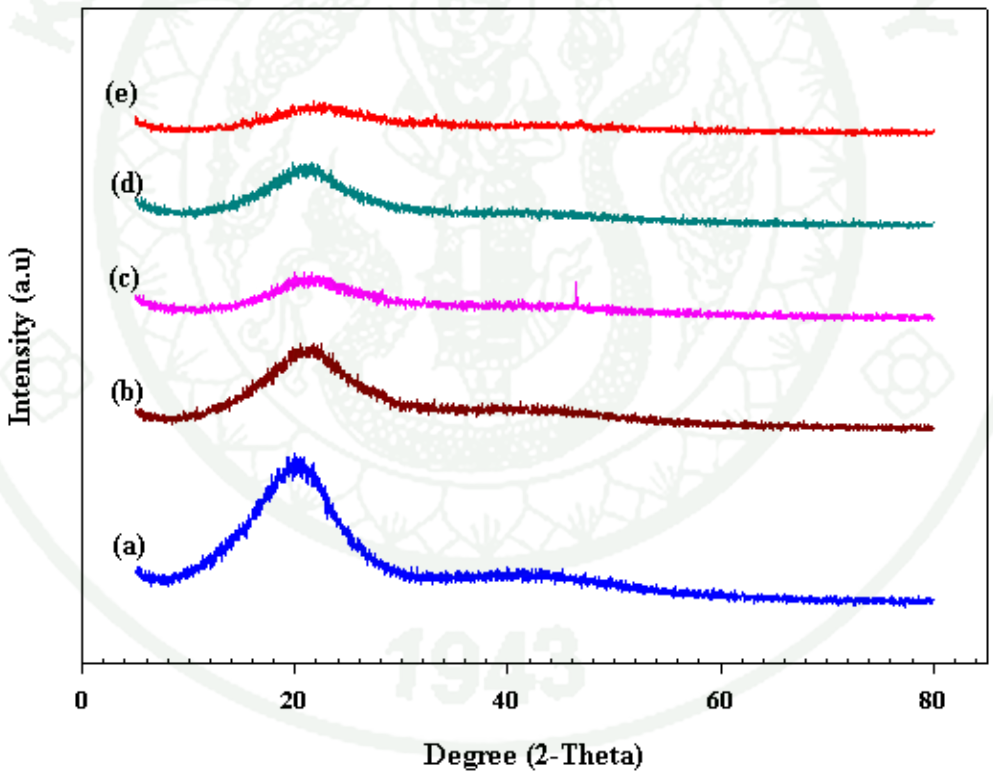

Figure 58 X-ray diffraction (XRD) patterns comparison of:(a) PU foam, (b) 10%gel_110+PU foam, (c) 20 %gel_110+PU foam, (d) 10%gel_300+PU foam and (e) 20%gel_300+PU foam

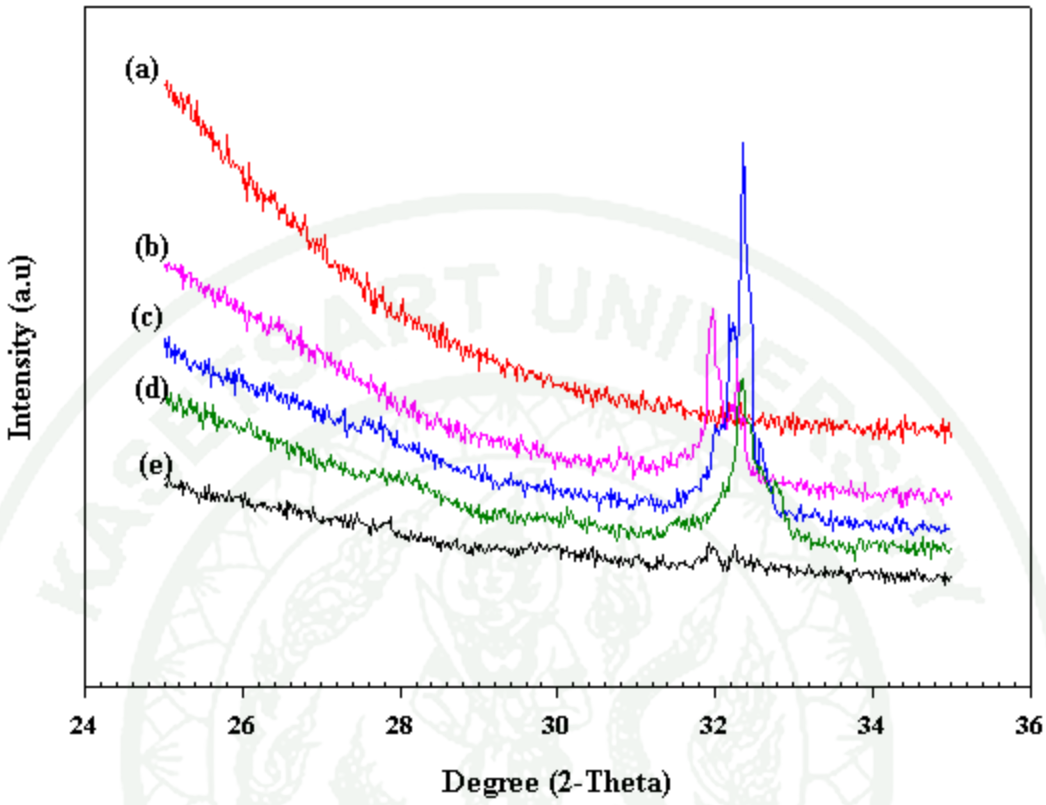

Figure 59 X-ray diffraction (XRD) patterns comparison of:(a) pure PU foam, (b) 10%gel_110+PU foam, (c) 20 %gel_110+PU foam, (d) 10%gel_300+PU foam and (e) 20%gel_300+PU foam

5.5 Fourier Transform Infrared Spectrometer (FT-IR)

The Figures 60d and 60e show spectra comparison of PU foam+10 vol% catalyst gel at 110°C (10%gel_110+PU foam) and PU foam + 10 vol% catalyst gel at 300°C (10%gel_300+PU foam), and pure PU foam. The 10%gel_110+PU foam shows peak positions at 470.89, 797.20 cm^{-1}, same as the peak positions of the 10%gel_300+PU foam at 463.43 and 794.40 cm^{-1} corresponding to the characteristics of β-Ca-O-Si and Ca-O-Si, respectively. The spectra of the pure PU foam acted as a matrix whereas the calcium zeolite type A ($CaNaAlSi_2O_7$) acted as the dispersed phase for making catalyst foam composites. It is found that the segmented structure of PU no major change the properties and the structure of $CaNaAlSi_2O_7$.

The FT-IR spectra of the polyurethane foams prepared from the FF 45804 and the SUPRASEC 2749 as shown in Figure 60f. This spectrum indicates peak positions belonging to polyurethanes at 3437.71 cm^{-1} consistent with -N-H stretching vibration of urethane groups (3200-3450 cm^{-1}) (Hassan *et al*., 2004). The broad band peak at 2800-3000 cm^{-1} corresponds to -C-H stretching (Scott *et al*., 2008). They do not show the peak position at 2250-2270 cm^{-1} consistent with the characteristic of isocyanate (-N=C=O) group because of polymerization (Corcuera *et al*., 2010), (Scott *et al*., 2008). The -C=O stretching of the urethane carbonyl peak at 1712.90 and 1730.79 cm^{-1} are observed and reported at 1702-1737 cm^{-1} (Yongshang and Richard, 2010). The peak at 1613.45 cm^{-1} indicates the carbonyl vibration (-C=O) reported at 1630-1637 cm^{-1} (Corcuera *et al*., 2010), (Scott *et al.,* 2008) while -NH bending is identified peak at 1512.21. Also, the peak at 1541.65 cm^{-1} originates from the coupling of -CN stretching and -NH bending. The FTIR peaks observed between 1400 and 1480 cm^{-1} (in this work occurred at 1414.57 and 1453 cm^{-1}) are attributed to $-CH_2$ scissoring vibrations. The weak peaks at 1345.96 and 1374.99 are connected to the wagging vibrations of methylene groups, whereas the peak at 1310.32 cm^{-1} is assigned to $-CH_2$ twisting. The FTIR spectra exhibit the characteristic peak at 1000-1400 cm^{-1} of C-N and C-O stretching. The presence of the FTIR peaks belongs to polyurethane foam.

5.6 Gas pycnometer

The data of true density of catalyst gel at 110°C (gel_110), catalyst gel at 300°C (gel_300) as shown in table 8 including pure PU foam, and 10%gel_300+PU foam, were analyzed by gas pycnometer, as shown in table11. Adding 10%gel_300 into pure PU foam can increase the true density value of composite foam from 1.13 to be 1.47g/cc.

5.7 Bulk density

Table 12 shows bulk density at different percentage of gel_110 or gel_300 composite with PU foam. Bulk density of gel_110 tends to increase when adding a higher percentage of polyurethane which is consistent with lower true density of Pure PU foam than 10%gel_300+PU foam comparison (Pure PU foam is 1.13 g/cc and 10% gel_300+PU foam is 1.47 g/cc).

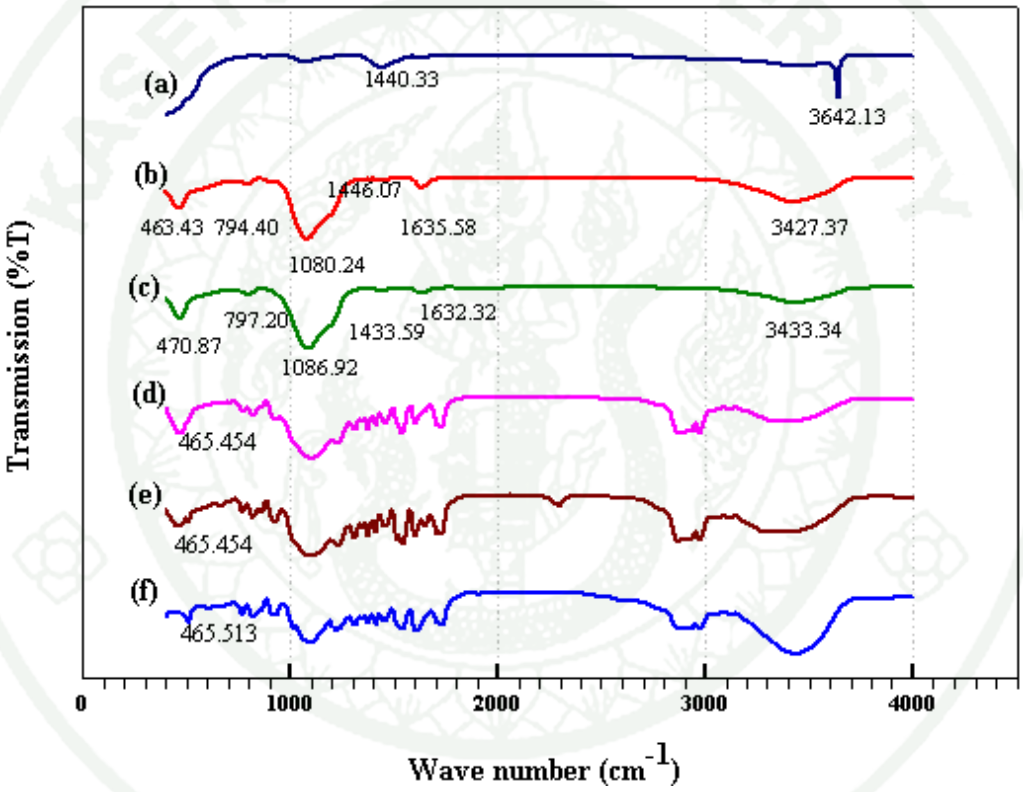

Figure 60 The Fourier Transformation Infrared Spectroscopy (FT-IR) spectra of (a) CaO, (b) gel_110, (c) gel_300, (d) 10 % gel_110+PU foam, (e) 10%gel_300+PU foam and (f) PU foam

5.8 Universal Testing Machine

The compressive strength and elastic modulus of PU foam+10 vol% catalyst gel at 300°C (10%gel_110+PU foam) compared to pure PU foam were measured by a compressive tester (Qmat 5.44 M-Series-10 KM) according to ASTM D 695 compression of rigid plastics (cross head). The dimensions of specimens are 25.4×25.4×12.7 mm^3 and the crosshead speed of compression was set at 1.2 mm/min. The elastic modulus and compressive strength of the composite foam are 0.0327±0.0078 and 0.0188±0.0017 Kgf/mm^2, respectively. The elastic modulus and compressive strength of pure PU foam are 0.1162±0.047 and 0.0245±0.0067 Kgf/mm^2, respectively. The mechanical properties (elastic modulus and compressive strength) of catalyst composite foams of adding catalyst gel at 300°C are less than that of pure PU foams due to H-bond formation among urethane groups that greatly contributes to the strength and modulus of PU foam. For the reason of catalyst gel at 300°C may intervene with the H-bond formation and no strong interaction or graft within PU matrix. Therefore, The PU foam composite has high elastic modulus and compressive strength. However, catalyst composite foams have high specific surface area, thermal resistance, and corrosion resistance useful for using as catalyst composite foams.

Table 11 True density of PU foam and composite foam (10%gel_300+PU foam) compared with gel_110 and gel_300

Sample names	True density (g/cc)
1. gel_110°C	1.90
2. gel_ 300°C	1.96
3.Pure PU foam	1.13
4. 10%gel_300+PU foam	1.47

Table 12 Bulk density of different percentage of foam composite (gel_110 or gel_300)

Sample names	Bulk density (g/cm^3)	Sample names	Bulk density (g/cm^3)
PU foam	0.214±0.012	PU foam	0.213±0.012
1.0%_110	0.141±0.009	-	-
1.5%_110	0.136±0.026	-	-
5.0%_110	0.152±0.020	-	-
10%_110	0.213±0.012	10%_300	0.296±0.030
15%_110	0.290±0.030	-	-
20%_110	0.292±0.015	20%_300	0.285±0.070

Note Uncertainty at 95%

CONCLUSIONS AND RECOMMENDATION

Conclusions

From the experimental results and discussion of this study, the conclusions can be noted as follows:

1. Calcium zeolite type A ($CaNaAlSi_2O_7$) was successfully synthesized fromeggshell as the starting material by the sol-gel process including fabrication by using CMC binder to produce granules and granules coated on filter papers, compressive force and polyurethane foam as template.

2. Granules of $CaNaAlSi_2O_7$ have small particles close to size and spherical in shape, but do not enough for coating on filter paper, however the granules can be applied use for the fixed bed, fluidized bed and moving bed.

3. Forming by compression creates a smooth surface but these results were not studied thoroughly. For application, it can be applied work as membrane to separate gas or liquid if there are good controlling.

4. Polyurethane foam can be used as a template to create a composite of PU and $CaNaAlSi_2O_7$ which has potential as catalyst foams in the chemical and petrochemical industries for use in ion exchange, use as filter and a desiccant.

Recommendation

1. All product samples should have been tested in order to know about their property then applying to confirm in real applications.

2. Try to use other materials for use as a starting material such as quail eggshell, duck eggshells.,*etc.*

3. Polyurethane has many types, the stirring time to finish reaction is not the same so the proper time should be tested before using.

LITERATURE CITED

Anonymous. 2012. **Polyurethane**. Avalaible source: http://www.exploratorium.edu/ cooking/ eggs/ eggcomposition.html, February 22, 2012.

_____. 2012. **Polyurethane.** Avalaible source: http://www.Sdplastics.com/polyuret.html, February 22, 2012.

_____. 2012. **Polyurethane.** Avalaible source: http://www.Sunilbhangale.tripod.com/pu.html, February 25, 2012.

_____. 2012. **Structure and frame structure of zeolite.** Avalaible source: http://www.teara.govt.nz./en/rock-limestone-and-clay/10/11, February 25, 2012.

_____. 2012. **The octahedron stucture.** Avalaible source: http://www.theory.org/geotopo/tt/html/truncatering.html, February 25, 2012.

_____. 2012. **Granulation process.** Avalaible source: http://www.pharmainfo.net/free-books/fluidized-bed-systems-review, February 25, 2012.

Chuapradita C., L. R. Wannatongb, D. Chotpattananonta, P. Hiamtupa, A. Sirivata and J. Schwank. 2004. Polyaniline/zeolite LTA composites and electrical conductivity response towards CO. **J.Polymer.** 46: 947-953.

Charles A. H. and M. P. Edward. 2003. **Plastics materials and processes**. A concise Encyclopedia. John wiley&sons, INC. Hoboken, New Jersey.

Corcuera M. A., L. Rueda, B. Fernandez d'Arlas, A.Arbelaiz and C. Marieta. (2010) I. Mondragon and A. Eceiza. **Polymer Degradation and Stability** 95 (11): 2175-2184.

Hanwatanakul J. 2007. **Polyurethane foam and Polystylene.** Available Source: http:// www.dss.go.th/dssweb/st-articles/files/bla_4_2550_foams.pdf, April 29, 2011.

Heydarzadeh H. D., G. D. Najafpour and A. A. Nazari-Moghaddam. 2009. Catalyst-Free conversion of alkali cellulose to Fine Carboxy methyl Cellulose at mild Conditions. **J. World Applied Sciences** 6(4): 564-569.

Khongnakhon T.. and S. Kittikul. 2009. **Preparation of Calcium Silicate Dielectric Compounds from Eggshell.** B.Eng. Thesis, Kasetsart University.

James S. R. 1989. **Introduction to the Principles of ceramic processing**. John wiley&Sons, INC., Singapore.

Joseph K., N.Matsue and T. Henmi. 2009. Synthesis of Linde type A zeolite-goethitenano composite as an adsorbent for cationic and anionic pollutants. **J.Hazardous Materials** 164: 929-935.

Martin C. 2011. **Carboxymethylcellulose (CMC)**. Avalaible source: http:// www.isbu.ac.uk/water/hycmc.html, February 29, 2012.

RAHAMAN M.N.. 1995. **Ceramic Processing and Sintering**. Marcel Dekker, New York.

Romanowski P. 2011. **Polyurethane.** Avalaible source: http://www.isbu.ac.uk/water/hycmc.html, February 29, 2012.

Suresh S, Narine, X. Kong, L. B. and S.P. Peter. 2007. Properties of Polyurethanes Produced from Polyols from Seed Oils: II. Foams. **J. Amer Oil Chem Soc**: 65-72. Accession no .DOI 10.1007/s11746-006-1008-2.

Shingjiang J.L. and T. Liaw 2005. eparation of xylene mixtures using polyurethane-zeolite composite membranes. **J. Desalination** 193: 137-143.

Songül S., B Belgin., A. Y. Gül. and A.U GÖk. 2008. Polyfuran/zeolite LTA composites and adsorption properties. **J. European Polymer** 44: 2708-2717.

Sridhar K., S. Sakka, P. P. Phule and M. Richard Laine. 1998. **Sol-Gel Processing of Advanced Materials: ceramic Transactions**. The American ceramic Society, Ohio.

Suresh S. N, X. Kong, L. Bouzidi and P. Sporns. 2007. Physical Properties of Polyurethanes Produced from Polyols from Seed Oil: II. Foams**. J. Amer Oil Chem Soc** 84: 65-72.

Tangboriboon N., S.Wongkasemjit, R. Kunanuruksapong and A. Sirivat. 2010. **An Innovative Synthesis of Calcium Zeolite Type A Catalysts from Eggshells via the Sol–Gel Process.** J.Inorg Organomet Polym. Accession no.DOI 10.1007/s10904-010-9413-2.

Thongthai W. 2011. Characterization of calcium oxide derived from waste eggshell and its application as CO_2 sorbent. **J.Ceramics International** 37: 3291-3298.

Toshi Y., Y. Takahata, T. Katauyama and Y. Mastsuda. 2001. A new teach for preparing ceramics for catalyst support exhibiting high porosity and high heat resistance. **J.Catalysis Today** 69: 11-15.

VAN DER WAAL J.C. and H. VAN BEKKUM. 1998. Molecular Sieves,Multifunctional Microporous Materialsin Organic Synthesis. **J.Porous Materials** 5: 289-303.

Xia Cao, L.J. Lee, T. Widya, C. Macoskob. 2004. Polyurethane/clay nanocomposite foams: processing, structure and properties. **J. Polymer** 46: 775-783.

Yujiro W., T. Ikoma, Y Suetsugu, H. Yamada, K. Tamura, Y. Komatsu, J. Tanaka and Y. Moriyoshi. 2005. Type-A zeolites withhydroxyapatite surface layers formed by an ion exchange reaction. **J. European Ceramic Society** 26: 469-474.

Ziku W., C. Xu and B.Lic. 2009. Application of waste eggshell as low-cost solid catalyst for biodiesel production. **J. Bioresource Technology** 100: 2883-1885.

APPENDICES

Appendix A

Figures

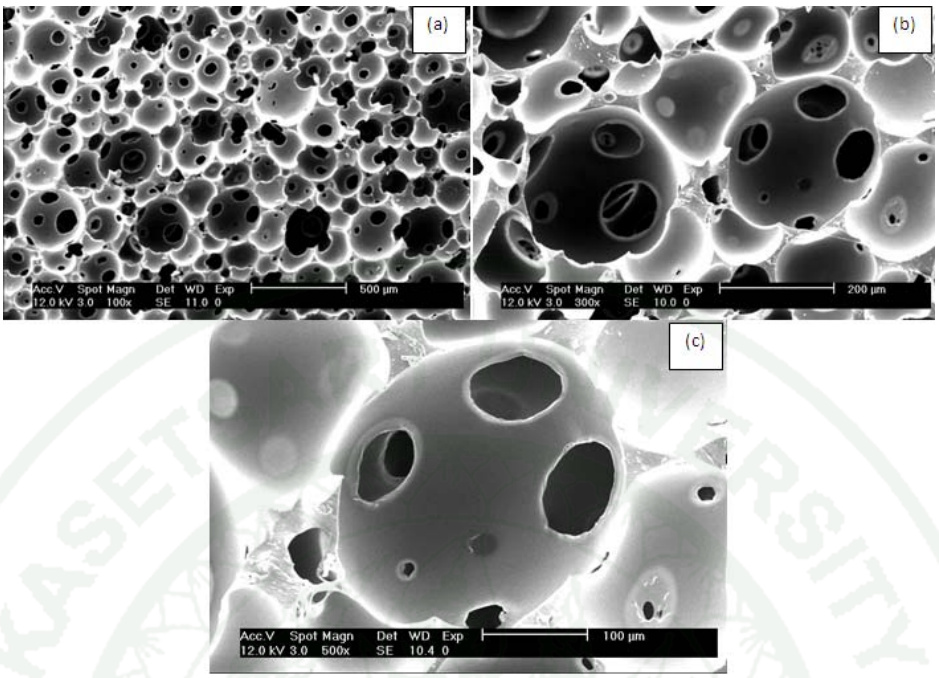

Appendix Figure A1 The SEM micrographs of of pure PU foam with different magnifications of (a) 100x, (b) 500x and (c) 3000x

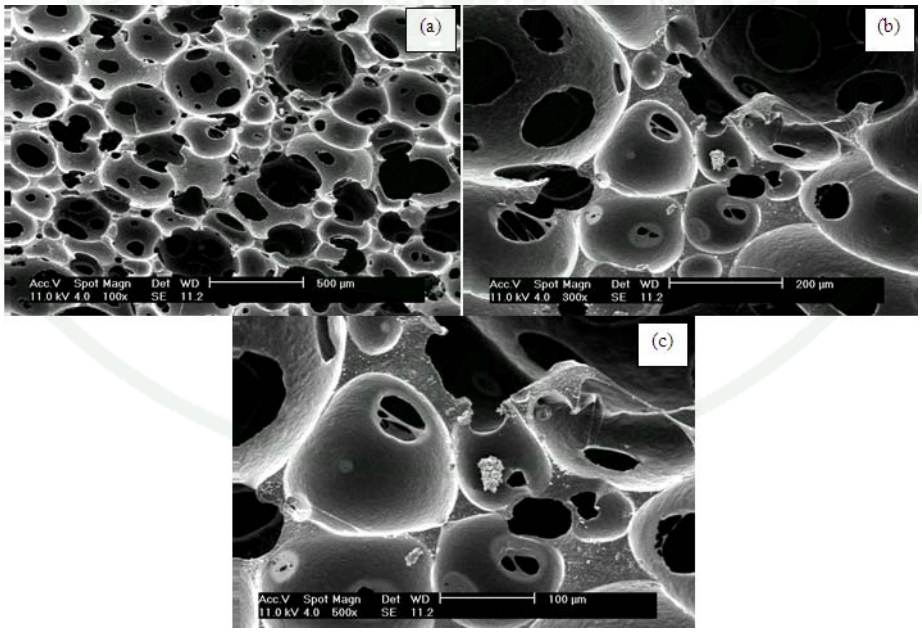

Appendix Figure A2 The SEM micrographs of 1%gel_110 distributed in PU foam (w/w) with different magnifications of (a) 100x, (b) 500x and (c) 3000x

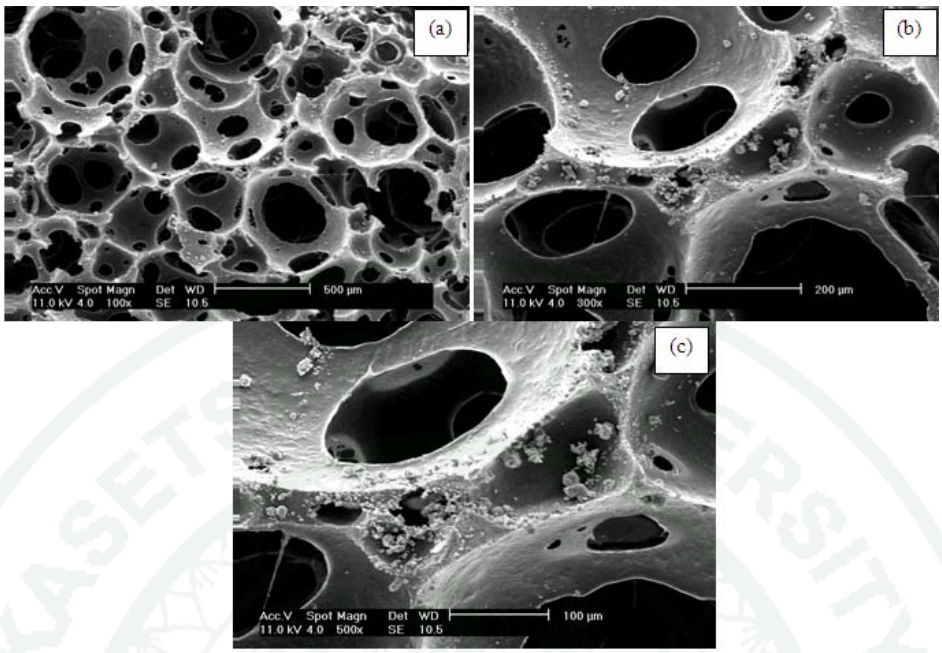

Appendix Figure A3 The SEM micrographs of 1.5%gel_110 distributed in PU foam (w/w) with different magnifications of (a) 100x, (b) 500x and (c) 3000x

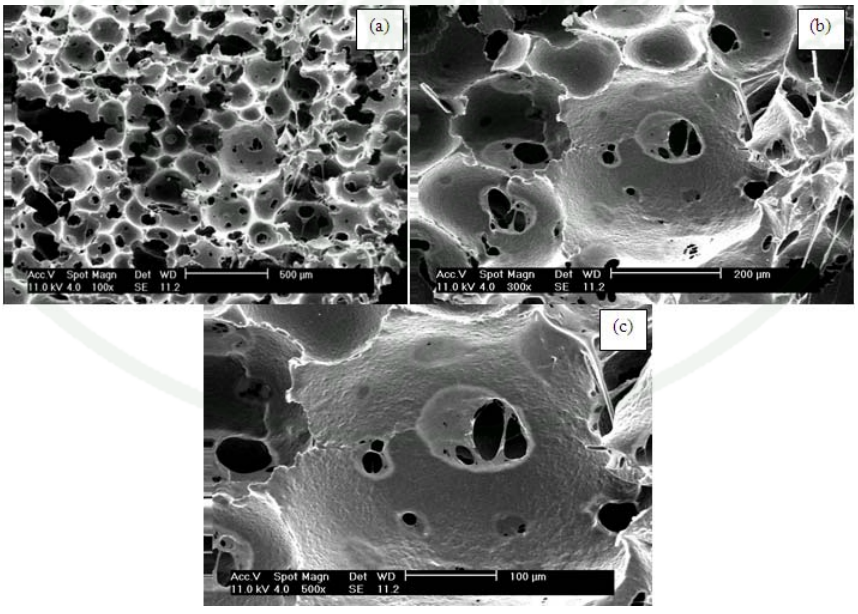

Appendix Figure A4 The SEM micrographs of 5%gel_110 distributed in PU foam (w/w) with different magnifications of (a) 100x, (b) 500x and (c) 3000x

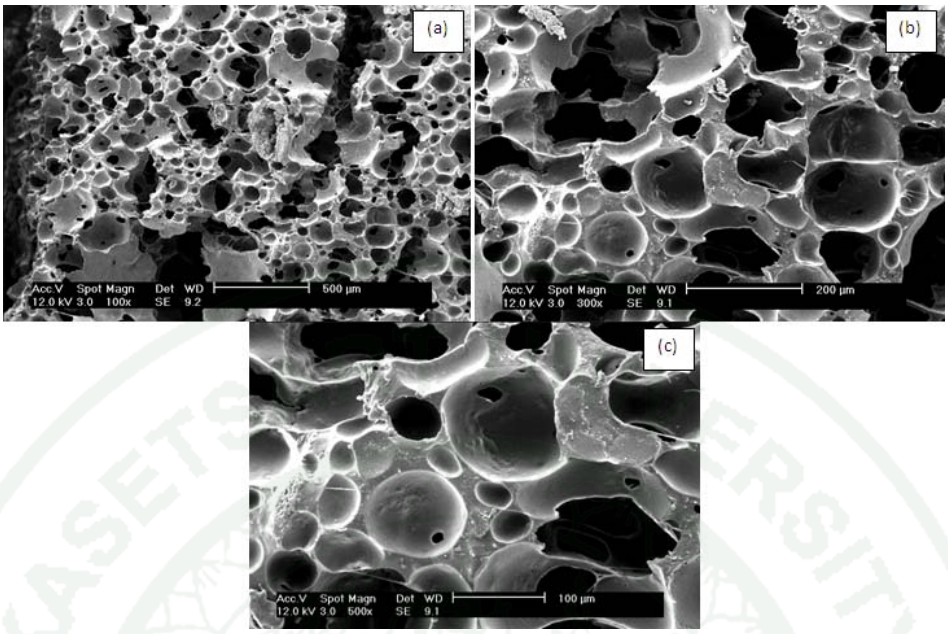

Appendix Figure A5 The SEM micrographs of 10%gel_110 distributed in PU foam (w/w) with different magnifications of (a) 100x, (b) 500x and (c) 3000x

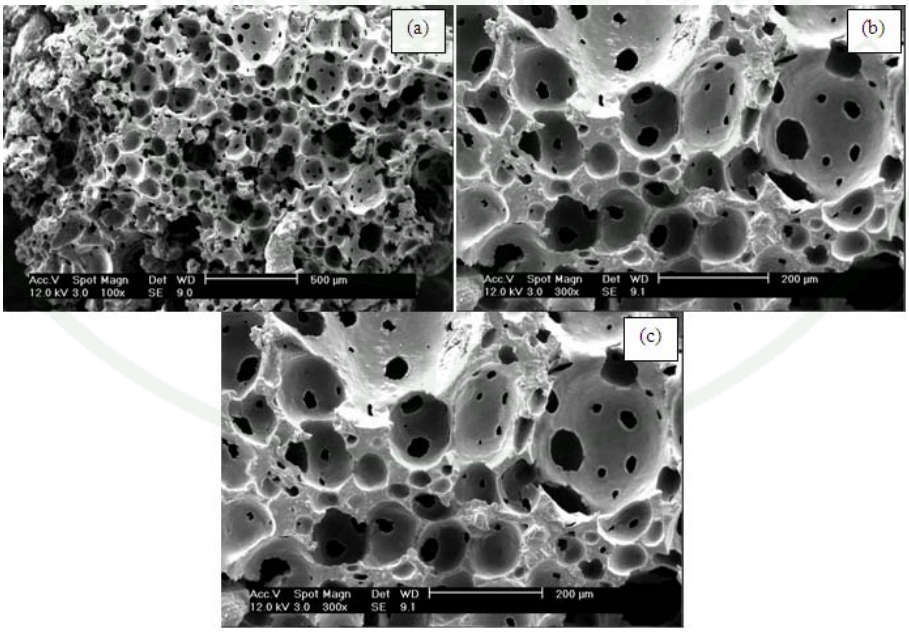

Appendix Figure A6 The SEM micrographs of 10%gel_300 distributed in PU foam (w/w) with different magnifications of (a) 100x, (b) 500x and (c) 3000x

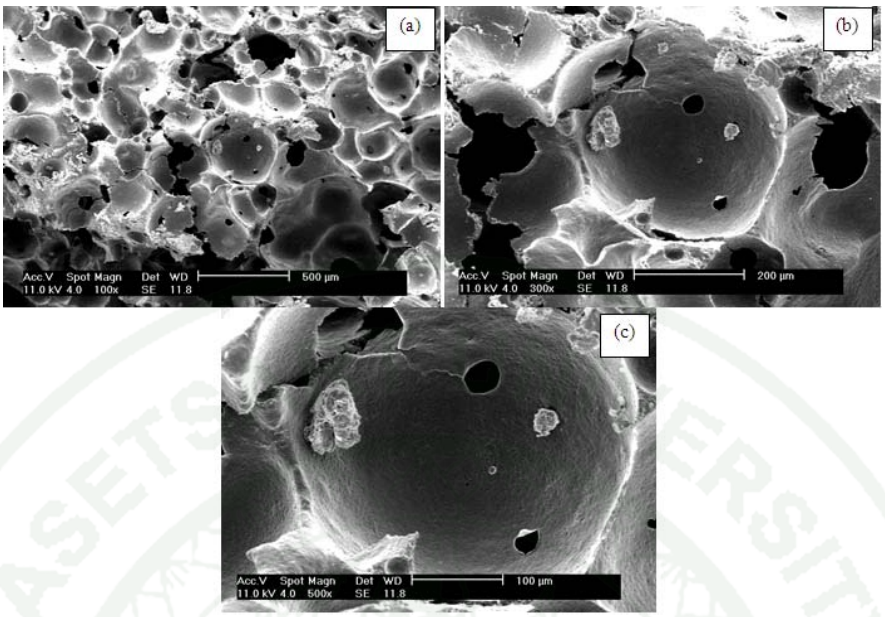

Appendix Figure A7 The SEM micrographs of 15%gel_110 distributed in PU foam (w/w) with different magnifications of (a) 100x, (b) 500x and (c) 3000x

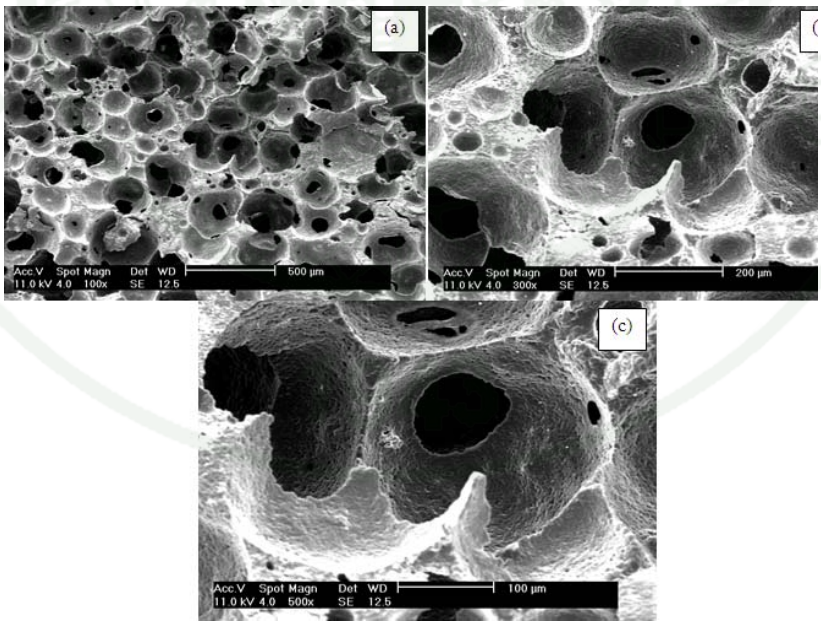

Appendix Figure A8 The SEM micrographs of 20%gel_110 distributed in PU foam (w/w) with different magnifications of (a) 100x, (b) 500x and (c) 3000x

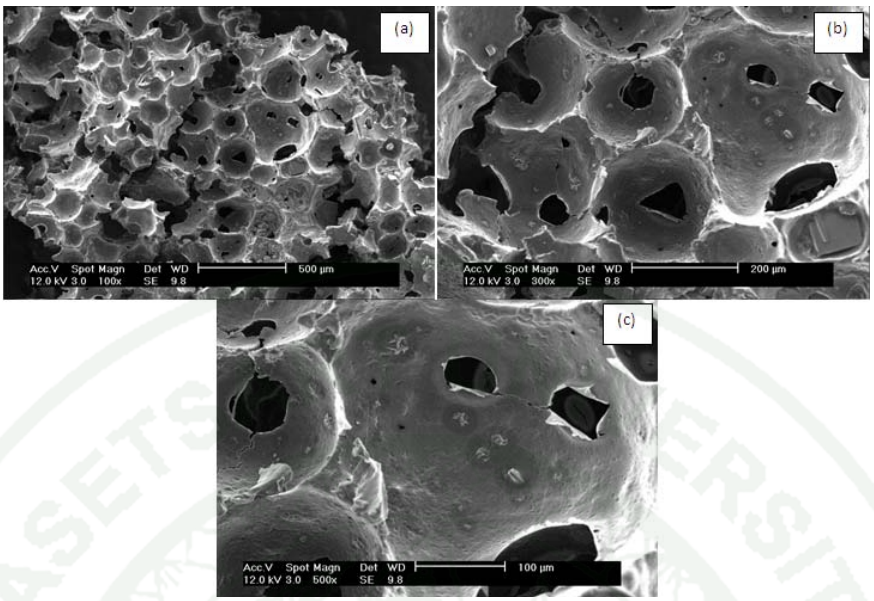

Appendix Figure A9 The SEM micrographs of 20%gel_300 distributed in PU foam (w/w) with different magnifications of (a) 100x, (b) 500x and (c) 3000x

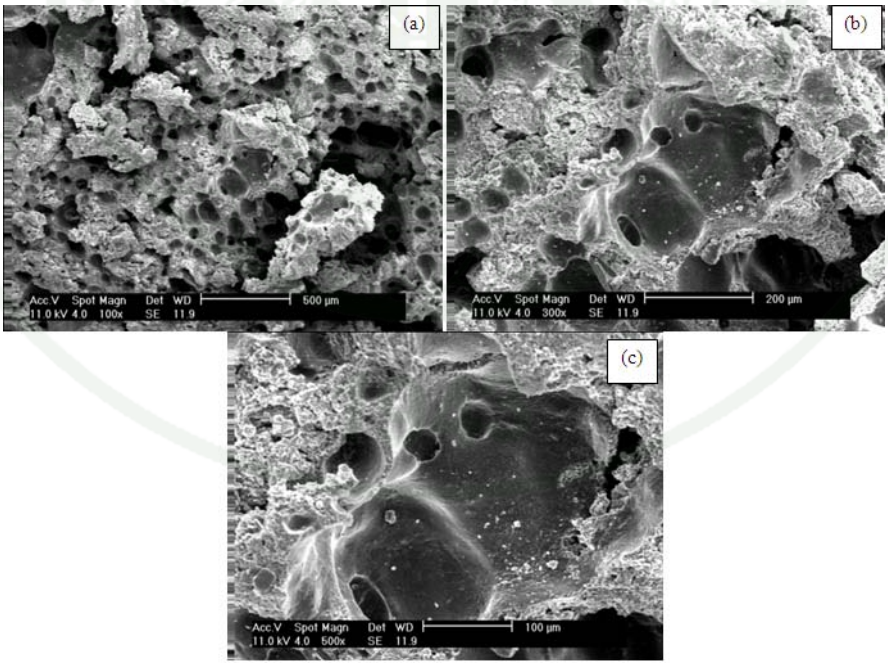

Appendix Figure A10 The SEM micrographs of 50%gel_110 distributed in PU foam (w/w) with different magnifications of (a) 100x, (b) 500x and (c) 3000x

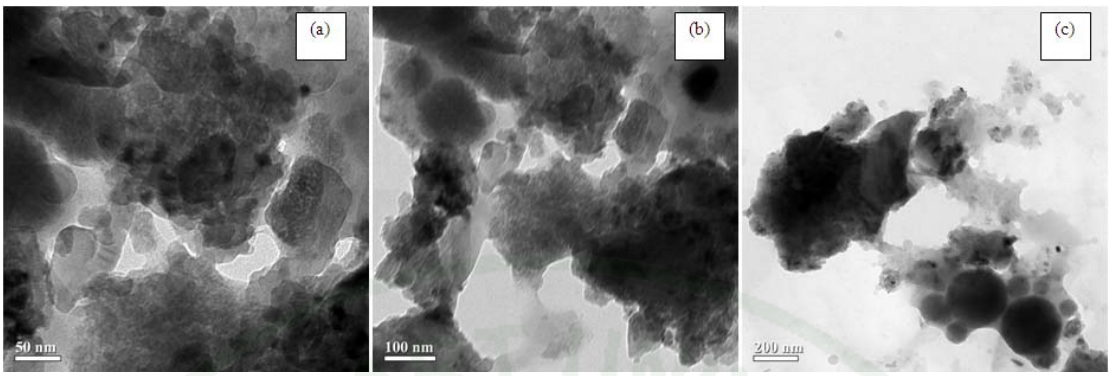

Appendix Figure A11 The micrographs of crushed quail-eggshell with different magnifications of (a) 50 k, (b) 30 k and (c) 12 k

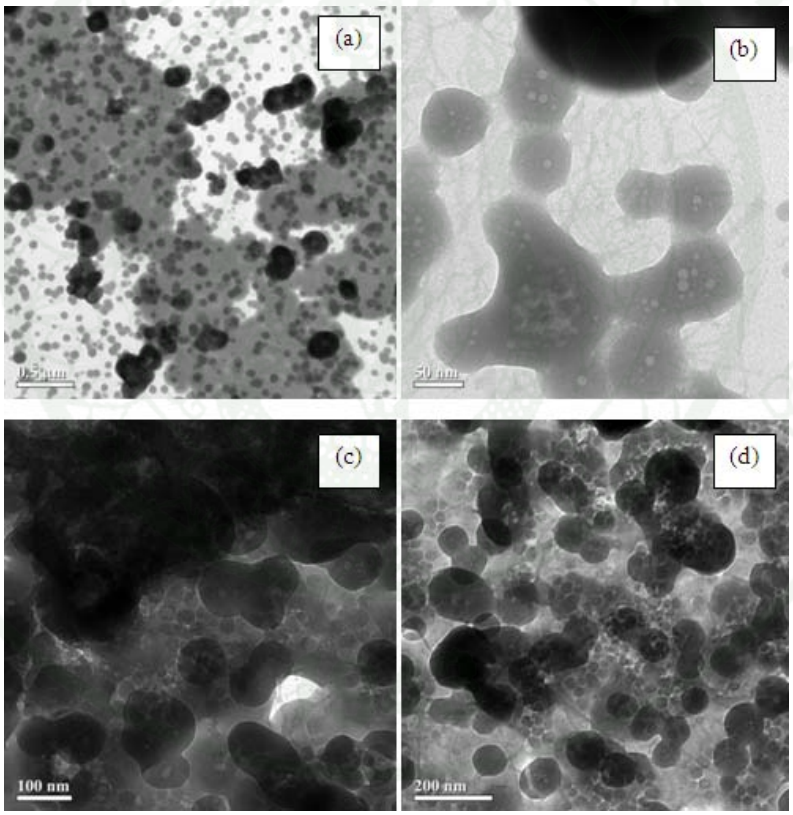

Appendix Figure A12 The TEM micrographs of calcined-quail eggshell at 900°C for 1 h with different magnifications of (a) 10k, (b) 50 k, (c) 30 k and (d) 12k

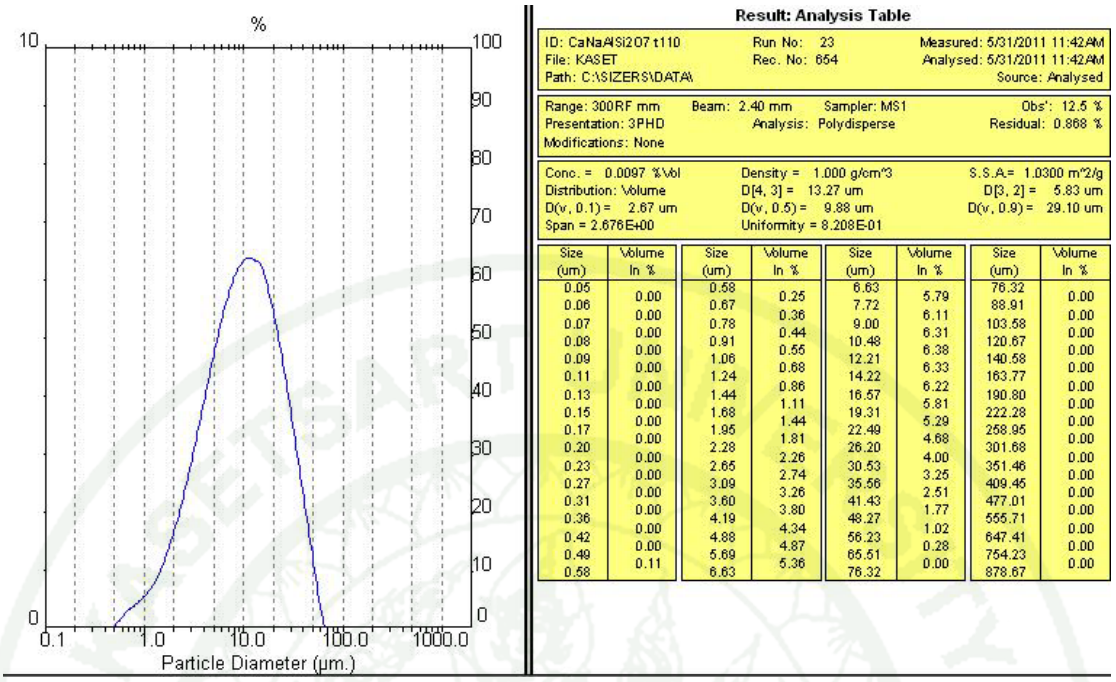

Result: Analysis Table

ID: CaNaAlSi2O7 t110 | Run No: 23 | Measured: 5/31/2011 11:42AM
File: KASET | Rec. No: 654 | Analysed: 5/31/2011 11:42AM
Path: C:\SIZERS\DATA\ | Source: Analysed

Range: 300RF mm | Beam: 2.40 mm | Sampler: MS1 | Obs': 12.5 %
Presentation: 3PHD | Analysis: Polydisperse | Residual: 0.868 %
Modifications: None

Conc. = 0.0097 %Vol | Density = 1.000 g/cm^3 | S.S.A.= 1.0300 m^2/g
Distribution: Volume | D[4, 3] = 13.27 um | D[3, 2] = 5.83 um
D(v, 0.1) = 2.67 um | D(v, 0.5) = 9.88 um | D(v, 0.9) = 29.10 um
Span = 2.676E+00 | Uniformity = 8.208E-01

Size (um)	Volume In %	Size (um)	Volume In %	Size (um)	Volume In %	Size (um)	Volume In %
0.05	0.00	0.58	0.25	6.63	5.79	76.32	0.00
0.06	0.00	0.67	0.36	7.72	6.11	88.91	0.00
0.07	0.00	0.78	0.44	9.00	6.31	103.58	0.00
0.08	0.00	0.91	0.55	10.48	6.38	120.67	0.00
0.09	0.00	1.06	0.68	12.21	6.33	140.58	0.00
0.11	0.00	1.24	0.86	14.22	6.22	163.77	0.00
0.13	0.00	1.44	1.11	16.57	5.81	190.80	0.00
0.15	0.00	1.68	1.44	19.31	5.29	222.28	0.00
0.17	0.00	1.95	1.81	22.49	4.68	258.95	0.00
0.20	0.00	2.28	2.26	26.20	4.00	301.68	0.00
0.23	0.00	2.65	2.74	30.53	3.25	351.46	0.00
0.27	0.00	3.09	3.26	35.56	2.51	409.45	0.00
0.31	0.00	3.60	3.80	41.43	1.77	477.01	0.00
0.36	0.00	4.19	4.34	48.27	1.02	555.71	0.00
0.42	0.00	4.88	4.87	56.23	0.28	647.41	0.00
0.49	0.00	5.69	5.36	65.51	0.00	754.23	0.00
0.58	0.11	6.63		76.32		878.67	0.00

Appendix Figure A13 Particle Diameter of gel_110 is analyzed the second time.

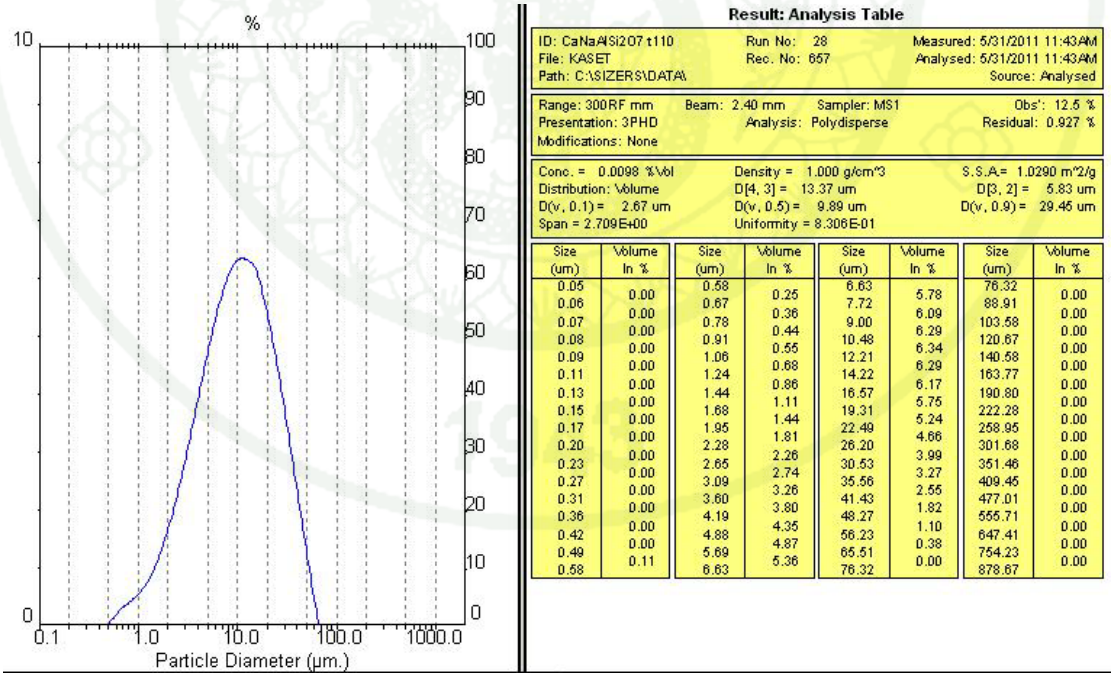

Result: Analysis Table

ID: CaNaAlSi2O7 t110 | Run No: 28 | Measured: 5/31/2011 11:43AM
File: KASET | Rec. No: 657 | Analysed: 5/31/2011 11:43AM
Path: C:\SIZERS\DATA\ | Source: Analysed

Range: 300RF mm | Beam: 2.40 mm | Sampler: MS1 | Obs': 12.5 %
Presentation: 3PHD | Analysis: Polydisperse | Residual: 0.927 %
Modifications: None

Conc. = 0.0098 %Vol | Density = 1.000 g/cm^3 | S.S.A.= 1.0290 m^2/g
Distribution: Volume | D[4, 3] = 13.37 um | D[3, 2] = 5.83 um
D(v, 0.1) = 2.67 um | D(v, 0.5) = 9.89 um | D(v, 0.9) = 29.45 um
Span = 2.709E+00 | Uniformity = 8.306E-01

Size (um)	Volume In %	Size (um)	Volume In %	Size (um)	Volume In %	Size (um)	Volume In %
0.05	0.00	0.58	0.25	6.63	5.78	76.32	0.00
0.06	0.00	0.67	0.36	7.72	6.09	88.91	0.00
0.07	0.00	0.78	0.44	9.00	6.29	103.58	0.00
0.08	0.00	0.91	0.55	10.48	6.34	120.67	0.00
0.09	0.00	1.06	0.68	12.21	6.29	140.58	0.00
0.11	0.00	1.24	0.86	14.22	6.17	163.77	0.00
0.13	0.00	1.44	1.11	16.57	5.75	190.80	0.00
0.15	0.00	1.68	1.44	19.31	5.24	222.28	0.00
0.17	0.00	1.95	1.81	22.49	4.66	258.95	0.00
0.20	0.00	2.28	2.26	26.20	3.99	301.68	0.00
0.23	0.00	2.65	2.74	30.53	3.27	351.46	0.00
0.27	0.00	3.09	3.26	35.56	2.55	409.45	0.00
0.31	0.00	3.60	3.80	41.43	1.82	477.01	0.00
0.36	0.00	4.19	4.35	48.27	1.10	555.71	0.00
0.42	0.00	4.88	4.87	56.23	0.38	647.41	0.00
0.49	0.00	5.69	5.36	65.51	0.00	754.23	0.00
0.58	0.11	6.63		76.32		878.67	0.00

Appendix Figure A14 Particle Diameter of gel_110 is analyzed the third time.

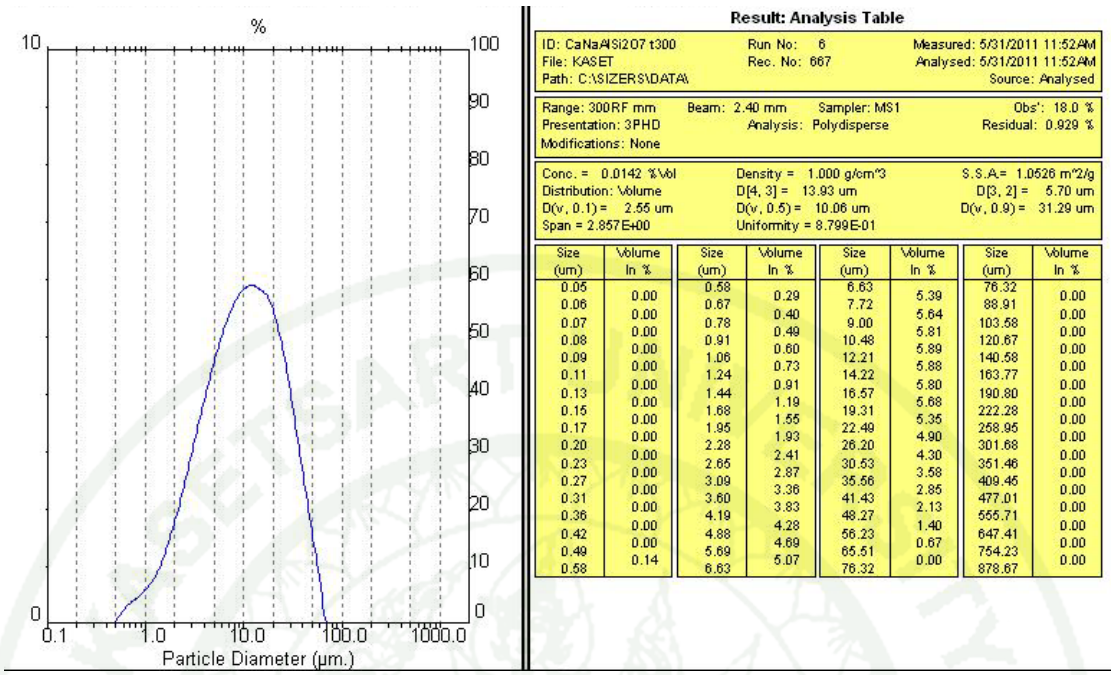

Appendix Figure A15 Particle Diameter of gel_300 is analyzed the second time.

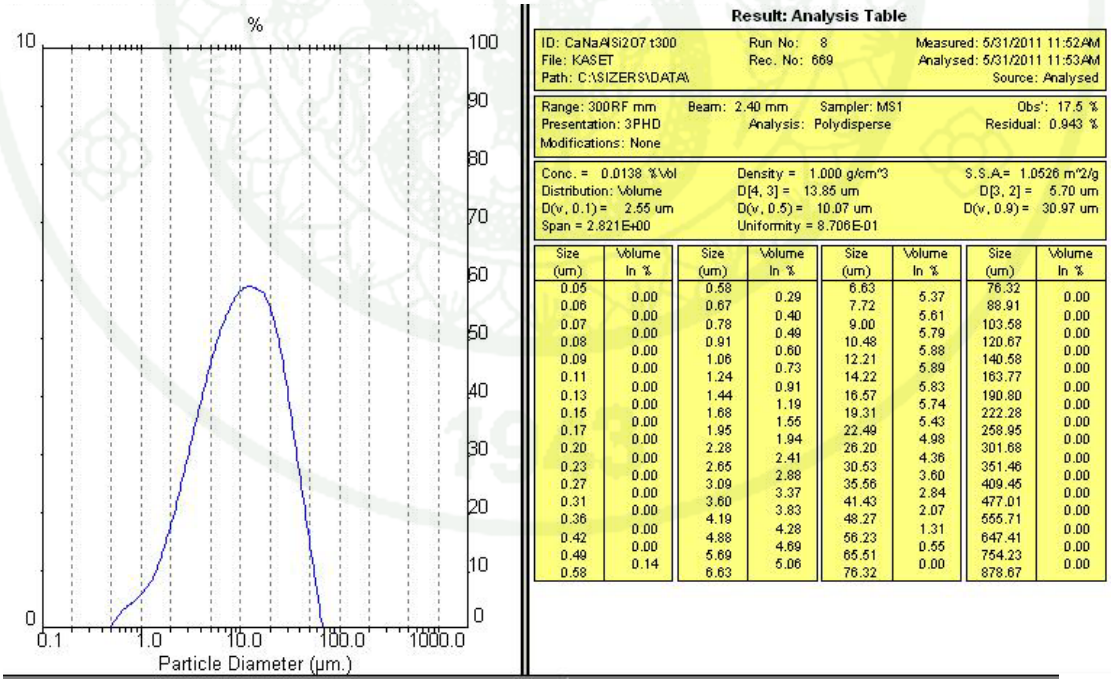

Appendix Figure A16 Particle Diameter of gel_300 is analyzed the third time.

Appendix Figure A17 Egg shell

Appendix Figure A18 Crushed egg shell

Appendix Figure A19 Calcined-eggshell at 900°C for 1 h

Appendix Figure A20 Quail egg shell

Appendix Figure A21 Crushed quail egg shell

Appendix Figure A22 Calcined-quail eggshell at 900°C for 1 h

Appendix Figure A23 Aluminosilicate powder

Appendix Figure A24 Fumed silica powder (SiO_2)

Appendix Figure A25 Calcium Zeolite Type A gel

Appendix Figure A26 Calcium Zeolite Type A dried at 110°C (gel_110)

Appendix Figure A27 Calcium Zeolite Type A calcined at 300°C (gel_300)

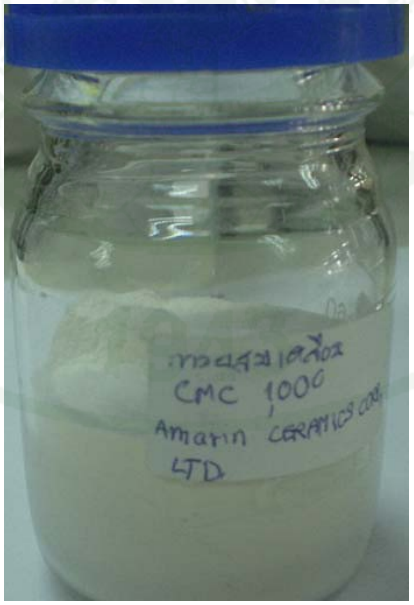

Appendix Figure A28 Caboxy Methyl Cellulose (CMC) powder

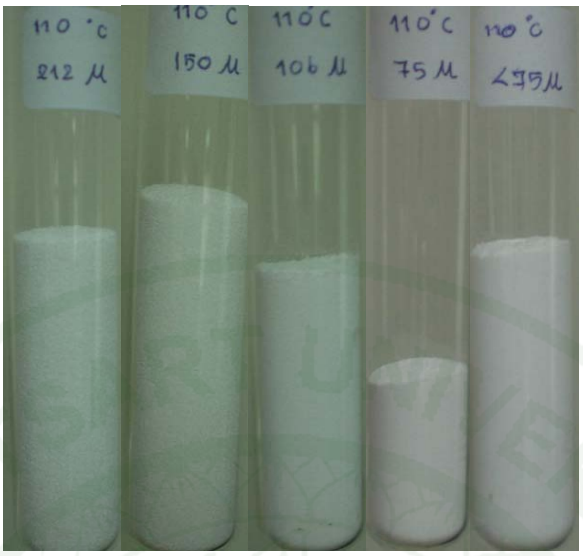

Appendix Figure A29 Different size granules (gel_110)

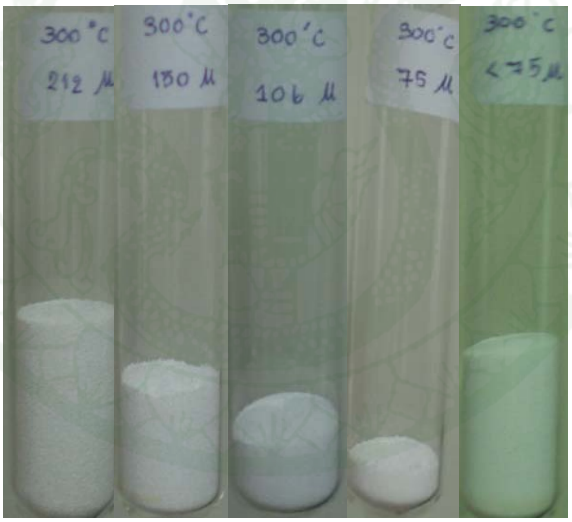

Appendix Figure A30 Different size granules (gel_300)

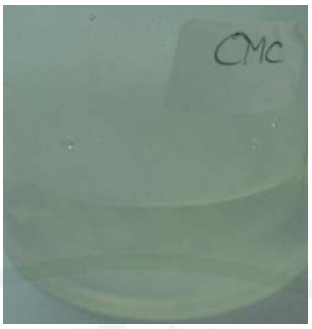

Appendix Figure A31 Caboxy Methyl Cellulose(CMC) dissolved in water

Appendix Figure A32 Foam cutter machine

Appendix Figure A33 Foam composite (Zeolite+gel_110/300)

Appendix Figure A34 High temperature furnace

Appendix Figure A35 Oven

Appendix Figure A36 Compressive force gel_110 and gel_ 300 products

Appendix Figure A37 Mechanical stirrer

Appendix B

Tables

Appendix Table B1 Machanical properties of PU foam

Sample names/No.	E.Modulus (kgf/mm^2)	0.2% Kgf/mm^2	Y.Strength (kgf/mm^2)	C.Strength (kgf/mm^2)	Diameter (mm)
PU foam 1	0.1611	0.0120	0.0300	0.0300	28.20
PU foam 2	0.0831	0.0020	0.0133	0.0133	28.73
PU foam 3	0.0875	0.0015	0.0255	0.0255	28.40
PU foam 4	0.0867	0.0039	0.0243	0.0243	28.25
PU foam 5	0.1626	0.0041	0.0295	0.0295	28.63
Mean	0.1162	0.0047	0.0245	0.00245	28.44
Std. Dev	0.0417	0.0042	0.0067	0.0067	0.2084

Note E.Modulus is Elastic Modulus, Y.Strength is Yield trength, C.Strength is Compressive Strength and the samples are characterize by ASTM D 695 Compression of Rigid Plastics[Xhead].

Appendix Table B2 Machanical properties of composite foam (10%gel_300+PU foam)

Sample names/No.	E.Modulus (kgf/mm^2)	0.2% Kgf/mm^2	Y.Strength (kgf/mm^2)	C.Strength (kgf/mm^2)	Diameter (mm)
10%gel_300 +PU foam 1	0.0404	0.0018	0.0200	0.0200	29.36
10%gel_300 +PU foam 2	0.0327	0.0022	0.0194	0.0194	29.43
10%gel_300 +PU foam 3	0.0281	0.0022	0.0206	0.0206	29.32
10%gel_300 +PU foam 4	0.0223	0.0016	0.0174	0.0174	29.10
10%gel_300 +PU foam 5	0.0400	0.0022	0.0168	0.0168	29.33
Mean	0.0327	0.0020	0.0188	0.0188	29.31
Std. Dev	0.0078	0.0003	0.0017	0.0017	0.1239

Note E.Modulus is Elastic Modulus, Y.Strength is Yield trength, C.Strength is Compressive Strength and the samples are characterize by ASTM D 695 Compression of Rigid Plastics[Xhead].

Appendix C

Conference

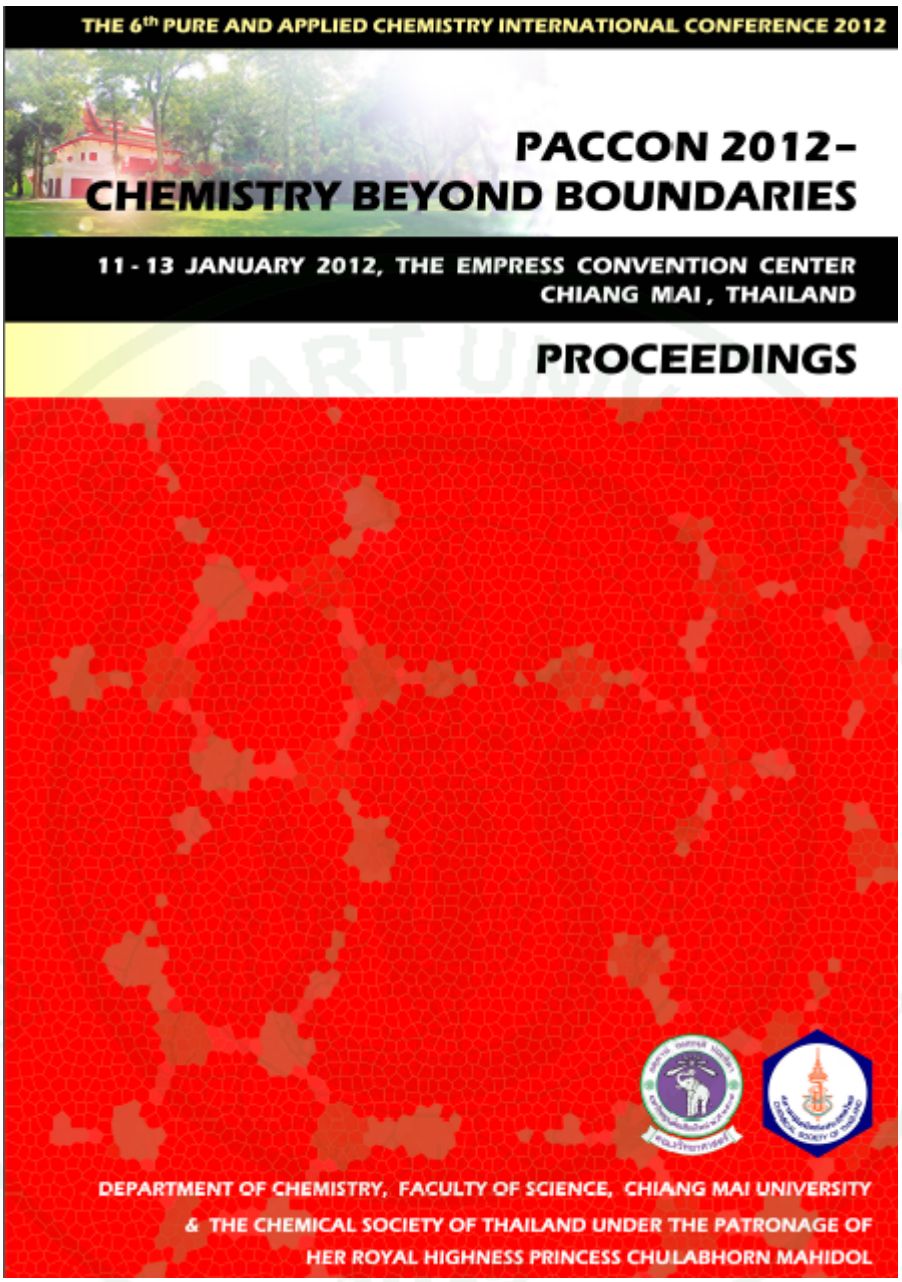

PACCON
PURE AND APPLIED CHEMISTRY INTERNATIONAL CONFERENCE 2012

"Chemistry Beyond Boundaries"

Content

PACCON 2012 proceedings are published in electronic form only. There is no index page but reader can search for interested keywords in this content by using pdf program searching tool. The full articles in the proceedings are grouped into various sessions and have been in separated files in order to reduce file size for convenient downloading. The sessions and associated files are listed below:

PREPARATION OF CATALYST FOAMS OF CALCIUM ZEOLITE TYPE A FROM EGGSHELLS AND POLYURETHANE TEMPLATE

La-Orngdow Mulsow[1] and Nuchnapa Tangboriboon[1*]

[1]*Department of* Materials Engineering, Faculty of Engineering, Kasetsart University, Bangkok 10900, Thailand

[*]Author for correspondence; E-Mail:fengnnpt@ku.ac.th, Tel. +662 942-8555 Ext. 2106, Fax. +662 955-1811

Abstract: This research aims to form polymer matrix composites (PMCs) between calcium zeolite type A ($CaNaAlSi_2O_7$) made from eggshells as the starting material via the sol-gel process and polyurethane foam (PU) matrix. The received PMCs samples phase formation was characterized by X-ray diffraction, microstructure by scanning electron microscopy, pore size and specific surface area by brunaues-emmet-teller, mechanical properties by compression test, the functional groups by the fourier transformation infrared spectroscopy, and the endothermic-exothermic reaction by differential thermal analysis. The $CaNaAlSi_2O_7$ acted as a dispersant in the polyurethane (PU) matrix, (PMCs). The best composition of composite materials is 10 %vol $CaNaAlSi_2O_7$ added into PU matrix. The average particle size of $CaNaAlSi_2O_7$ is approximately 10 µm, non-agglomeration, and good dispersion in the entire volume of PU foam. The composite foam cells are well ordered and uniform in size and shape. The true density, elastic modulus, compressive strength of $CaNaAlSi_2O_7$/PU composites are 1.47 g/cm^3, 0.0327 Kgf/mm^2, and 0.0188 Kgf/mm^2, respectively. The $CaNaAlSi_2O_7$/PU composites are semi-crystalline between tetragonal phase formations of $CaNaAlSi_2O_7$ and amorphous phase formation of PU.

1. Introduction

Over 200 years ago, a Swedish scientist discovered the first of a group crystalline microporous aluminosilicate known as zeolite; zeolite derived from the Greek word *Zeo* which means boil and *Lithos* meaning stone [1].

Zeolite consists of open cell, three dimensional framework of tetrahedral AlO_4 and SiO_4 units linked through shared oxygen molecules, crystalline microporous and aluminosilicate minerals. Due to their properties that have size and shape selectivity so its applications can be used in ion-exchange, purification, desiccant or adsorbent and as a catalyst. The catalysts are quite important in chemical, petrochemical and oil refining industries.

The zeolite type A is one kind of all zeolites which synthesize in different ways; such as electrostatic deposition, sol-gel process [2], mixed matrix membranes (MMM) as a promising morphology for gas separation and as a polymer matrix composite; for example, separation of xylene mixtures using polyurethane-zeolite composite membranes [3].

Owing to polyurethane (PU) has many good properties such as moisture resistance, high shear strength, excellent sound dampening, vibrational, and oscillation environment tolerance [4], so several researches have used their benefit with homogeneous pore cells in order to improve others research. The present study is using PU as a matrix for making catalyst composite foams.

This research aims to produce polymer matrix composite (PMCs) between calcium zeolite type A ($CaNaAlSi_2O_7$) made from eggshells as the starting material via the sol-gel process and polyurethane foam (PU) as a matrix. The constituent of eggshells contained 1wt% of magnesium carbonate, 4 wt% of calcium phosphate and organic matter, and 94 wt% of calcium carbonate which is an important source of calcium oxide as a starting material to prepare the catalyst powder [5].

2. Materials and Methods

2.1 Calcium Chloride Solution Preparation

Calcium oxide (CaO) was prepared from eggshells by the following steps; washed and dried at room temperature, crushed and calcined under atmospheric pressure at 900°C for 1 h with a heating rate of 10°C/min, then 0.5g of air cooled CaO was dissolved in 20 mL of 1 M HCl (Analytical Reagent, AR, Lab-Scan Co., Ltd., Thailand) to obtain the solution [2].

2.2 Sodium Aluminosilicate Solution Preparation

Sodium aluminosilicate solution was obtained by mixing 0.8 g of fumed silica powder (SiO_2, WACKER Chemie, AG, Germany), 5.0 g of precipitated sodium aluminosilicate(United Silica(Siam Ltd, Thailand)) and 1.0 g of sodium hydroxide (NaOH, Molecule Co., Ltd., Thailand) with 20 ml distillated water[2].

2.3 Synthesis of Calcium Zeolite type A

The calcium zeolite type A ($CaNaAlSi_2O_7$) was obtained by pouring the mixture solution of 2.1 into the mixture solution of 2.2 stirred then left at room temperature for 24 h, called the sol-gel process [2]. The gel sample was dried at 110°C for 24 h (gel_110) and calcined at 300°C for 1 h (gel_300) to obtain $CaNaAlSi_2O_7$ powder.

2.4 $CaNaAlSi_2O_7$-PU catalyst foam (PMCs) preparation

PMCs was prepared by using polyurethane foam (PU) as a template (DALTOPED®FF 45804 and SUPRASEC®2749 from Huntsman (Thailand)). The FF 45804 is polyol and the SUPRASEC 2749 is di-isocyanate used as pre-polymer. The weight ratio of FF 45804 and SUPRASEC 2749 is 100:98.

The PMCs were prepared by stirring the FF 45804 with a speed of 1200 rpm for 3 min then added 10 vol% of catalyst gel into the FF 45804, after that added the SUPRASEC 2749 rapidly into the mixture. The mixture stirred uniformly until to complete exothermic reaction to obtain the catalyst foam, observed by heating to skin hand.

3. Results and Discussion

The thermal stability of catalyst and PU composite foam was determined by differential thermal analysis (DTA, Perkins-Elmer TAC7/DX, DTA7, USA) under a nitrogen atmosphere (Fig 1). The samples were heated from 30°to 950°C with a heatting rate 10°C/min. The result shows an exothermic reaction of PU foam started to degrade from 530°C to 650°C(Fig 1a). Furthermore, the catalyst-composite foams (PU foam + 10 vol% catalyst gel at 300°C) have an endothermic peak at 790°C shown onset at 786°C (Fig 1b) due to re-crystalline of catalyst gel in PU foam matrix.

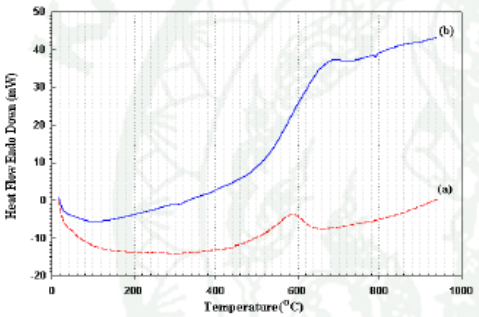

Figure 1 Differential thermal analysis (DTA) of (a) PU foam, (b) PU foam+10% vol of catalyst gel at 300°C.

Table 1: True density test result

Sample names	True density (g/cc)
1.Catalyst gel at 110°C	1.90
2.Catalyst gel at 300°C	1.96
3.Pure PU foam	1.13
4.PU foam+10 vol% catalyst gel at 300°C	1.47

The data of true density of catalyst gel at 110°C, catalyst gel at 300°C , pure PU foam, and PU foam + 10 vol% catalyst gel at 300°C, were analyzed by gas pycnometer, as shown in table1. Adding 10 vol% catalyst gel at 300°C into pure PU foam can increase the true density value of composite foam from 1.13 to be 1.47g/cc. The specific surface area, total pore volume, and average pore diameter of catalyst gel were analyzed as shown in table 2. The catalyst gel at 300°C exhibited higher surface area, pore volume and pore diameter values than the data values of catalyst gel at 110°C due to densification, internal voids in the material reduce the mass and diffusion of some residue gas such as carbon dioxide (CO_2) gas out of the material.

Table 1: BET analysis of catalyst gel samples

Sample names	Multipoint BET (m^2/g)	Total pore volume (cc/g)	Average pore diameter (Å)
1.Catalyst gel at 110°C	37.91	0.2917	307.8
2.Catalyst gel at 300°C	38.89	0.3728	383.4

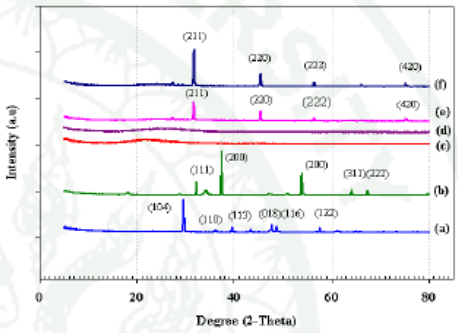

Figure 2 X-ray diffraction (XRD) patterns comparison of (a) eggshell, (b) CaO, (c) fumed SiO_2, (d) aluminosilicate, (e) gel_110 and (d) gel_300.

The XRD peak pattern of eggshell is shown in Fig 2a with the number of 01-085-1108 according to the International Center for Diffraction Data (JCPDS) of 2θ and (hkl) values equal to 29.466 (104), 36.039 (110), 39.489 (113), 43.244 (2302), 47.685 (018), 48.615 (116), and 48.615(122), indicating the rhombohedral formation of calcium carbonate ($CaCO_3$). The Fig 2(b) shows a peak pattern of CaO, number 00-037-1497 with 2θ and (hkl) are equal to 32.604 (111), 37.347 (200), 53.856 (220), 64.154 (311), 67.375 (222) and 79.665 (400) indicating the cubic phase formation. Furthermore, the Fig 2(c) and 2(f) demonstrated peak patterns of catalyst gel at 110°C and catalyst gel at 300°C with the JCPDS numbers 01-076-0479 and 01-071-2066 of 2θ and (hkl) are equal to 31.805 (211), 45.432 (220), 56.452 (222), 29.310 (201), 68.714 (521), and 75.263 (420), indicating the tetragonal formation of calcium sodium aluminosilicate.

The Fig 3, shows XRD peak pattern comparison between pure PU foam and catalyst composite foams. The step scan used present time at 1s with 2θ = 5°-80°. The XRD peak patterns of pure PU foams and catalyst composite foams exhibited amorphous regions, so the step scan measured in the range of 2θ = 5°-80°. However, the XRD peak patterns of

$CaNaAlSi_2O_7$powder show crystalline phase in the range of 2θ equal to 25°-35° as shown in Fig.4. The peak patterns of Figs. 4b, 4c, 4d and 4e were demonstrated at 2θ about 32° which indicated the tetragonal formation of calcium sodium aluminosilicate.

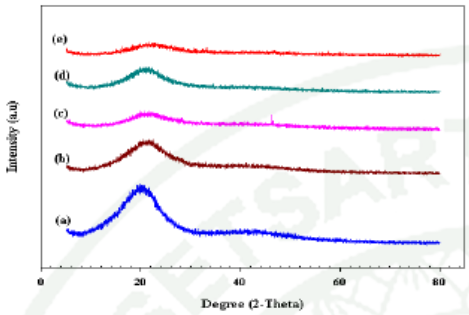

Figure 3 X-ray diffraction (XRD) patterns comparison of (a) pure PU foam, (b) PU foam+10 vol % catalyst gel 110°C , (c) PU foam+20 vol% catalyst gel at 110°C , (d) PU foam+10 vol% catalyst gel at 300°C, and (e) PU foam+20 vol% catalyst gel at 300°C.

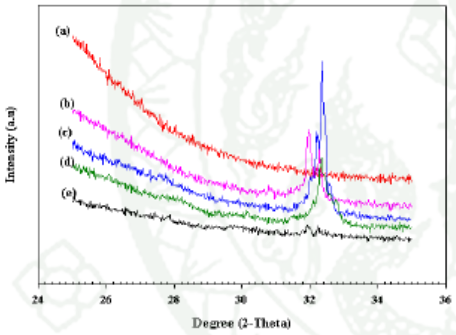

Figure 4 X-ray diffraction (XRD) patterns comparison of (a) pure PU foam, (b) PU foam+10 vol% catalyst gel at 110°C, (c) PU foam+20 vol% catalyst gel at 110°C, (d) PU foam+10 vol% catalyst gel at 300°C and (e) PU foam+20 vol% catalyst gel at 300°C.

The Fig 5(a) shows the FT-IR (Perkin Elmer, Spectum one) spectrum of the calcined eggshell to be CaO. The wave number of peak at 3642.13 cm^{-1} belongs to OH of $Ca(OH)_2$ due to moisture absorption of CaO. The broad band peak occurs around 1440.33 cm^{-1} corresponding to the Ca-O. Figs 5(b) and 5(c) are FTIR spectra of catalyst gel at 110°C and catalyst gel 300°C at 500-550 cm^{-1} indicating Al-O-C, Si-O-Al, Si-O, and Si-O-Si bonding consistent with the data reported [2]. In addition, the FTIR spectra at 463.43, 794.40, and 1446.04 cm^{-1} show the characteristic of the β-Ca-O-Si, Ca-O-Si, and strong C=O vibration, respectively, which indicated the $CaNaAlSi_2O_7$.

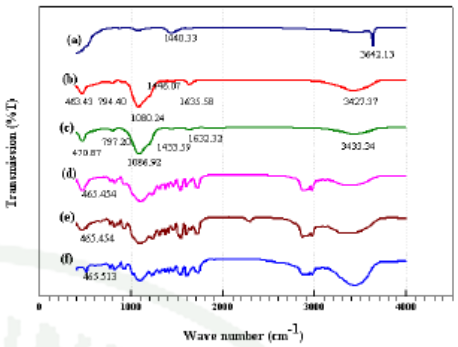

Figure 5 The Fourier Transformation Infrared Spectroscopy (FT-IR) spectra of (a) CaO (b) catalyst gel at 110°C (c) catalyst gel at 300°C (d) PU foam+10 vol% catalyst gel at 110°C (f) pure PU foam.

The Fig. 5(d) and 5(e) show spectra comparison of PU foam+10 vol% catalyst gel at 110°C and PU foam + 10 vol% catalyst gel at 300°C, and pure PU foam. The PU foam+10 vol% catalyst gel at 110°C shows peak positions at 470.89, 797.20 cm^{-1}, same as the peak positions of the PU foam+10 vol% catalyst gel at 300°C at 463.43 and 794.40 cm^{-1} corresponding to the characteristics of β-Ca-O-Si and Ca-O-Si, respectively. The spectra of the pure PU foam acted as a matrix whereas the calcium zeolite type A ($CaNaAlSi_2O_7$) acted as the dispersed phase for making catalyst foam composites. It is found that the segmented structure of PU no major change the properties and the structure of $CaNaAlSi_2O_7$.

The FT-IR spectra of the polyurethane foams prepared from the FF 45804 and the SUPRASEC 2749 as shown in Fig 5(f). This spectrum indicates peak positions belonging to polyurethanes at 3437.71 cm^{-1} consistent with –N-H stretching vibration of urethane groups (3200-3450 cm^{-1}) [4]. The broad band peak at 2800-3000 cm^{-1} corresponds to –C-H stretching [6]. They do not show the peak position at 2250-2270 cm^{-1} consistent with the characteristic of isocyanate (-N=C=O) group because of polymerization [6, 8]. The –C=O stretching of the urethane carbonyl peak at 1712.90 and 1730.79 cm^{-1} are observed and reported at 1702-1737 cm^{-1} [7]. The peak at 1613.45 cm^{-1} indicates the carbonyl vibration (-C=O) reported at 1630-1637 cm^{-1} [6, 8] while –NH bending is identified peak at 1512.21. Also, the peak at 1541.65 cm^{-1} originates from the coupling of –CN stretching and –NH bending [9]. The FTIR peaks observed between 1400 and 1480 cm^{-1} (in this work occurred at 1414.57 and 1453 cm^{-1}) are attributed to $–CH_2$ scissoring vibrations. The weak peaks at 1345.96 and 1374.99 are connected to the wagging vibrations of methylene groups, whereas the peak at 1310.32 cm^{-1} is assigned to $–CH_2$ twisting. The FTIR spectra exhibit the characteristic peak at 1000-1400 cm^{-1} of C-N and C-O stretching. The presence of the FTIR peaks belongs to polyurethane foam.

Fig.6 shows the SEM photographs analyzed by Scanning Electron Microscope (SEM) (Philips, XC,

Netherland) of pure PU foam and pure PU foam added with 10 vol% catalyst gel at 300°C. The cell edges and cell walls of pure PU foam are distinctly visible with almost uniform cell structures throughout. Cell size as seen in the (SEM) is approximately 200-250 µm. The samples added with 10 vol% catalyst gel at 300°C are shown in Figs. 6(d), 6(e), and 6(f). The 15 vol%, 20 vol%, 30 vol%, and 50 vol% of catalyst gel at 300°C were added into PU foam. The higher percentage of catalyst added into PU foam is not good for making catalyst composite foam formation due to the agglomeration of catalyst within the interconnecting cells of PU foam. Therefore, the best composition of composite materials is adding 10 vol% $CaNaAlSi_2O_7$ into PU matrix with uniform structure and non-agglomeration of catalyst powder. The composite foam cells still are well ordered and uniform in size and shape. However, open cells of the composite foam seem smaller than that of pure PU foam. According to the SEM image results of catalyst composite foam added 10 vol% catalyst gel at 110°C into PU foam matrix are similar SEM micrographs of catalyst composite foams added with 10 vol% catalyst gel at 300°C into PU foam matrix.

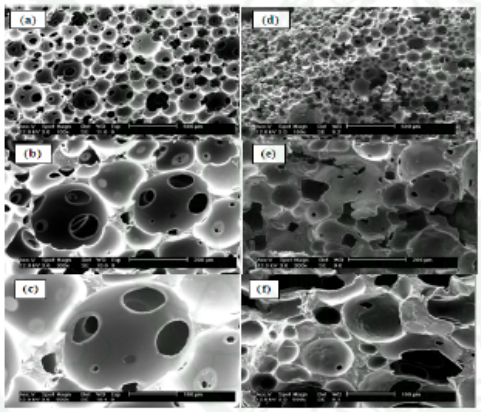

Figure 6 SEM picture of (a) pure PU foam at 500 µm (b) pure PU foam at 200 µm (c) pure PU foam at 100 µm (d) pure PU foam+10 vol% catalyst gel at 300°C at 500 µm (e) pure PU foam+10vol% catalyst gel at 300°C at 200 µm (f) pure PU foam+10 vol% catalyst gel at 300°C at 100 µm.

The compressive strength and elastic modulus of PU foam+10 vol% catalyst gel at 300°C compared to pure PU foam were measured by a compressive tester (Qmat 5.44 M-Series-10 KM) according to ASTM D 695 compression of rigid plastics [XHead]. The dimensions of specimens are 25.4×25.4×12.7 mm^3 and the crosshead speed of compression was set at 1.2 mm/min. The elastic modulus and compressive strength of the composite foam are 0.0327±0.0078 and 0.0188±0.0017 Kgf/mm^2, respectively. The elastic modulus and compressive strength of pure PU foam are 0.1162±0.047 and 0.0245±0.0067 Kgf/mm^2, respectively. The mechanical properties (elastic modulus and compressive strength) of catalyst composite foams of adding catalyst gel at 300°C are less than that of pure PU foams due to H-bond formation among urethane groupsthat greatly contributes to the strength and modulus of PU foam. For the reason of catalyst gel at 300°C may intervene with the H-bond formation and no strong interaction or graft within PU matrix. Therefore, The PU foam composite has high elastic modulus and compressive strength. However, catalyst composite foams have high specific surface area, thermal resistance, and corrosion resistance usefulas catalyst composite foams.

4. Conclusions

The catalyst foam was successfully made from eggshells as the catalyst-starting material via the sol-gel process composite to PU as the matrix. The $CaNaAlSi_2O_7$/PU composites have potential as catalyst foams in the chemical and petrochemical industries for use in ion exchange, filter, and desiccant.

Acknowledgements

The authors would like to thank the Department o Material Engineering at Kasetsart University fo financial and analytical equipment support, th Petroleum and Petrochemical College, the Scientifi and Technological Research Equipment Centre, a Chulalongkorn University for using of analytica equipment, and the Hutsman (Thailand) Ltd., fo providing the chemical substance to prepar polyurethane as a PU foam.

References

[1] J.C. Van der waal and H.Van bekkum, *J. Poroı Mat*.5(1998)289—303.
[2] T. Nuchnapa, W. Sujita, K. Ruksapong and S. Anuva *J. Ionrg Organomet Polym* (2010).
[3] S.Denger, K.Halil and Y.levent, *J.mem.sci*.303(2007) 194-203.
[4] M.Hassan, R.Vijaya, I.Mohammad and J.Shaik, *part a* 35 (2004) 453—460.
[5] W.Ziku, X.Chunli and L.Baoxin, *J.Bio.tech.* (2009 2883-2885.
[6] G.A. Scott, S.Abiraman, D.E. Jerald, D.E.Jonathan, M.Sean and H.O.Jeffrey, *Biomaterials*, Vol. 29, Issue12,(2008)1762—1775.
[7] L.Yongshang and L.Richard, *Progress in Organic Coatings* 69(2010)31-37.
[8] M.A. Corcuera, L. Rueda, B. Fernandez d'Arlas, A. Arbelaiz, C. Marieta, I. Mondragon and A. Eceiza, *Polymer Degradation and Stability* 95, Issue 11(2010) 2175-2184.

PACCON
PURE AND APPLIED CHEMISTRY INTERNATIONAL CONFERENCE 2012

Certificate of Participation

This is to certify that

La-Orngdow Mulsow

Kasetsart University

has participated as an

Poster Presenter

in the 6th Pure and Applied Chemistry International Conference (PACCON 2012)
at The Empress Convention Center, Chiang Mai, Thailand
11 – 13 January 2012

Professor Dr. Kate Grudpan
Chairman
Academic Committee

Associate Professor Dr. Jintana Siripitayananon
Chairman
Organizing Committee

CIRRICULUM VITAE

NAME : Mrs. La-Orngdow Mulsow

BIRTH DATE : March 30, 1986

BIRTH PLACE : Roi-Et, Thailand

EDUCATION :

YEAR	**INSTITUTE**	**DEGREE/DIPLOMA**
2010	Silpakorn University	B.Eng. (Petrochemical) and Polymeric Materials)

CONTACT : laorngdow191@hotmail.com, 085-8477614